

**Master of Urban Climate and Sustainability (MUrCS)**

**Assessment of Wind Characteristics and Urban  
Heat Island Dynamics for Urban Planning: A  
Case Study of Toulouse, France**

**Henry Adeniyi Ibitolu**

**August 2020**

**ASSESSMENT OF WIND CHARACTERISTICS AND URBAN  
HEAT ISLAND DYNAMICS FOR URBAN PLANNING: A  
CASE STUDY OF TOULOUSE, FRANCE**

**HENRY ADENIYI IBITOLU**

**S1839388**

Submitted in partial fulfilment for the requirements of  
Master of Urban Climate & Sustainability (MUrCS)

Glasgow Caledonian University, UK;  
LAB University of Applied Sciences, Finland;  
University of Huelva, Spain

Supervisors: Prof. José Enrique García Ramos (UHU)

Dr Caroline Gallagher (GCU)

**August 2020**

## DECLARATION

*“This dissertation is my own original work and has not been submitted elsewhere in fulfilment of the requirements of this or any other award”*

## ABSTRACT

To build liveable, resilient and climate responsive cities today, there is a need for city planners to understand the local complexities of the urban environments, especially in a changing urban climate. The prevailing wind flow over a city determines to a great extent the urban heat island (UHI) intensity in the city, thus it is important to understand the wind pattern in a city, since natural wind ventilation is one of the most effective energy-saving strategy to improve the overall thermal comfort level at the city scale.

This study has attempted to do exactly that, by employing the Local Weather Type (LWT) classification to conduct a spatio-temporal wind analysis of the Toulouse Metropolitan region in France under the warm and dry summer months of 2004. The administrative urban database describing the surface properties and the wind simulation output from the mesoscale atmospheric model Meso-NH at 250 m x 250 m horizontal resolution across the city of Toulouse was used in this research. The simulation provided city-wide wind data at 10 m above average building height, hence representative of the prevailing wind situation over Toulouse. To quantify the wind characteristics, a mean and frequency statistical approaches were evaluated in R. Results revealed that the frequency cartographic maps tend to show more details of the distinct shape of the densely built urban centre. Also, it was revealed that the mean analysis over-estimated the wind velocity by 1-2 m/s during daytime for all local weather types. At night, both methods show similar velocity intensity from East to West, though LWT-9 tends to under-estimate the wind speed by 2 m/s around the airport for the frequency analysis.

Furthermore, using the local climate zones (LCZs) classification describing the built urban morphology in the city, attempts were made to understand how the nocturnal UHI varies between LCZs in relations to changes in wind intensity. The results show that compact buildings LCZ-1/2/3 (compact high/mid/low-rise) which are predominant in the city-centre recorded the strongest average nocturnal UHI intensity of 2.57°C. Not surprising, this same compact LCZs had the highest decrease in the wind intensity (-0.20 m/s) from daytime to night-time. Meanwhile, the highest increase in wind intensity (0.47 m/s) is observed in LCZ-9 (Sparsely built) which corresponds to the weakest nocturnal UHI intensity of 0.32°C. This is expected since the urban-rural thermal gradient is at the highest at night-time because of the thermal properties of the building materials. Additional analysis reveals that the intra-LCZ variabilities of UHI and wind intensity can be explained by the distance to the city centre.

Consequently, the anticyclonic urban breeze circulation on 4<sup>th</sup> July 2004 documented in previous work was represented here on a cartographic map to help urban planners better understand this phenomenon. The map revealed that for the few hours between 15:00 – 18:00UTC there was a NW-SE breeze pattern, with near-surface wind advection from the less built-up northern part of the city, towards the urban centre. This breeze can also accentuate the diffusion of pollution from the industrial campuses in the suburban into the centre especially as the extent of the breeze covers a large portion of the NW-SE mesoscale cross-section.

Finally, the characteristics of the pedestrian wind velocity ratio in relation to the building volume density was analysed. The results revealed that the higher the building volume density per unit area, the lower the velocity ratio at the pedestrian level. Ultimately, this study has proven that city-scale urban climate study can greatly assist urban planning professionals design and make data-driven decisions that will lead to more sustainable future cities.

## ABSTRACT (Finnish Version)

Rakentaakseen asuttavia, kestäviä ja ilmastoresponsiivisia kaupunkeja muuttuvien kaupunki-ilmastojen aikana, tulee kaupunkisuunnittelijoiden ymmärtää paikallisia urbaaneja ympäristöjä niiden koko kompleksisuudessaan. Koska kaupungin yli puhaltava pääasiallinen tuulivirta määrittää merkittävästi urbaanin lämpösaarekkeen (ULS) intensiteettiä, on tärkeää ymmärtää tuulen liikettä kaupungin sisällä. Luonnollisen tuulen liikkuvuuden säätely on yksi energiatehokkaimmista strategioista kaupungin lämpötilan kokonaistason parantamiseksi.

Tässä tutkimuksessa käytettiin Paikallisen Säätötyypin (PST) luokittelujärjestelmää spatiotemporaalisen ilmavirta-analyysin suorittamiseksi Tolousin metropolialueella Ranskassa, kuivien ja lämminten kesäkuukausien aikana vuonna 2004. Aineistona olivat kaupungin tietokannat sisältäen kaupungin pintaominaisuudet sekä tuulisimulaation tulokset mesoskaalan ilmastomallissa Meso-NH horisontaalisella tarkkuudella 250 m x 250 m läpi kaupungin. Simulaatio tuotti kaupunginlaajuista ilmavirta-aineistoa 10 metriä Toulousin rakennuskorkeuden yläpuolelta. Tämä edustaa Toulousissa vallitsevaa tuulitilannetta. Tuulten kvantitatiivisten ominaisuuksien määrittämiseksi käytettiin keskiarvoihin ja frekvensseihin pohjaavia menetelmiä R:ssä. Tulokset osoittivat frekvenssien katografisten karttojen näyttävän suurempaa yksityiskohtaisuutta tiheästi rakennetun kaupunkikeskustan selväpiirteisistä muodoista. Lisäksi keskiarvoanalyysi yliarvioi päiväajan tuulennopeuden 1–2 m/s kaikilla paikallisilla säätötyypeillä. Yöllä molemmat menetelmät näyttävät samansuuruisia nopeuksia idästä länteen, joskin PST-9 oli frekvenssianalyysissä taipuvainen aliarvioimaan tuulennopeuden lentokentän alueella 2 m/s.

Käyttämällä kaupungin rakennettua morfologiaa kuvailevaa paikallisten ilmastovyöhykkeiden (PIV) luokittelujärjestelmää pyrittiin ymmärtämään yöllistä ULS:en vaihtelua PIV:den välillä suhteessa tuulen intensiteettiin. Tulokset osoittivat, että tiiviit LCZ-1/2/3 -rakennukset (tiiviit korkeat/keskikorkeat/matalat rakennukset) jotka ovat vallitsevia kaupungin keskustassa, osoittivat suurimman 2.57°C keskimääräisen yöllisen ULS-intensiteetin. Kuten odottaa saattaa, tällä samalla kompaktilla LCZ:lla oli myös suurin lasku tuulen intensiteetissä (-0.20 m/s) päivästä yöhön siirryttäessä. Toisaalta suurin nousu tuulen intensiteetissä (0.47 m/s) havaittiin vyöhykkeellä LCZ-9 (harvaan rakennettu), jossa oli heikoin yöllinen ULS-intensiteetti (0.32°C). Tämä oli odotettavissa, sillä urbaani–ruraali lämpögradientti on rakennusmateriaalien lämpöominaisuuksien vuoksi yöllä korkeimmillaan. Lisäanalyysit paljastivat että PIV:den sisäinen ULS -vaihtelu ja tuulen intensiteetti voidaan selittää etäisyydellä kaupungin keskustasta.

Näin antisykloninen kaupunkituulen kierto neljäs heinäkuuta 2004, joka on dokumentoitu aiemmassakin tutkimuksessa, on tässä työssä esitetty kartografisella kartalla kaupunkisuunnittelijoiden ilmiötä koskevan kasvavan ymmärryksen mahdollistamiseksi. Kartta osoitti, että muutaman tunnin ajan 15:00–18:00UTC, tapahtui koillinen–lounas -tuulikaava pinnanläheisellä advektiolla kaupungin vähemmänrakennetulta pohjoisosalta kohti kaupungin keskustaa. Tuuli saattoi myös painottaa saasteen diffuusiota lähiöiden teollisuusalueilta kohti kaupungin keskustaa, erityisesti kun tuulen mittakaava kattoi suuren osan koillinen–lounas poikkileikkauksesta mesomittakaavalla.

Lopuksi analysoitiin ominaisuuksia jalankulkijatuulen nopeudesta suhteessa rakennustiheyden volyyymiin. Tulokset osoittivat, että mitä suurempi rakennustiheyden volyyymi yksikön aluetta kohti, sitä pienempi nopeussuhdanne jalankulkijoiden tasolla. Tämä tutkimus on osoittanut, että kaupunkimittakaavan ilmastotutkimus voi merkittävästi opastaa kaupunkisuunnittelun ammattilaisia paremmin suunnittelemaan ja tekemään tietoon pohjaavia päätöksiä jotka johtavat kestäväen kehityksen tulevaisuuden kaupunkeihin.

## DEDICATION

*This piece of work is dedicated to the blessed memories of my Dad, **Late (Mr) Augustine Ojo Ibitolu**, and my two cousins: **Late Motunrayo** and **Late Iyanuoluwa Ibitolu**.*

## ACKNOWLEDGEMENTS

All glory and honour be to the lord most high for his unwavering grace in my life and through whom all knowledge spring-forth. May his name be praised both now and forever, amen. My sincere appreciation goes to the European Commission under the Erasmus Mundus Joint Masters programme for providing the funding for me to undertake this degree as part of the inaugural cohort for the Joint Master of Urban Climate and Sustainability (MUrCS). I will be forever grateful for this life-changing opportunity. With a grateful heart, I acknowledge the immeasurable support of Prof Rohinton Emmanuel and Dr Eeva Aarveaara for your guidance and always going all out to make sure we have the best of experience in this 2-years journey. Also, special thanks go to my supervisors (Prof. José Enrique García Ramos and Dr Caroline Gallagher) and all the staff affiliated to the MUrCS programme. I cannot thank you all enough.

I wish to express my deep gratitude to Dr Julia Hidalgo for her support during my internship placement at the LISST-CIEU Laboratory in Toulouse, it was through her professional guidance this thesis came to fruition. Also, I appreciate the suggestions from Dr Robert Schoetter (Meteo-France) and Renaud Jouglu for helping me with my R script. I am thankful to the community members of Stack Overflow whose extensive archive of information and forum support greatly helped me to troubleshoot my script and enabled me to significantly improve my programming skills and R statistics knowledge during the course of this project.

To my family; my mum, and my Uncle, Engr. and Mrs M.B. Ibitolu. I thank you for all the sacrifices you have made, and for your spiritual and emotional support. I pray for a sound health and long life for you to reap the fruits of your labour. A special thanks to my siblings; Seun, Ayo and Victoria, and to my cousins; Femi, Biodun, Tunde, and my great friend-brother, Festus. You all are very dear to me and I remain indebted to you for your prayers and love.

And finally, I am especially grateful to my classmates, those with whom I have journeyed this past two years together as the first set of the MUrCS programme. I appreciate you all for electing and entrusting me with the responsibility to co-represent your interest despite having only spent a week together. I am sincerely thankful for this. Particularly, I thank Samira, Marina (my newfound Pakistani sisters) and Mahmudul – the times we shared together are the memories that makes us more like family than classmates. Thank you all for making every second of this whirlwind journey a once a lifetime unique experience. Our paths have crossed for good, and my heart is overwhelmed with emotions to say goodbye, but I wish you all the very best.

Cheers to a greater height in no distant future, as we work to make the world a more sustainable and liveable place for everyone!

# TABLE OF CONTENTS

<b>1. INTRODUCTION .....</b>	<b>1</b>
1.1 BACKGROUND.....	1
1.2 PROJECT OUTLINE .....	3
1.2.1 <i>Project Overview</i> .....	3
1.2.2 <i>Research Question</i> .....	3
1.2.3 <i>Aim and Objectives</i> .....	3
1.2.4 <i>Description of Study Area</i> .....	4
1.2.5 <i>Report Structure</i> .....	6
<b>2. LITERATURE REVIEW .....</b>	<b>7</b>
2.1 WIND FLOW PATTERN AND UHI .....	9
2.2 LOCAL WEATHER TYPES (LWT) CLASSIFICATION APPROACH .....	11
2.3 LOCAL CLIMATE ZONE (LCZ) CLASSIFICATION.....	13
2.4 BRIEF DESCRIPTION OF CONCEPTS.....	14
<b>3. METHODOLOGY .....</b>	<b>17</b>
3.1 OVERVIEW OF DATASET.....	17
3.1.1 <i>Atmospheric Data</i> .....	17
3.1.2 <i>Surface/Urban Dataset</i> .....	19
3.1.3 <i>Software used</i> .....	20
3.2 DESCRIPTION OF METHODS.....	21
3.2.1 <i>Statistical Evaluation</i> .....	21
3.2.2 <i>GIS Analysis</i> .....	24
3.2.2 <i>Methodology Framework</i> .....	26
<b>4. RESULTS AND DISCUSSION .....</b>	<b>27</b>
4.1 MEAN WIND ANALYSIS VS MOST FREQUENT WIND ANALYSIS.....	27
4.2 VARIATIONS IN WIND INTENSITY AND NOCTURNAL UHI INTENSITY ACROSS BUILT LOCAL CLIMATE ZONES (LCZs) IN TOULOUSE .....	31
4.3 VISUALIZING URBAN BREEZE CIRCULATION IN TOULOUSE .....	34
4.4 WIND VELOCITY RATIO ANALYSIS.....	36
<b>5. CONCLUSIONS .....</b>	<b>42</b>
5.1 SUMMARY OF RESULTS.....	42
5.2 IMPLICATION OF THIS STUDY .....	44
5.3 LIMITATIONS OF THE STUDY .....	44
5.4 RECOMMENDATIONS FOR FUTURE RESEARCH.....	45
<b>6. REFERENCES.....</b>	<b>46</b>
<b>APPENDIX .....</b>	<b>54</b>



## LIST OF FIGURES

FIGURES	DESCRIPTION	PAGE
Figure 1:	Location Map of the Study Area with the various communes .....	5
Figure 2:	Climatological data for Toulouse (1981-2010) .....	5
Figure 3:	Typical Temperature Profile across an UHI .....	8
Figure 4:	3D model of UHI and wind speed under various cloud conditions .....	9
Figure 5:	Built Local Climate Zone Classification .....	13
Figure 6:	Representation of the urban-breeze circulation in a hinterland city.....	15
Figure 7a:	Main urban ventilation corridors at the city level and the regional level .....	15
Figure 7b:	Main and secondary urban ventilation corridors at the district and the city level..	16
Figure 8:	The grid points of the atmospheric simulation domains (250 m x 250 m) .....	18
Figure 9:	Three scales of urban building morphology.....	20
Figure 10:	Screenshot for the R script used for Step-I analysis phase.....	22
Figure 11:	Screenshot of the R script for converting of U-V wind component to FF-DD....	22
Figure 12:	The Methodology Framework used in the research .....	26
Figure 13a:	Summer day wind characteristics for the mean and frequency approaches.....	27
Figure 13b:	Summer night wind characteristics for the mean and frequency approaches....	28
Figure 14a:	East – West Profile of the wind velocity across the city .....	29
Figure 14b:	Comparison of the East–West Profile of wind velocity (m/s) for the mean and frequency methods for each LWT-7,8,9 during the day and night .....	29
Figure 15:	Comparison of (a) change in wind intensity map between the night-time and daytime, (b) Local Climate Zones re-grouped, and (c) the Nocturnal Urban Heat Island Intensity.....	31
Figure 16:	Distribution of area covered by each of the Built LCZs and Natural LCZs.....	31
Figure 17:	Urban Breeze Situation at 10m above ground in Toulouse Metropole on 4th/July/2004.....	34
Figure 18:	The mean wind velocity ratio at pedestrian level-2m during the daytime (17h - 20h local time) and night-time (03h – 06h local time) across the different local weather type 7, 8 and 9.....	36
Figure 19:	Aggregated mean velocity ratio across all local weather types during the daytime and night with the marked case study areas.....	38
Figure 20:	The Building Volume Density map for Toulouse based on the building unit scale(left) and the RSU scale (right) at 100m resolution.....	39
Figure 21:	Spatial average of wind velocity ratio as compared with the building volume density for the different case studies during the daytime and night.....	40

## LIST OF TABLES

TABLE	DESCRIPTION	PAGE
Table 1:	Number of days of occurrence and brief description of the LWT Clusters.....	12
Table 2:	Summary of all the dataset used in the research.....	19
Table 3:	Adapted Beaufort scale wind classification.....	23
Table 4:	Summary of UHI Intensity and Wind Intensity across the LCZs.....	32
Table 5:	Summary of the velocity ratio for the different local weather types during the daytime and night-time.....	37
Table 6:	Summary of the relationship between building volume density and mean velocity ratio during the day and night.....	40

## LIST OF ABBREVIATIONS

ABL	Atmospheric Boundary Layer
BVD	Building Volume Density
CAPITOUL	The Canopy and Aerosol Particles Interactions in Toulouse
CFD	Computational Fluid Dynamics
DEM	Digital elevation Model
DD	Wind direction
FF	Wind speed
GIS	Geographic Information System
i_H	Building height (i_H)
i_Vol	building volume (i_vol)
ISBA	Interaction between Soil, Biosphere, and Atmosphere Model
IPCC	Intergovernmental Panel on Climate Change
LWT	Local Weather Types
LCZs	Local Climate Zones
LONS	Longitude
LAT	Latitude
MApUCE	Modelling and Urban Planning Law: Urban Climate and Energy project
Meso-NH	Non-hydrostatic Mesoscale Atmospheric Model
PAM	Partitioning Around Medoid
PET	Physiological Equivalent Temperature
REFER	Reference Simulation
RSU	Reference Spatial Unit
SHP	Shapefile
SVAT	Soil-Vegetation-Atmosphere Transfer
SVF	Sky View Factor
TEB	Town Energy Balance Model
UHI	Urban Heat Island
URBINC	Urban Increment Simulation
VRAT	Velocity Ratio
WMO	World Meteorological Organisation

# 1. INTRODUCTION

The urban population of the world has grown rapidly from 751million in 1950 to 4.2 billion in 2018, and over 68% of the world population is projected to live in urban areas by 2050 (United Nations, 2018). This rapid urbanization has significantly turned cities into densely packed urban areas with less greenery, more pollution sources and impervious surfaces. The presence of artificial materials in buildings and public spaces increases the heat storage in the ground layer and building fabrics and contributes to the higher level of air and surface temperature in urban areas compared to their surrounding rural areas (Oke, 1982). This phenomenon is known as “Urban Heat Island” (UHI).

Consequently, cities are becoming more and more densely built-up with compact and high-rise buildings composed mostly in the city-centres and other Central Business District (CBD) where a vast number of the population spend their entire day working. Hence, UHI has become a rising concern to the quality of life within the built urban environments (Wong & Yu, 2005). These effects are evident in the increasing energy use, water consumption, human thermal comfort issues, and various health complications which accounts for the increase in health budget and hospital admissions. Nevertheless, climate change induces warmer summers and more frequent and intense heat waves, thereby increasing human mortality and energy demand for cooling purpose. This is particularly critical in urban areas where climate variables such as temperature, wind and radiation are modified by the urban morphology, the absence of pervious soils and the human activities. As the urban population is projected to grow, it is imperative to understand better how urban growth and design interplays with weather variables, especially wind flow patterns which is critical to making cities cooler.

## 1.1 Background

According to the latest IPCC assessment report, the global climate has warmed by 1°C above the pre-industrial conditions in 2017 (IPCC, 2018), however, land surfaces especially urban environments, are warming faster than water surfaces, thus the locations most relevant to the human population wellbeing are therefore becoming more exposed to frequent heat stress than the global average temperature rise. Meanwhile, countries in southern Europe and the Mediterranean basin are particularly vulnerable to a rise in climate change extreme events. No event made this more apparent in France, than the 2003 heatwave, which saw around 15000 heat-exposure-related deaths in France, and about 70000 deaths across Europe(Watts *et al.*, 2018). Sadly, in summer 2019, this extreme weather was repeated, but at greater intensity, as the southern commune of Gallargues-le-Montueux recorded France’s highest ever temperature

of 45.9°C breaking the previous 2003 record of 44.1°C. Not surprising, more than 50 French cities exceeded their previous high temperature records in the 2019 heat wave (WMO, 2019).

The existence of the local heat island effect and the characteristics of existing urban morphology and the kinds of building materials that traps heat for longer period makes urban areas in Europe more vulnerable to the regional heat extreme events. Hence, it is important to understand how the morphology of urban environments affects Urban Heat Island generation and dynamics. Furthermore, data on weather and climate, air quality and energy use are valuable for the decision-making process of urban infrastructure planning and development. Consequently, factors such as temperature, humidity, and wind velocity all play a key role in human comfort (Stathopoulos, Wu & Zacharias, 2004), but are often ignored during planning due to its unavailability or cost of measurement, and lack of communication between urban planners and climate experts (Eliasson, 2000).

Additionally, urban development itself can have a significant effect on the surrounding microclimate (Rajagopalan, Lim & Jamei, 2014a) since some common building materials trap heat, causing urban heat islands to form (Akbari, Pomerantz & Taha, 2001) and likewise humidity is typically lower during the day compared to the exterior suburban vegetated areas (Eliasson, 2000). Over the last few decades, significant progress has been made to associate the properties of urban surfaces to the atmosphere. Despite this, huge gaps still remain in our understanding of these processes, but it is generally recognized that the outstanding issue for urban climate science is the need for knowledge transfer from urban research into urban decision-making (MAPUCE, 2016). Unfortunately, most urban planners do not have the required knowledge to quantify the effect that different urban planning scenarios could have on UHI intensity. For instance, a survey to which 25 French urban planning agencies answered showed two major limitations that inhibit the adoption of climate sensitive building topics to be considered in the everyday planning strategies; the first limit is linked to the lack of knowledge of these actors on these important topics, while the second is the lack of pertinent data (MAPUCE, 2019).

Therefore, it is pertinent that necessary climate data analysis is made available to assist urban planners to better understand this crucial topic, thereby informing the development of a broad climate sensitive planning framework. However, for this case study based on the city of Toulouse in France, attempts will be made to push these limits back by analysing the wind regimes on the city-scale, in addition to understanding “how and to what extent wind flow can exert effects on regulating the Urban Heat Island dynamics in the context of Toulouse city”.

## 1.2 Project Outline

The purpose of this section is to summarise the project goals, give a description of the study area and outline the motivated research questions.

### 1.2.1 Project Overview

This project involves quantitative statistical analysis using R and geo-analysis from various sources. It explores the potential of the mesoscale atmospheric numerical model MésosNH-SURFEX simulation output at 250x250m of horizontal resolution to identify wind characteristics in summer 2004 from the microclimatic point of view, while also accessing the plurality of weather representative of the local climate of Toulouse using the Local Weather Type approach (Hidalgo, Julia, Masson & Baehr, 2014). The later stages involved the evaluation and visualization of the statistical results obtained in a Geographic Information System (GIS) environment using QGIS to understand the relationship of wind characteristics with urban heat island dynamics.

### 1.2.2 Research Question

The hypothesis of this research is highlighted in the research questions below:

- “Does the wind (velocity and direction) dynamics have any influence on the night-time Urban Heat Island (UHI) intensity in relation to the urban morphology of Toulouse?”
- If so: “What magnitude of influence does these wind characteristics (wind corridors, urban/slope breeze etc.) exert on the Urban Heat Island (UHI) intensity in the city of Toulouse?”
- “How well can we display/visualize city-wide mesoscale wind simulation output data of Toulouse?”

### 1.2.3 Aim and Objectives

Wind flow in urban centres are generally warmer with weaker speed than in the rural/suburban due to the blockage of high-rise buildings and the surface roughness (Yim, Fung, Lau & Kot, 2009). The UHI mitigation strategies suggested by Santamouris et al. (2016) includes using cool materials with higher albedo on buildings & pavements, the use of green systems- such as trees, hedges, shrubs and grasses in cities, and the introduction of water bodies, such as lakes, fountains and ponds. However, wind ventilation corridor is a viable approach to introduce cooler wind into built areas, which can help reduce urban temperature and mitigate the urban heat island effect. The corridor is a function of urban forms, previous

studies mainly focus on wind ventilation around isolated buildings or just a small cluster of buildings.

Therefore, the overall goal of this research is to explore how and to what extent the wind dynamics can exert effects on modulating the Urban Heat Island intensity on a city scale for urban planning and recommendation purposes in the context of Toulouse, France. This new knowledge will be integrated in the Geographical Information System software QGIS in order to make it easily available to researchers working with urban issues as well as urban planners. Thus, to achieve this goal, the Meso-NH numerical simulation model output and the Local Weather Types (LWT) classification approach will be used with the following objectives:

- Identification and characterization of wind pattern in the city;
- Analysis and visualization of the daytime urban breeze circulation (Hidalgo, J., Pigeon & Masson, 2008; Hidalgo, J., Masson & Pigeon, 2008) from the Meso-NH model output;
- Assessment of the relationship between wind intensity and nocturnal UHI characteristics across various urban morphology in the city;
- Visualization and Cartographic representation of the wind analysis from the MApUCE urban/surface database.

#### **1.2.4 Description of Study Area**

For this project, the city of Toulouse was selected as the study area due to the availability of the weather types data acquired during the CAPITOUL experiment (Masson *et al.*, 2008) and the data simulation output from the Meso-NH atmospheric model. Toulouse is situated in the South-West of France at 80km north of the Pyrenees mountain range, 150km west from the Mediterranean Sea and 250 km east to the Atlantic Ocean as shown in Figure 1.

The climatological data according to the current WMO climatological normal period (1981-2010) at the Toulouse-Blagnac station is given in Figure 2. The relief is marked by the convergence of the Garonne affluent valleys. The minimum and maximum height is approximately 102m and 273m respectively (MAPUCE, 2016). On a regional level, the city of Toulouse exerts a notable influence on the surrounding territory. Once the capital of the region of Midi-Pyrenees, the city is now, as a result of the territorial reform of 2014, the capital of the large region of Occitanie (Zimmermann & Feiertag, 2017).

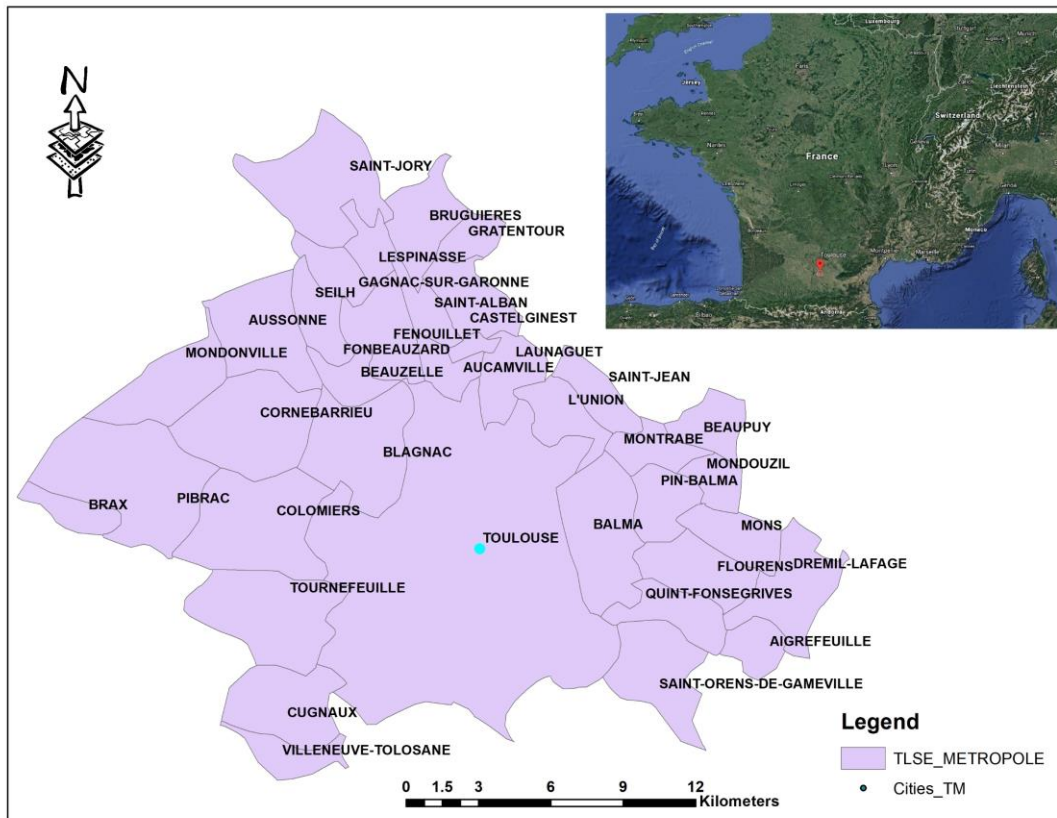


Figure 1: Location Map of the Study Area with the various communes

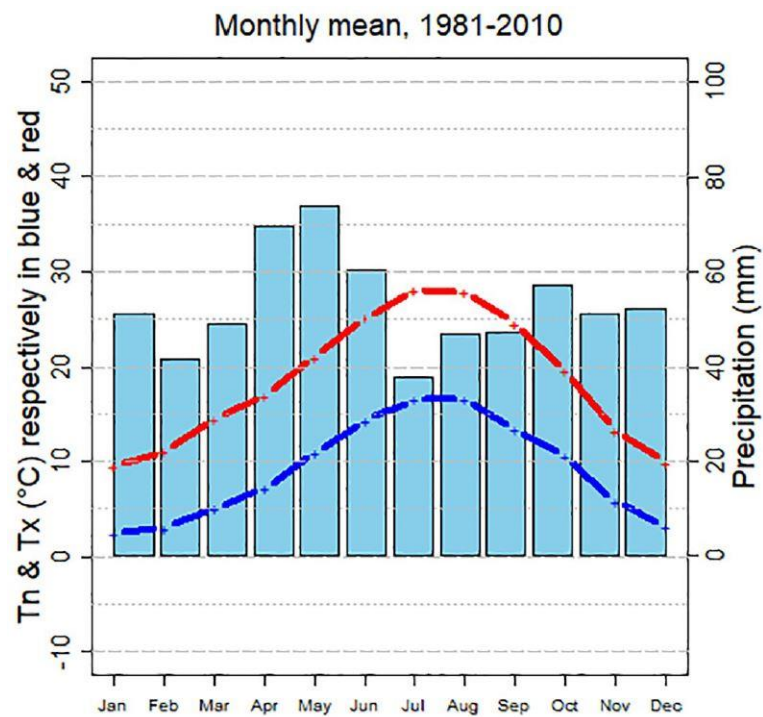


Figure 2: Climatological data for Toulouse (1981-2010)  
Source: Météo-France



However, Toulouse is the fourth-largest city in France (after Paris, Lyon and Marseille) with a population of about 800,000 occupying 1175 km<sup>2</sup>; its large surface area is comparable to that of Paris but with one tenth the number of inhabitants making Toulouse one of the least dense cities with density of 1665 hab/km<sup>2</sup> in 2016. The old downtown has an area of approximately 3.5 km<sup>2</sup> with relatively homogeneous building height (approximately 20m) and construction materials composed mostly of red brick walls and tile roofs (Masson *et al.*, 2008). The city has few polluting industries, the main economic activity being mainly space and aeronautics.

### 1.2.5 Report Structure

The layout of this dissertation as to how the remaining sections are outlined, are described in more details in this section. The report underwent the following structure:

- Literature Review
- Methodology
- Results and discussions
- Conclusion, recommendation, and direction for future work

Section 2 presents the Literature Review, which discusses the previous related research in this field. It covers the literatures in the areas of Urban Heat Island investigations, wind flow analysis and urban building geometry. This analysis of research papers gave an insight of what prior research has covered and thus identified research/knowledge gaps.

Section 3 explains the various technical methods implemented for the data analysis to achieve the aim of the project. It describes the different dataset used, and the step-by-step methods were summarized in the methodology framework.

Section 4 presents the results of the analysis in maps, graphs, and tables. Also, it compares these results to previous published work, and discusses similarities and differences.

Section 5 concludes the dissertation by summarizing the findings to complete the ambiguity in research. Further, it proposes some recommendations and direction for future work.

## 2. LITERATURE REVIEW

In recent years, urban climate literatures have been composed of studies aimed at understanding and modelling the thermal characteristics of the main urban phenomena: the “Urban Heat Island (UHI)”. The UHI effects has been well documented as a consequence of anthropogenic activities, posing significant challenges to urban livelihood and ecosystems services. However, cities are significantly warmer than the surrounding rural areas since the urban morphology and their artificial surfaces have varying radiative and aerodynamic characteristics, which modifies the surface energy balance and interact with the local circulation pattern. There are two factors affecting the occurrence and intensity of heat island in an urban environment, and this can be broadly classified into two categories; first category is the meteorological factors including wind speed and direction, relative humidity and air temperature; the second category is urban design factors, such as density of built up areas, aspect ratio of urban canyons, sky view factor (SVF) and construction materials (Rajagopalan, Lim & Jamei, 2014b).

A first compilation on investigations of Urban-Induced Rainfall was made by (Shepherd, 2005) and the potential of remote sensing on urban climate studies was demonstrated by (Voogt & Oke, 2003). Nevertheless, cities undergo more frequent short and intense rainfall, less cloud coverage, earlier dissipation of morning fog and lower relative humidity (He, 2018). These climatic factors are the causes of various problems including deteriorated air quality, increasing energy consumption and higher rates of mortality and morbidity (Santamouris, M. *et al.*, 2017; Santamouris, Mat & Kolokotsa, 2016). These problems are indication that traditional planning approach is no longer suitable for the creation of safe, reliable and resilient built community. Hence, there is an urgent demand for creative and innovative planning strategy, where the performance-based planning that has been argued as an alternative may allow urban planners and decision makers to tackle urban climate problems (Frew, Baker & Donehue, 2016).

Within the city, there are diverse structures of urban morphology, and these has been attributed as an explanation for variations of urban climate (Adolphe, 2001; Edussuriya, Chan & Ye, 2011; Stewart & Oke, 2012). It is important to clearly describe interactions between urban morphology and climatic conditions (Wang, Li & Hang, 2017). For instance, Adolphe (2001) developed a spatial model to standardize the complexity of urban morphology and the variety of climatic conditions. Particularly, for urban temperature, Stewart and Oke (2012) defined the local climate zones (LCZ) to differentiate generic temperature patterns over city fabrics.

Furthermore, UHI occurs both during the day and at night (Figure 3), but the maximum intensity of heat island is felt 3–5 hours after sunset(Oke, 1987), because the urban features such as asphalt roads, buildings, and other structures retains much of their heat longer.

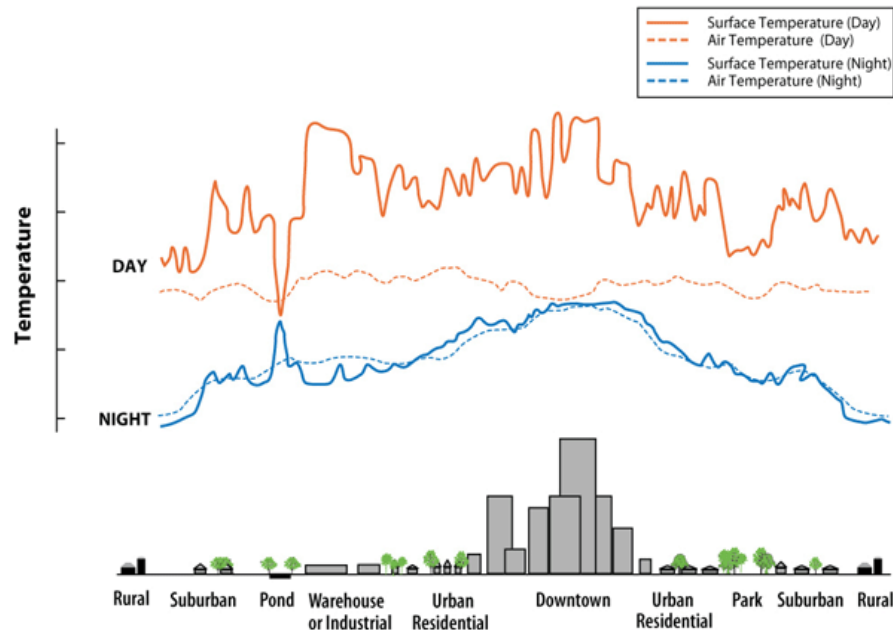


Figure 3: Typical Temperature Profile across an UHI. Source: Wijeyesekera et al., 2012

Several studies have been undertaken to investigate the heat island effect by various methods in climatic characteristics (Santamouris, M. & Georgakis, 2003; Santamouris, Mat, 2011). During the cold winter seasons, urban heat island maybe considered an asset, since it helps in reducing the energy needed for heating purposes. On the other hand, in a very warm summer, heat island becomes a liability since it causes further reliability on air conditioning systems and thus higher energy use. Meanwhile, in comparison with similar cities on the same latitude, the UHI in Toulouse is more intense during the night-time than during day-time and more intense in summer and winter than in spring and autumn (MAPUCE, 2016) . The UHI intensity increases from February to August and then it diminishes from September to January with a maximum of intensity from June to September and a minimal extension during winter-time (Pellerin et al., 2007).

Consequently, the application of air conditioning itself will increase the outdoor temperatures by emitting the excess heat to the urban air and more cooling will be required(Baker *et al.*, 2002). Nevertheless, urban wind flow, have great implications on energy efficiency (Shirzadi, Naghashzadegan & A. Mirzaei, 2018), urban pollutant dispersion (Hang & Li, 2011), outdoor thermal comfort (Niu *et al.*, 2015) and it has widely been reported to have lessened the intensity of heat island effect in urban areas (Kim & Baik, 2002; Memon & Leung, 2010; Morris, C. J. G., Simmonds & Plummer, 2001).

## 2.1 Wind Flow Pattern and UHI

Understanding the relationship between urban forms and wind induced airflow is important, particularly in a changing climate and the ever-increasing population growth and urbanization. Generally, winds are categorized into three groups depending on the intensity of the built environment: isolated roughness flow, wake interference flow and skimming flow which are classified by the ratio ( $H/W$ ) of building height ( $H$ ) to the distance between building arrays ( $W$ ) (Oke, 1987).

Wind velocity is an important parameter in urban environment influencing the air quality, health, outdoor/indoor comfort and the energy consumption of buildings (Memon & Leung, 2010; Rajagopalan, Hien & Wai David, 2008; Yang & Li, 2011). Wind provides cooling effects that helps to mitigate the adverse effects of heat island on the environment and human thermal comfort. For example, within the tropics, a wind velocity of 1–1.5 m/s can create cooling effect which is equivalent to a 2°C drop in temperature (Erell, Pearlmutter & Williamson, 2011). With appropriate wind induced airflows air pollution in cities can be dissipated (Kato & Huang, 2009).

Wind pattern is affected by building height and orientation (Rajagopalan *et al.*, 2014) and according to Roth (2013), wind speed exerts a strong control on the magnitude of heat island, which tends to be larger under weaker wind regimes (Figure 4).

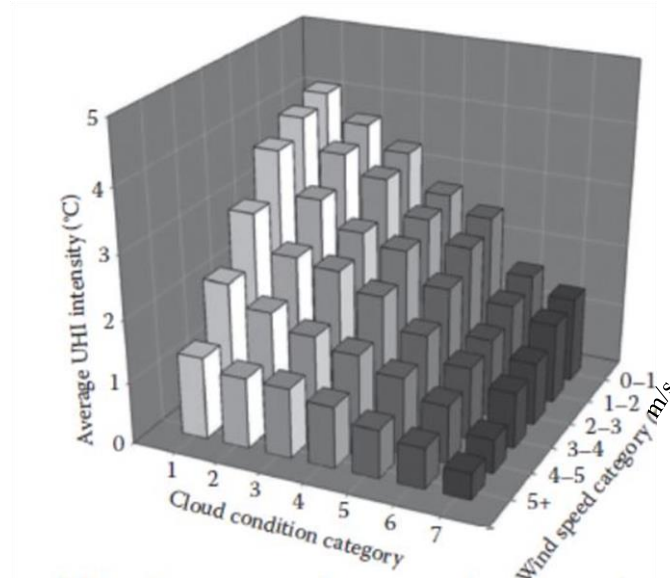


Figure 4: 3D model of UHI and wind speed under various cloud conditions (Source: Roth, 2013)

Several studies have investigated the role of urban geometry on microclimate. Investigations by (Shashua-Bar, Tzamir & Hoffman, 2004) revealed that areas with shallow open spaces and wider spacing recorded temperatures 4.7°C higher than measurements taken

from a meteorological reference. Surveys showed that higher relative humidity levels are more acceptable by people when there is substantially more airflow (Rajagopalan *et al.*, 2014). However, increasing airflow does not necessarily increase the acceptance of higher temperature levels (Ahmed, 2003). In addition, in a research investigating the relationship between thermal performance and urban morphology, (Golany, 1996) noted that the configuration of a city can assist wind circulation and affects wind velocity which in turn influences the temperature variations. He made clear that morphology of a city directly affects the movement of the wind within it, depending on its design, shape, and orientation of the roads within it.

In an experiment using wind tunnel and CFD simulation, (Zhang, Gu, Cheng & Lee, 2011) examined the wind pattern around different building arrangements. The results showed that maximum wind speed and vortex occur on the windward surface. Also, they found that the pattern of the wind around the buildings is strongly depending on the building geometry and wind direction. Furthermore, in a study by (Morris *et al.*, 2001), which investigated the corresponding relationship between urban heat island intensity, wind speed and cloud cover from a network of monitoring stations in the city of Melbourne. His findings proved that calm winds and clear skies result in increased means of urban heat island values. In summer, he found that an increase of wind speed by 1 m/s causes a 0.14°C reduction in the intensity of heat island. It was also revealed that, by increasing the cloud cover by 1 okta, UHI decreases by about 0.12°C.

In summary, an extensive review of literatures available in the field of urban microclimate and the impacts of building geometry and urban forms highlights few investigations relating UHI to urban planning and morphology on a city scale (Taleb & Abu-Hijleh, 2013). Many studies provide strong evidence and findings which are limited to building-to-building relationships, defined as different ratios (Abreu-Harbich, Labaki & Matzarakis, 2014; Giannopoulou *et al.*, 2010; Hwang, Lin & Matzarakis, 2011) Therefore, the goal of this dissertation is aimed at attempting to bridge this gap in city-scale urban climate research related to urban planning using the Local Weather Types (LWT) classification and how different urban morphology may impact temperature and wind variations.

## 2.2 Local Weather Types (LWT) Classification Approach

This study uses the Local Weather Types (LWT) classification approach for the study area proposed by (Hidalgo *et al.*, 2014); and further studied by (Hidalgo, Julia & Jougla, 2018), which is critical for identifying the plurality of weather situations representative of a place. According to Hidalgo & Jougla (2018), a local weather type refers to the description of the atmospheric situation directly stemming from the analysis of climatic data from the atmospheric boundary layer. Also, the term “local” refers to the atmospheric conditions representative of the background suburban/rural area surrounding the city.

(Hidalgo *et al.*, 2014) used the LWT classification strategy to describe the climate variability of Toulouse and Paris by leveraging on the statistical clustering k-means method for the period 1998–2008, to increase the temporal frequency of atmospheric inputs at an hourly time-step to force existing climate projections like the Soil-Vegetation-Atmosphere Transfer (SVAT) models for use in impact climate studies. Further, the authors ((Hidalgo & Jougla, 2018) pursued this method more thoroughly for the same construction period (1998-2008), by recommending the statistical Partitioning Around Medoid (PAM) method which allows a dissimilarity matrix to be used thereby facilitating the treatment of wind direction as a qualitative variable based on Gower distance as a metric.

Nevertheless, both statistical methods produce similar results, and that is why, the PAM method was the most preferred approach used in the nationally funded MAPUCE project for obtaining the LWT for fifty cities in France (MAPUCE, 2016). The spatial distribution, frequency, length and succession enables the reality of weather conditions over a given land area to be understood and their corresponding consequences for the urban environment. This weather type classification approach is useful because it allows for shifting from a mean climate conditions typically driven by long-term climatic variables to a shorter meteorological time-scales which is a more realistic representation of the daily cycle of the atmosphere and thus have an immediate impact on the human comfort level.

Previous studies have also used the weather types classification approach for urban climate research. For example, (Alcoforado, Andrade & Viera, 2004) applied the weather type classification to better understand tourist’s numbers along the Lisbon coast. For that study, on-site meteorological data were measured during 120 field surveys carried out in summertime in 1994, 1995 and 1996. Two types of indicators of tourist numbers were selected: number of cars parked by the beach, and subjective classification of business by two restaurants/coffee shops. For the same time periods, LWT classification was carried out for each survey based on cloudiness (3 classes) and Physiological Equivalent Temperature-PET indicator (3 classes), thus proving significant correlation between weather types and tourist turnout. Furthermore,

(Cantat, 2004) explored the extent of the Urban Heat Island in the city of Paris according to the weather types intensity, frequency, duration and shape. In that paper, statistical analysis were used to highlight the essential influence of cloud cover and wind on the formation of the UHI and how the corresponding weather types could cause the urban-rural temperature difference to go from 0 to over 10°C.

Cantat (2014), went further to use this method and applied it to 60 meteorological reference stations near urban sites in the whole of France for the period 1991–2010, by including the influence of temperature and precipitation to obtain on an annual basis, 64 possible typologies (four classes for wind, four classes for cloud cover, two classes for temperature and two for precipitation) of weather types. Thus, since every typology is result of a classification, weather types can simply be differentiated according to their “use” (Carrega, 2004). However, (Cantat & Savouret, 2013) went beyond this default structure of this typology to develop a supervised classification module of ‘weather types’ (with free selection from among 12 parameters), thus enabling pertinent subject areas to be focused more precisely.

However, in both studies (Hidalgo *et al.*, 2014; Hidalgo & Jougla, 2018), it was evident that 11 clusters was enough to adequately describe the local weather conditions in Toulouse in terms of the diurnal temperature ranges, precipitation, wind regimes and humidity amplitude. Therefore, in order to achieve the goal of this dissertation, Table 1 summarizes the general LWT overview when applied to a classic urban boundary layer scenario in Toulouse during the CAPITOUL experiment (Feb 2004 and Mar 2005) as detailed in (Masson *et al.*, 2008).

Table 1: Number of days of occurrence and brief description of the LWT Clusters. (Hidalgo & Jougla, 2018)

LWT	Number of days	Brief Description of LWT
0	38	Typical winter day with low rainfall
1	9	Rainy day with less frequent South-Easterly wind
2	25	Autan wind day (Frequent in spring and autumn)
3	91	Day with strong North-Westerly wind typical of intermediate seasons and winter
4	7	Rainy day
5	58	Typical sunny winter day with weak South-Easterly wind
6	15	Cloudy day with strong NW wind and precipitation
7	44	Typical sunny summer day with weak South-Easterly wind
8	51	Typical sunny summer day with Westerly-NorthWesterly wind
9	56	Sunny day, very hot in summer, with North-Westerly wind
10	0	Very heavy rainy day



### 2.3 Local Climate Zone (LCZ) Classification

The local climate zone (LCZ) classification system defines regions of uniform urban and rural morphology types, characterized by a standardized definition of heat island magnitude. In essence, the LCZ system was developed to help to fill a crucial void in UHI research methodology, i.e.- the lack of an accepted global methodology to report heat island observations in the canopy layer, thus allowing the objective comparison of UHI magnitude in cities around the world (Stewart and Oke, 2012).

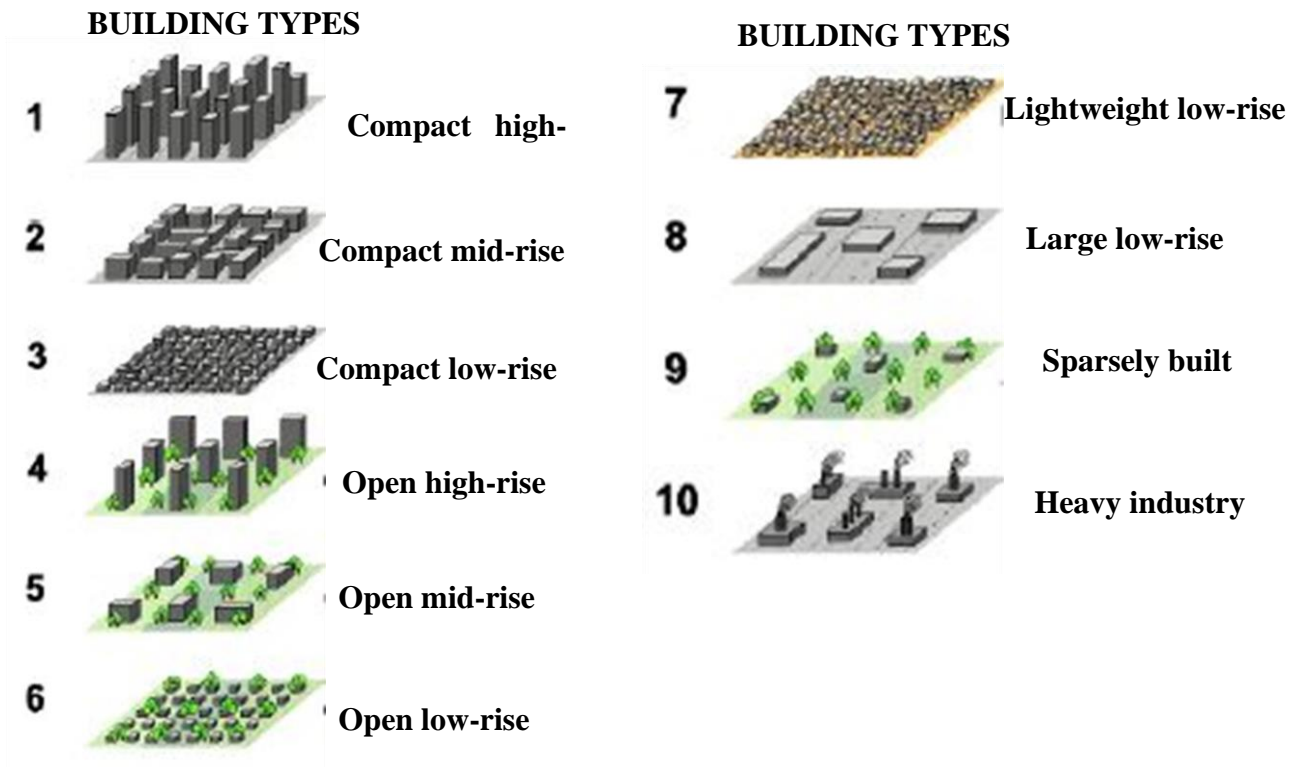


Figure 5: Built Local Climate Zone Classification (Stewart, 2011)

Therefore, the LCZ scheme comprises 10-“built” and 7-“land cover” classes, which are defined as ‘regions of uniform surface-air temperature distribution at horizontal scales spanning hundreds of meters to a few kilometres. The physical surface properties considered include; the sky view factor (SVF), building surface fraction, impervious surface fraction, terrain roughness, surface albedo, and anthropogenic heat flux (Stewart and Oke, 2009). However, in the study the focus will solely be on the built LCZ classes (Figure 5).

Whilst the mapping of LCZ classes should ideally be based on detailed urban morphological data, recent studies have developed new methods based on remote sensing technologies to classify LCZ data for cities in which urban information is not available (Geletic and Lehnert, 2016; and Bechtel et al., 2015). Hence, the inter-LCZ temperature difference could be used to quantify the UHI intensity (Stewart et al., 2014).



## 2.4 Brief Description of Concepts

### - Wind circulation system

The prevailing wind regime in descending order of predominance in Toulouse is characterized by the humid westerly wind from the Atlantic Ocean coupled with a moderate south-easterly wind (mostly strong-Autan wind) from the Mediterranean Sea and finally the southerly wind. Meanwhile, local wind resources and circulation system (including mountain and valley wind, land-sea breeze, lake-land breeze, and urban-rural breeze) can be assessed by using statistical methods and numerical simulations. The expected results should determine prevailing wind directions and obtain the effective time periods and impact areas of these local wind circulations. Toulouse is situated at the crossroads of three types of temperate climates: an oceanic climate influenced by the Mediterranean and continental effect. Therefore, unlike coastal or mountainous cities, due to this peculiar geographic location of Toulouse, it cannot benefit from the cooling brought by the Sea and Valley breeze.

### - Urban Air Stagnation

Urban Air stagnation is a phenomenon which occurs when air flow remains over an area for an extended period either due to natural topography, urban infrastructure blockage or as a result of weaker wind regime. In summertime, air stagnation can cause excessive heat to build up in blocked urban areas especially in the city centre, thus causing UHI to build-up and other heat-related human discomfort. Also, air stagnation and ventilation are used as collective measures of mixing and transport that affect air quality in urban areas.

For this study, due to the coarse resolution of the model output (250mx250m), it is difficult to access the stagnation areas in Toulouse at a city scale, hence, a topographic map (Digital elevation Model-DEM) from the MApUCE project, which is at a finer scale of (25m) will be used instead.

### - Urban Breeze

The difference in the distribution of the surface energy balance (SEB) between the urbanised and rural zones is the key to the Urban Breeze generation. In an anti-cyclonic condition where the winds are moderate, the urban plume can transport the heat from the city centre to the surrounding area (Oke, 2005). If the mean wind speed is low, then an “urban breeze” could develop (Figure 6). The urban-breeze is a closed circulation associated with the UHI and is characterized by a surface convergent flow from the countryside to the city centre and a divergent flow at the top of the Atmospheric Boundary Layer (ABL) (Hidalgo et al. 2008)

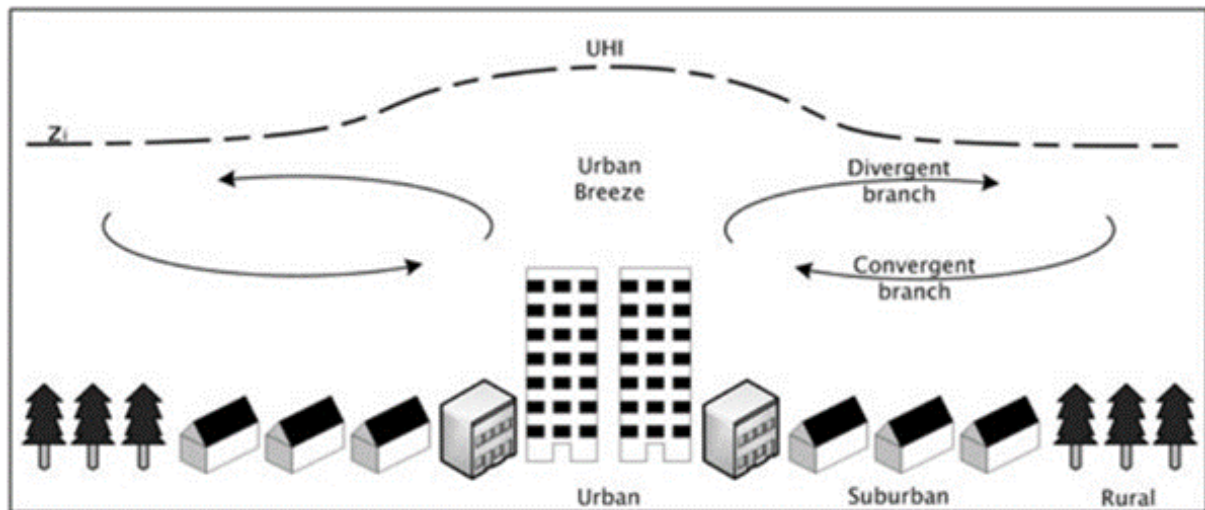


Figure 6: Representation of the urban-breeze circulation in a hinterland city.  
Source: (Hidalgo et al. 2008)

### ➤ Urban Ventilation Corridor

The concept of ‘urban ventilation corridor’ can also be called ‘wind corridor’ originated from the German word “Ventilationbahn” developed by Kress (1979). He suggested that to improve air exchange and ventilation conditions of urban areas, people should consider two important elements, namely the ‘**functioning area**’ and the ‘**compensating area**’, before creating any urban ventilation corridor which serves to link these two areas together to let cool fresh air move more easily within the city centre.

According to the German national guideline ‘Environmental meteorology climate and air pollution maps for cities and regions (VDI 3787-Part 1)’, ventilation corridor (also known as “Ventilation lane”) is the “Area for the mass transport of air near the ground owing to direction, nature of the surface and width.” (VDI, 1997). This wind corridor is shown in Figure 7 (a & b).

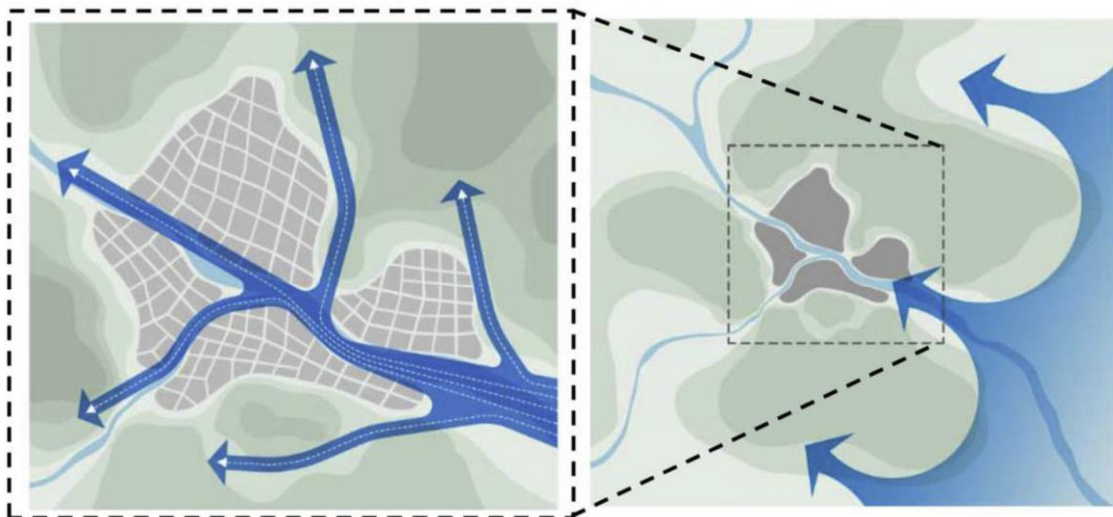


Figure 7a: Main urban ventilation corridors at the city level (left) and the regional level (right).  
(Ren et al., 2018)

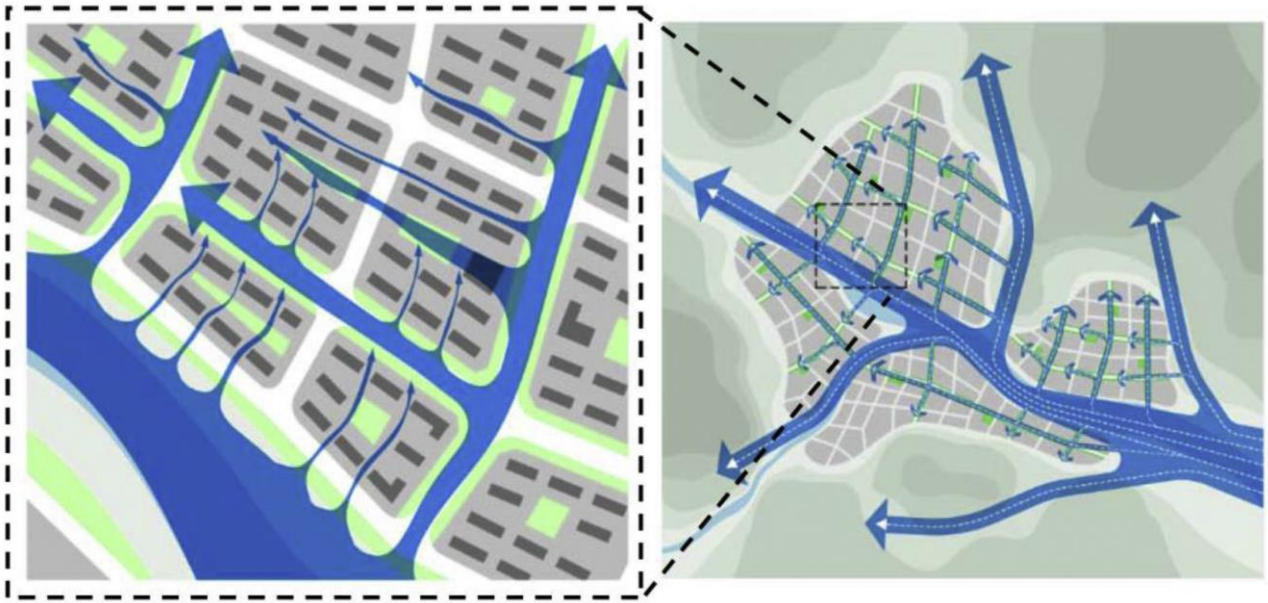


Figure 7b: Main and secondary urban ventilation corridors at the district (left) and the city level (right).  
(Ren et al., 2018)

### 3. METHODOLOGY

The following chapter presents the methodology adopted to achieve the goal of the project. The section starts by describing the different dataset used, and the step-by-step methods implemented for the data analysis were summarized in a flowchart methodology framework. The overarching methodology in this project involved quantitative data analysis which included statistical evaluation of atmospheric data and GIS analysis for visualization.

#### 3.1 Overview of Dataset

The dataset used in this study is primarily divided into 2 different types i.e. the Atmospheric dataset and the Surface/Urban dataset files.

##### 3.1.1 Atmospheric Data

The atmospheric weather data used included the U and V (i.e. the zonal and meridional) wind components at 10m together with the wind velocity ratio (VRat) at 2m pedestrian level derived from the MésoNH-SURFEX atmospheric model output. The simulation output was each collected as hourly wind data from 01-03-2004 to 28-02-2005. In this study, only the summer season (June-August 2004) was investigated. Meanwhile, the simulation data was sub-classified into Constant and Time-Dependent fields. The constant fields included data that stay the same all through the entire simulation process, such as LONS-Longitude, LATS-Latitude, HEIG-Elevation above sea level[m]. On the other hand, the time-dependent wind variables were extracted from two numerical simulation scenarios- Reference (REFER) and Urban Increment (URBINC) situations as described below.

The reference (REFER) numerical simulation scenario was performed such that, the MésoNH-SURFEX model was coupled with the surface scheme - Town Energy Balance (TEB) to simulate the urbanised areas (Masson, 2000) and with the Interaction between Soil, Biosphere, and Atmosphere (ISBA) scheme to simulate natural covers. Consequently, the “urban increment” (URBINC) scenario was also run to estimate the current impact of the blue and green belt within the mixing layer by comparison with the REFER simulation. For this scenario, the natural features were removed (i.e. the vegetated and watered grid box in the ISBA and TEB schemes were replaced with the characteristics of the most common urban land use category in the zone). The grid resolution of the atmospheric data is 250m x 250m horizontal scale within a horizontal domain of 30km x 30km covering the entire communes of the metropolitan area of Toulouse as shown in figure 8;



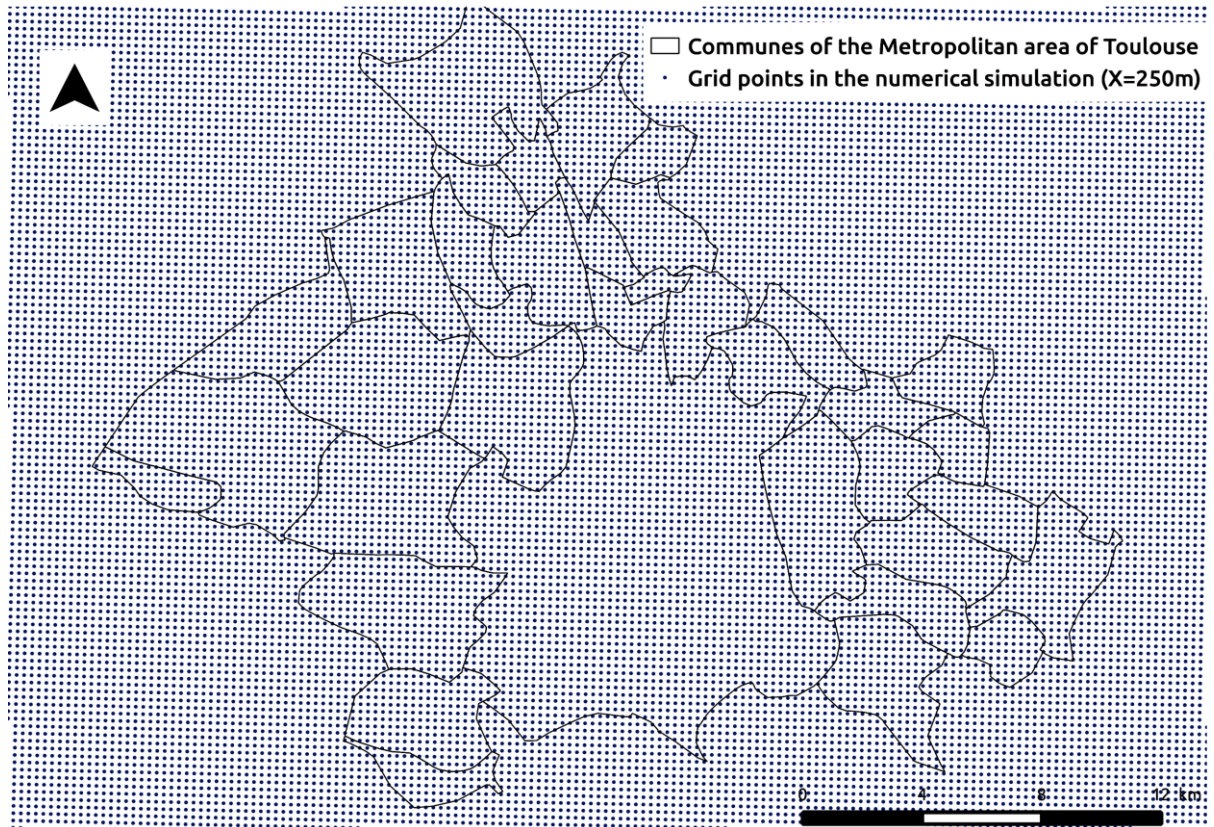


Figure 8: The grid points of the atmospheric simulation domains (250m x 250m). Source: Author

The simulation output data were stored in binary R files with each day of simulation contained in a folder. Each file contains a list named "LST" which contains the array "vals" for constant fields or "vals\_day" for time-dependent fields. The constant fields ("vals") are available as a vector whose length corresponds to the number of grid points (NGRIDPOINTS), while the time-dependent fields ("vals\_day") are stored as arrays with the dimensions (NGRIDPOINTS,24). The 24 values per grid point correspond to the time of day in UTC starting one hour after midnight (1 UTC to 24 UTC).

Furthermore, the local weather type situation for each day (01-03-2004 to 28-02-2005) was stored in a text (.txt) file shown in APPENDIX. However, for this study, only the summertime (June-July-August) weather situations was analysed. According to Hidalgo & Jougla, (2018), LWT - 7, 8 and 9 are the most persistent weather situation during summertime. They represent 85% of summer days in the simulation with an occurrence frequency of 24 days (26%), 37 days (40%) and 18 days (20%) respectively.

### 3.1.2 Surface/Urban Dataset

The surface data was acquired from the MApUCE project urban database which includes the urban data in GIS shapefile (.shp) format and the Digital Elevation Map (.geotiff format) in 25m x 25m resolution. The urban data include the LCZ maps-which shows the different local climate zones across the city land-scape and the UHI maps- showing the night-time temperature as compared to the previous daytime temperature. All these data are summarized in Table 2.

Table 2: Summary of all the dataset used in the research

Atmospheric Data	Time-dependent fields	REFER & URBINC Simulation	U-Wind component V-Wind Component	250m x 250m	01-03-2004 to 28-02-2005
	Constant fields	LONS, LATS, HEIG	VRat - Velocity Ratio		Hourly Summer data was analysed
Surface (Urban) Data	Local Climate Zone Map	The map with the local climate zones across the metropolitan area including the urban and natural surfaces			
	Urban Heat Island Map	For each Local Weather Type situation in the study period [LWT 7, 8, 9]			
	Topography Map	25m x 25m			
	Toulouse Metropole Urban Database with Building information	<div>- At individual building scale (see figure 9)</div> <div>- At the Reference Spatial Unit- RSU scale (See figure 9)</div>			

Where;

REFER: represents the reference simulation

URBINC: represents The urban increment simulation

LONS: Geographical longitude of grid cell center [degrees east]

LATS: Geographical latitude of grid cell center [degrees north]

HEIG: Elevation above sea level [m]

The Toulouse building information dataset used in the study was provided in 2 different scales (Erwan et al, 2018), namely the “building scale” and the “Reference Spatial Unit -RSU”. The RSU is the aggregation of buildings into blocks. Also, any well-defined geographical entity may be used as an RSU, such as the urban block defined by the road network [Lesbegueries et al., 2012]. A block is an aggregation of individual buildings that intersect each other with at least one point in common. All these scales are illustrated in Figure 9.

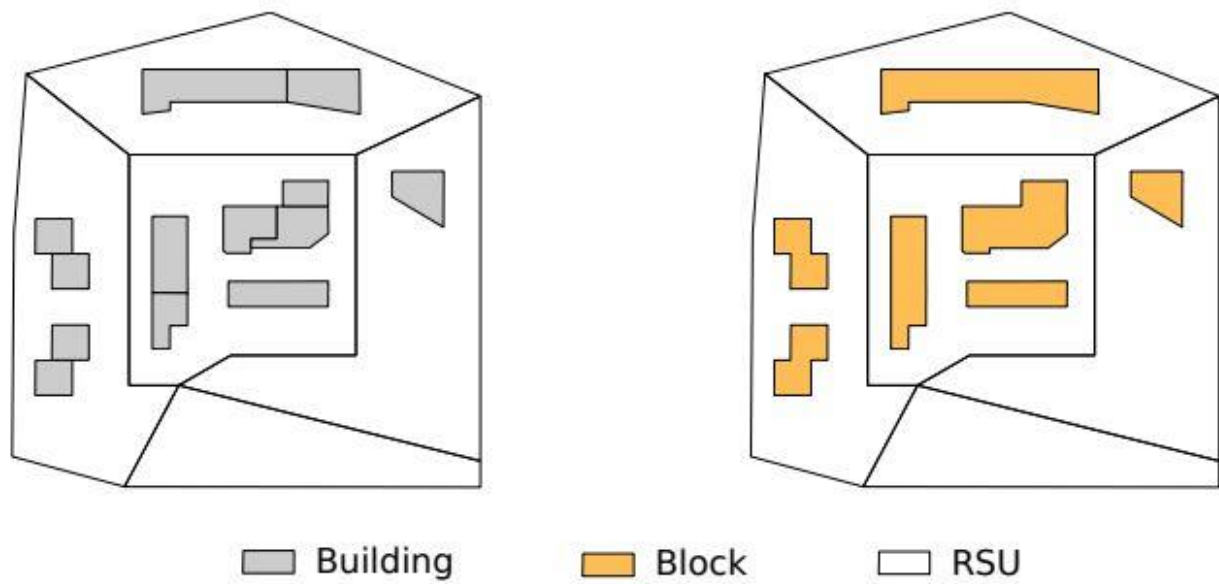


Figure 9: Three scales of urban building morphology (Erwan et. al, 2018)

Nonetheless, each one of these urban form resolutions have their unique pros and cons which makes either of them the best fit based on different urban-based research scenarios. For instance, if a research is aimed at understanding an urban change at a neighbourhood, then the best fit in this case will be the “building scale” which provides a more detailed information at a higher resolution. On the other hand, if a study is aimed at evaluating urban change in a city, or region, the RSU resolution will be the most appropriate. However, in this study, the building information attributes used include building height (*i\_H*), and building volume (*i\_vol*).

### 3.1.3 Software used

The various software used in this thesis research include; *R Studio*- which is the programming package used for writing and running the R script in the statistical analysis methodology, while both *QGIS* and *ArcGIS* software were used for the GIS visualization and geo-analysis. Lastly, *Microsoft Excel* was used for plotting the graphs in this study.

## 3.2 Description of Methods

The methodology executed in this study involved both the statistical evaluation of the Meso-NH model data and GIS post-analysis for cartographic visualization purpose. However, it should be noted that the reason for using this methodology in this study was mainly due to the type of available dataset in order to visualize the wind characteristics in the city.

### 3.2.1 Statistical Evaluation

The main goal for implementing the statistical evaluation method is to read-in the binary files and make sense of the data by processing and producing a map from the MésóNH-SURFEX model for each simulation scenarios. To do this, the methodology for the statistical evaluation was carried out in two phases:

- Wind Preparation Phase
- Wind main Analysis Phase

#### ➤ Wind Preparation Phase

The goal of this phase is to write the script that will read-in the hourly wind simulation file (VRat, U and V components), identify the days that each local weather types (7,8,9) occurs from the LWT (.txt) file and then combine these two subroutines to extract the hourly Velocity Ratio and the U-V components for each day of occurrence of LWT 7, 8, 9. Given that the goal of this study is to access how wind dynamics impacts urban heat island effects with respect to urban characteristics during the summer season when UHI is more prominent. Hence, the focus was to extract those days in summer when LWT7, 8 and 9 occurs.

Specifically, in order to access the day\_time and night\_time wind characteristics, 36 hours was extracted for each day, such that 12 hours after each day was included to signify the night\_time wind effect due to the prior day\_time). The result of this phase was outputted into a (.txt) file for each LWT, which then served as input for the second phase.

However, the R file was read using the freely available R program (R team, 2019) with the script command shown in equation 1a and 1b below:

```
load(file="inputfile")  
vals=LST$vals    (for constant fields)           [1a]  
or
```

```
vals_day=LST$vals_day (for time-dependent fields) [1b]
```

Nevertheless, the full R script written for this phase is attached in the APPENDIX.

#### ➤ Wind main Analysis Phase

The aim of this second phase is to read in the hourly wind data (.txt) file derived from previous phase one, and thereafter carry out various analysis on it. In this phase, two distinct procedures were analysed i.e. Mean\_Analysis and Frequency\_Analysis approach.



The mean-analysis was implemented in other to evaluate the average wind characteristics per day for each day of the specific local weather type. While the frequency analysis was also applied so as to access the most frequent wind characteristic per day for each day of the local weather type. The following paragraphs details the step-by-step methodology:

#### ○ **Step I - Reading in the data into a variable**

The first major step is to read in the 36-hourly wind data file derived from phase one. This file is stored in a variable “data\_temp” as shown in figure 10 below;

```
#####
print(" Step 1 - Reading the data into a variable")
Data_variab = c('UMME', 'VMME')

for (d in 1:length(Data_variab)) { # for each variable
  Data_var = Data_variab[d]
  print(Data_var)

data_temp <- read.table(file=paste('results/data_main/TT_',tt,'/sais_',sais,'/36hours_', Data_var,'_TT',tt,'_sais',sais,'.txt',sep=''))
}
```

Figure 10: Screenshot for the R script used for Step-I analysis phase

#### ○ **Step II - Extracting the required time interval**

This step involves extracting the required time interval for the day\_time and night\_period. Hence, in this study, the aim is to evaluate the wind data between the time interval:

15h -18h GMT (i.e. 17h - 20h local time) ---> to represent the day\_time,

01h -04h GMT (i.e. 03h – 06h local time) --> to represent the night\_time

#### ○ **Step III – Calculating the Mean or Frequency**

The average wind characteristics (VRat, U and V components) within the time interval for each LWT was calculated for the mean analysis approach. While the frequency of occurrence of the wind characteristics per day for each LWT was also evaluated.

#### ○ **Step IV – Converting the U-V components into speed and direction**

In this step, the mean U-V components derived from previous step was converted into the wind speed (FF) and wind direction (DD) using a function written for that purpose. The R function script is attached in figure 11 below

```
ffdd2uv = function(FF,DD) {
  u = -FF*sin(DD*pi/180)
  v = -FF*cos(DD*pi/180)
  return(list(u,v))
}

uv2ffdd = function(u,v) {
  FF = sqrt(u^2+v^2)
  theta = ifelse(v>=0,180,ifelse((u<0 & v<0),0,360))
  DD = (atan(u/v))*(180/pi)+theta
  return(list(FF,DD))
}

#####
#### END ####
#####
```

Figure 11: Screenshot of the R script for converting of U-V wind component to FF-DD

○ **Step V – Wind Threshold Classification**

For the purpose of a cartographic visualization of the wind data, the wind speed (FF) and wind direction (DD) was combined based on the Beaufort scale wind speed classification (WMO, 2018). This classification and the corresponding implication on wind ventilation is summarized in table 3 below

Table 3: Adapted Beaufort scale wind classification (WMO, 2018)

<b>Beaufort Scale</b>	<b>Wind Speed (m/s) at 10m above ground</b>	<b>Wind Category</b>	<b>Characteristics</b>
Calm / Light air	< 1.5	Very Weak Wind	Calm; smoke rises vertically Direction of wind shown by smoke-drift but not by wind vanes
Light Breeze	1.51 – 3.3	Weak Wind	Wind felt on face; leaves rustle; ordinary vanes moved by wind
Gentle Breeze	3.31 – 5.4	Intermediate Wind	Leaves and small twigs in constant motion; wind extends light flag
Moderate/ Fresh	>5.4	Strong Wind	Raises dust and loose paper; small branches are moved

It should be noted that this wind categorization used in this study does not correspond to "strong wind" in the meteorological sense, which will rather start at 15 m/s. However, based on the above Beaufort scale wind classification, the wind speed (FF) was combined with the wind direction (DD) to create 32 unique wind classes as described below;

windspeed (FF) = (0, 1.5, 3.3, 5.4) m/s

wind direction (DD) = (22.5, 67.5, 112.5, 157.5, 202.5, 247.5, 292.5, 337.5) °

**Wind Classification (32 classes)**

C1: N-no ventilation | C2: N-weak ventilation | C3: N - Intermediate ventilation | C4: N-good ventilation;

C5: NE-no ventilation | C6: NE-weak ventilation | C7: NE-Intermediate ventilation | C8: NE-good ventilation;

C9: E-no ventilation | C10: E-weak ventilation | C11: E-Intermediate ventilation | C12: E-good ventilation;

C13: SE-no ventilation | C14: SE-weak ventilation | C15: SE-Intermediate ventilation | C16: SE-good ventilation;

C17: S-no ventilation | C18: S-weak ventilation | C19: S-Intermediate ventilation | C20: S-good ventilation;

C21: SW-no ventilation | C22: SW-weak ventilation | C23: SW-Intermediate ventilation | C24: SW-good ventilation;

C25: W-no ventilation | C26: W-weak ventilation | C27: W-Intermediate ventilation | C28: W-good ventilation;

C29: NW-no ventilation | C30: NW-weak ventilation | C31: NW-Intermediate ventilation | C32: NW-good ventilation;

#### ○ **Step VI – Conversion to Shapefile (.shp)**

Upon completing the wind threshold classification, the final step involved in the statistical analysis in R, is the conversion into shapefile format. This shapefile (.shp) is the required format needed to carry out further analysis and visualization in the GIS environment. The entire R script used for the statistical analysis is attached in APPENDIX.

### **3.2.2 GIS Analysis**

For the GIS analysis, the shapefile (.shp) output from the statistical evaluation served as input data for the GIS visualization. These input datasets were combined with the urban/surface dataset (LCZ maps, UHI maps and Elevation maps) acquired from the MAppUCE database (<http://mapuce.orbisgis.org/>). The GIS methods and analysis were executed:

- Clipping and masking of vector and raster dataset
- Aggregation and resampling of data
- Overlay analysis and a color-coded symbology style was created for visualization purpose.

#### **➤ Building Volume Density (BVD) Map**

Building density is a key concept that must be considered in the description of a city's urban spatial structure. Hence, from the urban building information dataset described in section 3.1.2, the Building Volume Density (BVD) for was derived using the following GIS operation;

- The input Toulouse\_Building.shp shapefile was converted to raster with the building height attribute field “i\_H” selected as raster values at 1x1m resolution (Rasterization),
- Then, the resultant raster was aggregated into 100x100 resolution by using the “sum” option;
- Lastly, the raster was further divided by the value of the biggest building volume (420,000 m<sup>3</sup>) using ArcGIS raster calculator.

➤ **Analysis of wind intensity vs UHI intensity across built local climate zones (LCZ)**

To understand the variation in wind intensity ( $\Delta\text{Wind(m/s)}$ ) and the Nocturnal UHI intensity ( $\Delta\text{UHI(^{\circ}\text{C})}$ ) across the different LCZ in Toulouse, it was important to aggregate the wind intensity parameters from the various summertime LWT-7,8,9 together with the Nocturnal UHI corresponding to the LCZs spatially. Specifically, the model wind velocity output at 250-m horizontal grid and the UHI map was overlaid onto the LCZ map in ArcGIS. Using the “*Extract Values to Point*” toolset, each grid of the wind intensity and UHI data point is matched with its underlying LCZ.

However, after a preliminary visual inspection, for smaller sized LCZ classes with an area less than 10,000 m<sup>2</sup>, the more dominant LCZ within a 250m buffer radius around it is assigned to the class instead. This was done to match the model resolution of 250m, which cannot capture the sub-scale variation of meteorological parameters. Hence, to avoid sample sizes that are too small for a fair statistical evaluation of the differences across LCZs, the built LCZs was regrouped into five classes (i.e. LCZ-1/2/3, LCZ-4/5, LCZ-6, LCZ-8, LCZ-9) based on their geographic proximity and/or similar thermal properties.

In conclusion, all the methodology implemented in this study are summarized in a methodology framework in Figure 12.

### 3.2.2 Methodology Framework

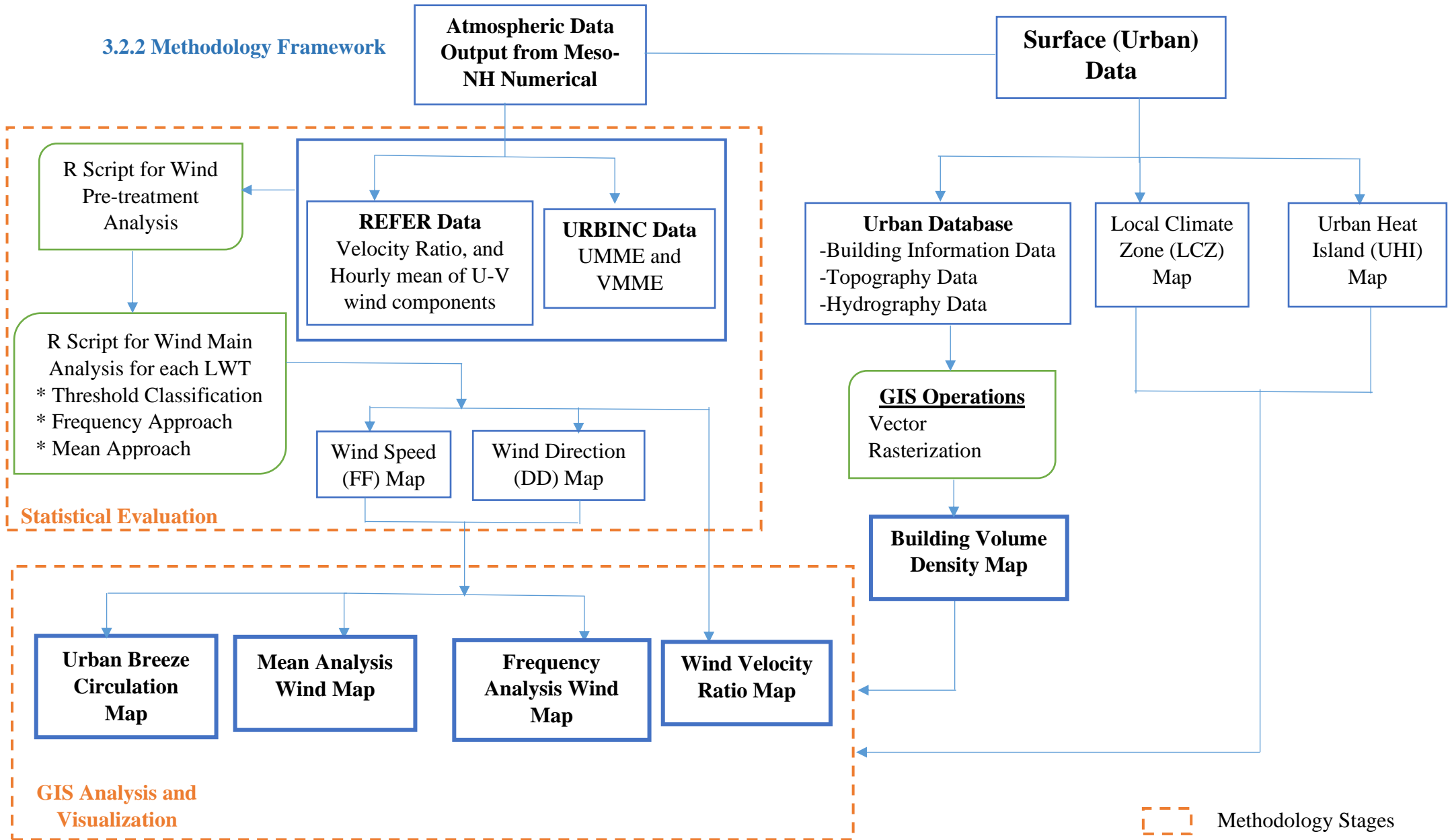


Figure 12: The Methodology Framework used in the research

## 4. RESULTS AND DISCUSSION

The following chapter presents and discussed the various results and map visualizations from the statistical data evaluation and the GIS post-analysis. Also, attempts were made to compare these results to previous published research.

### 4.1 Mean Wind Analysis vs Most Frequent Wind Analysis

To accurately understand and quantify the wind characteristics over the period of study (summer: June-August 2004) in Toulouse, two descriptive statistical methods were evaluated and compared: *Mean Approach* and *Frequency Approach*. The mean approach simply averages the hourly wind velocity and direction for each grid per day of occurrence of the different local weather types. On the other hand, the frequency approach evaluates the most frequent wind velocity and direction for each grid per day of occurrence of the weather types.

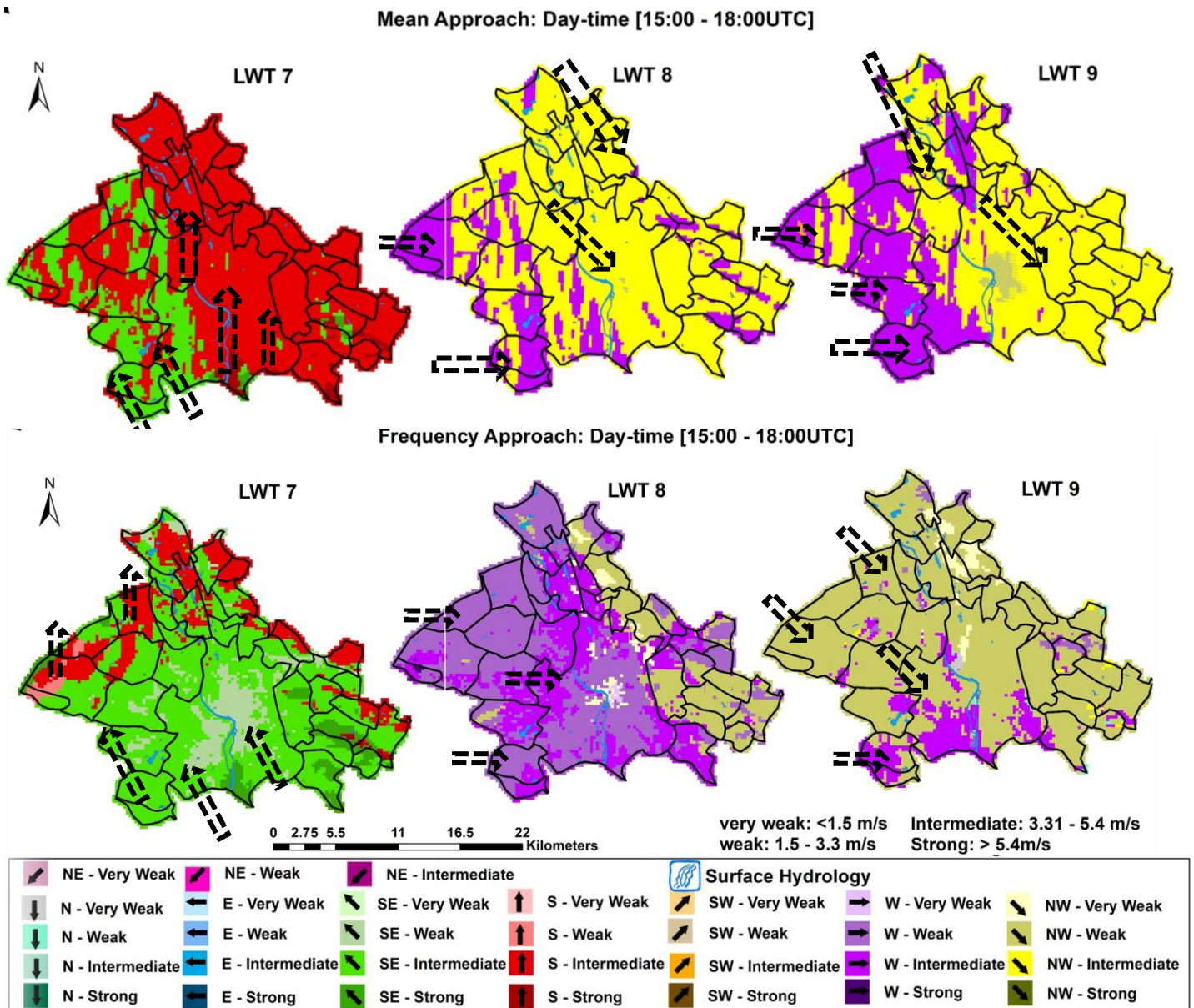


Figure 13a: Summer day wind characteristics for the mean and frequency approaches



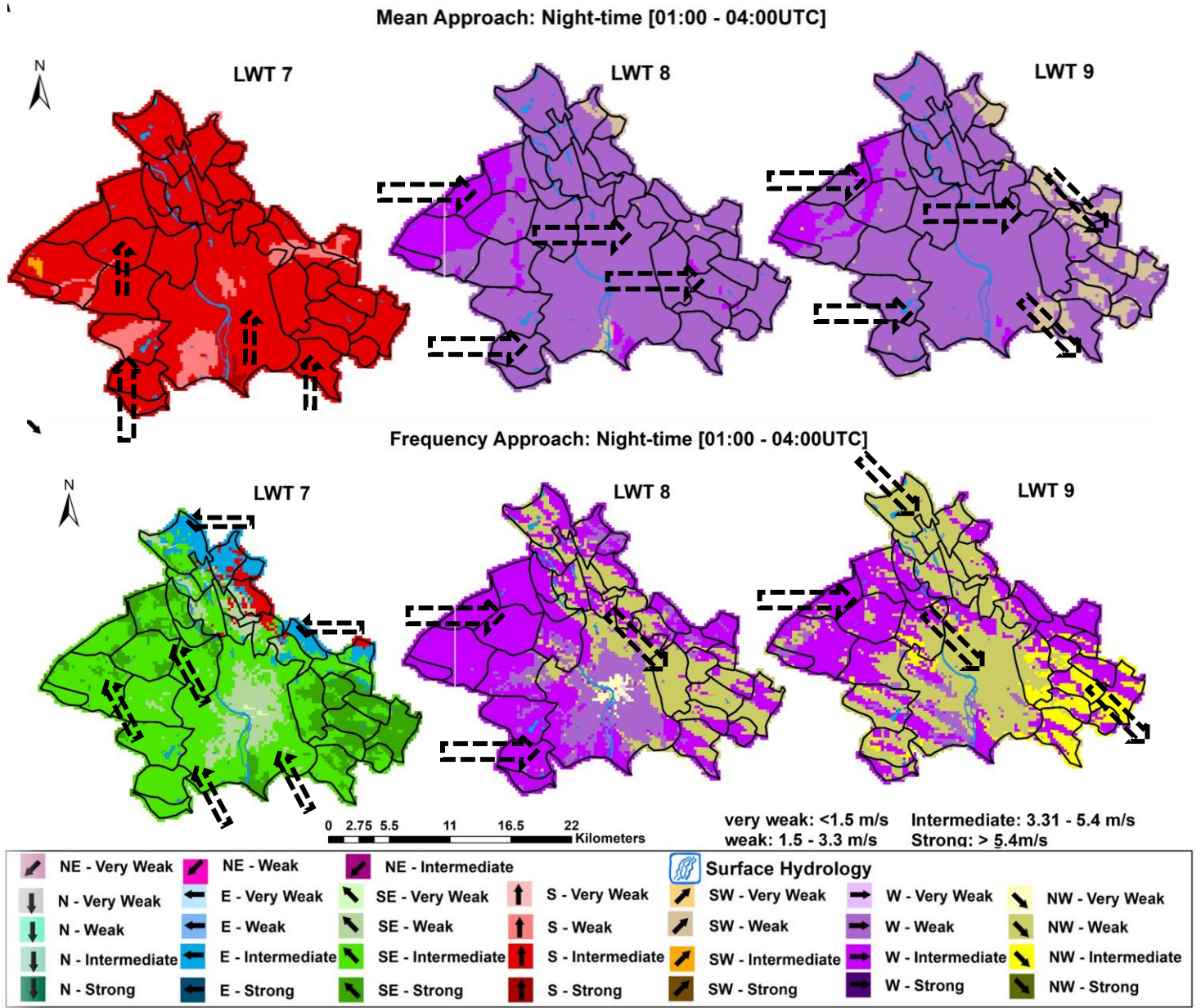


Figure 13b: Summer night wind characteristics for the mean and frequency approaches

A first visual glance of figure 13 (a & b) above clearly shows that the frequency analysis approach tends to show more details as compared to the mean analysis approach. More so, both the daytime and night-time frequency analysis maps reveal the distinct shape of the densely built-up areas in the city centre. As shown on the maps, the most persistent summer wind characteristics for LWT 7 is the south-easterly wind with stronger velocity(>5.4m/s) along the fringes of the Eastern part of the city, and the wind speed slows down towards the core of the city centre. While for LWT 8 & 9, the predominant wind regime is the westerly and north-westerly wind. This result is consistent with previous findings by Hidalgo & Joula (2018).

However, aside from these cartographic comparison between the wind maps derived from both the mean and frequency statistical methods, it was imperative to quantitatively assess how both approaches perform in relation to estimating the wind variables on the city scale.

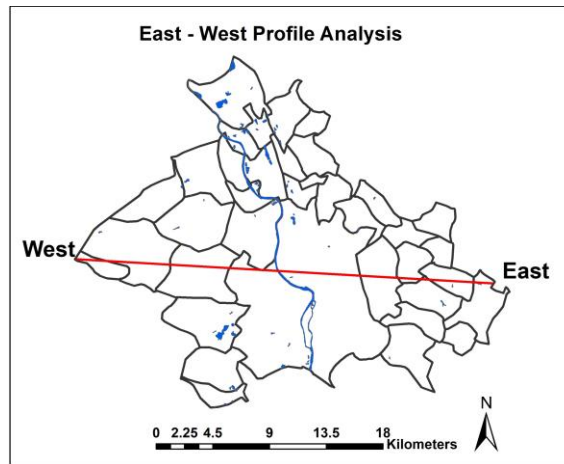


Figure 14a: East – West Profile of the wind velocity across the city

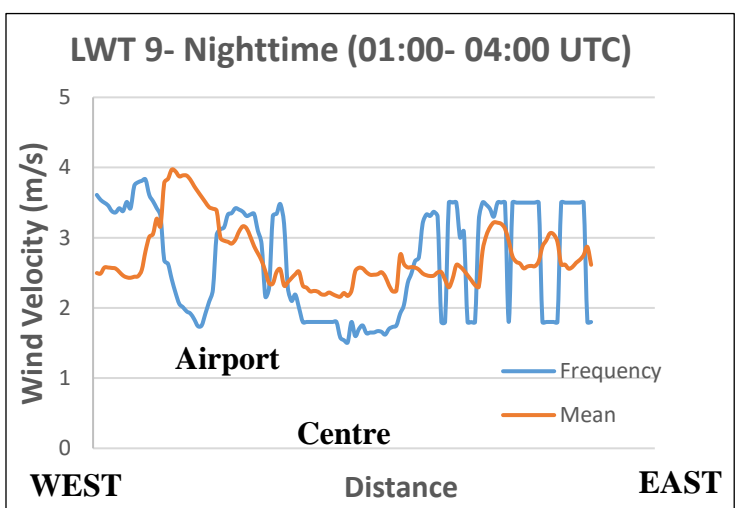
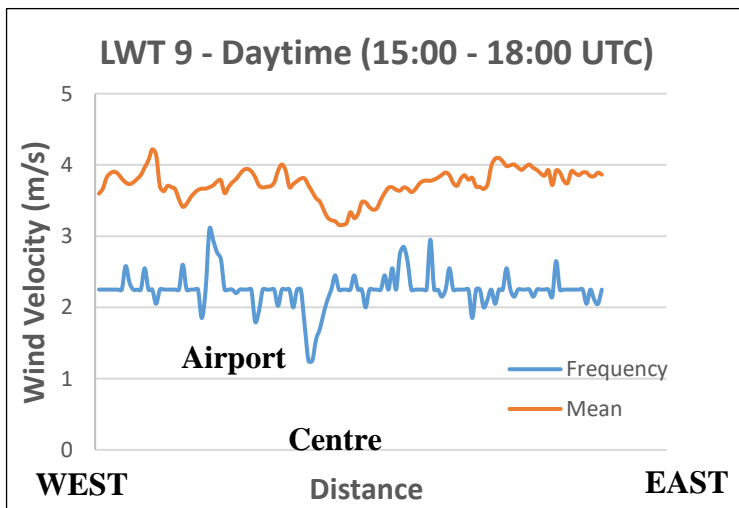
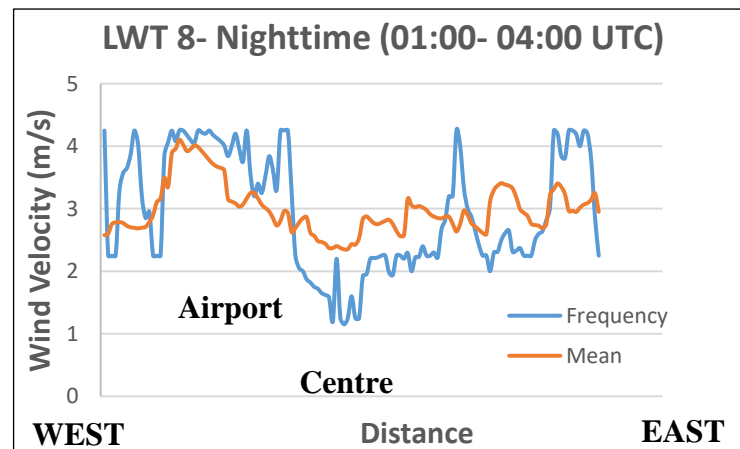
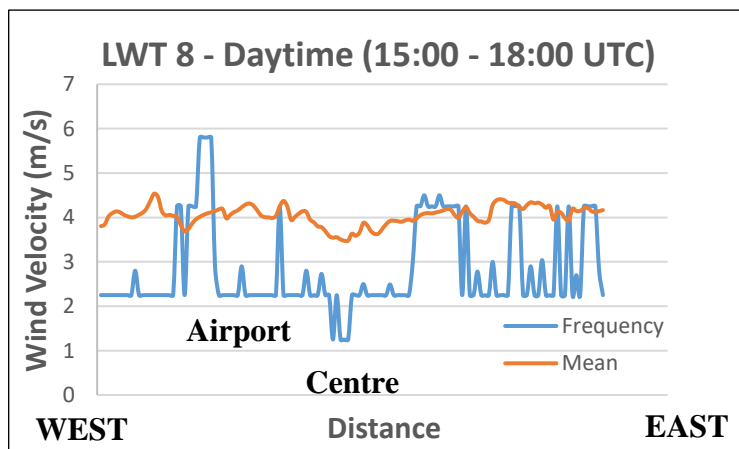
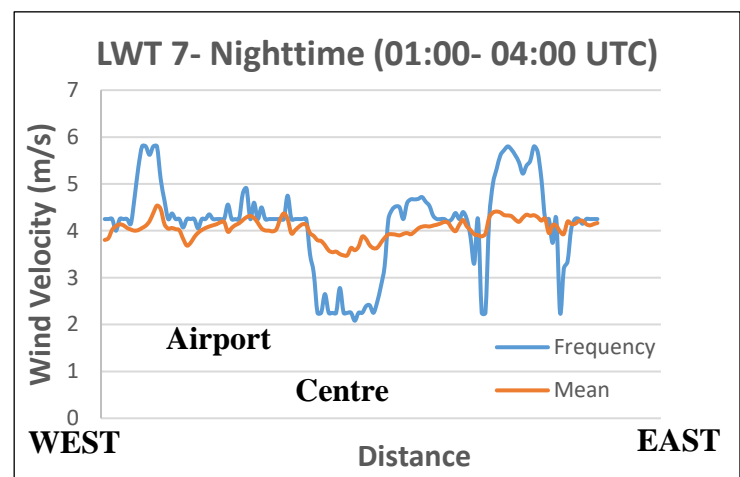
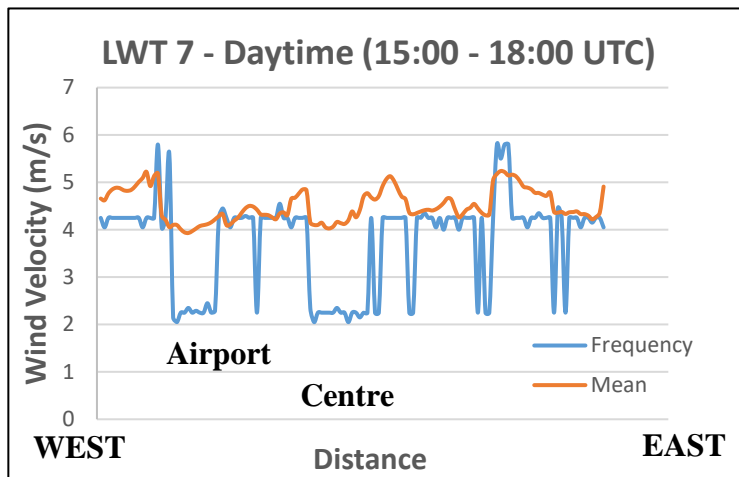


Figure 14b: Comparison of the East–West Profile of wind velocity (m/s) for the mean and frequency methods for each local weather types (LWT 7,8,9) during the daytime and night-time



Hence, this quantitative comparison was evaluated only based on the wind velocity values derived by each method. This was done because from a visual look at Figures 13a & 13b, both methods tend to describe the wind direction regime in a similar pattern, which to a great extent corroborates previous study (Hidalgo et al 2008; Hidalgo & Jouglu, 2018) as earlier noted. To achieve this comparison, a cross-section of the East-West wind velocity profile (Figure 14a) was extracted using ArcGIS spatial analyst tool and then plotted in a graph (Figure 14b).

Figure 14b shows the East-West profile of the wind velocity in the city for each statistical method and each local weather types during the daytime and night-time. This graph tried to quantify to what extent both methods either over-estimated or under-estimated the wind velocity in Toulouse. At first look, it is evident that the mean statistical approach tends to over-estimate the wind velocity by 1-2m/s during the daytime for all local weather types. While at night, the case is different with both methods showing almost similar wind velocity intensity from East to West, with occasional spikes in the frequency method. Furthermore, observed temporal similarities between the mean and frequency East-West profile is that they both show the distinct presence of the urban centre with a drop in the wind speed across all local weather types irrespective of the time of day. This is due to the dense built-up which slows down the wind speed as it approaches the centre (Santamouris, M., Georgakis & Niachou, 2008)

To be more specific, for LWT-7 during the daytime, the mean analysis over-estimated the wind velocity by an average of 1m/s as compared to the frequency analysis. While at night, the E-W mean wind velocity tends to hover around 4m/s with slight decrease in the city centre. Further, for LWT-8 during the daytime, the mean analysis over-estimated the wind intensity by almost 2m/s. Here, the frequency approach recorded a sudden spike in the wind speed (5.8m/s) around the airport area. This is expected as the presence of large open spaces in the airport accentuates the wind speed with less surface friction as in the centre. Also, similar over-estimation of 2m/s is recorded for LWT-9 during the daytime. But at night, LWT-9 tends to under-estimate the wind speed around the airport.

In general, as shown in Figure 14b, the intensity of the most frequent wind velocity tends to fluctuate a lot from East to West, as compared with the East-West mean wind velocity which remains almost stable. This is quite expected since mean analysis does not give the absolute values of the wind velocity but rather aggregates this into daily average wind velocity. Thus, mean might not account for any consistent outlier that might occur during the day. On the other hand, the frequency analysis evaluates the most frequent absolute wind velocity per day, hence this accounts for why this method describes the wind intensity as close to what is expected in the prevailing urban climatic conditions.

## 4.2 Variations in Wind Intensity and Nocturnal UHI intensity across Built Local Climate Zones (LCZs) in Toulouse

This session presents the results of the analysis carried out to understand how nocturnal UHI intensity is influenced by changes in the wind intensity from the daytime to night-time across the different LCZs. The LCZ map of Toulouse generated at the building block scale in a GIS platform as part of the MAPUCE project (Bocher et al., 2018) is presented in Figure 16b. More so, the difference between the daytime and night-time average wind velocity across the local weather types 7,8 and 9 is presented in Figure 16a.

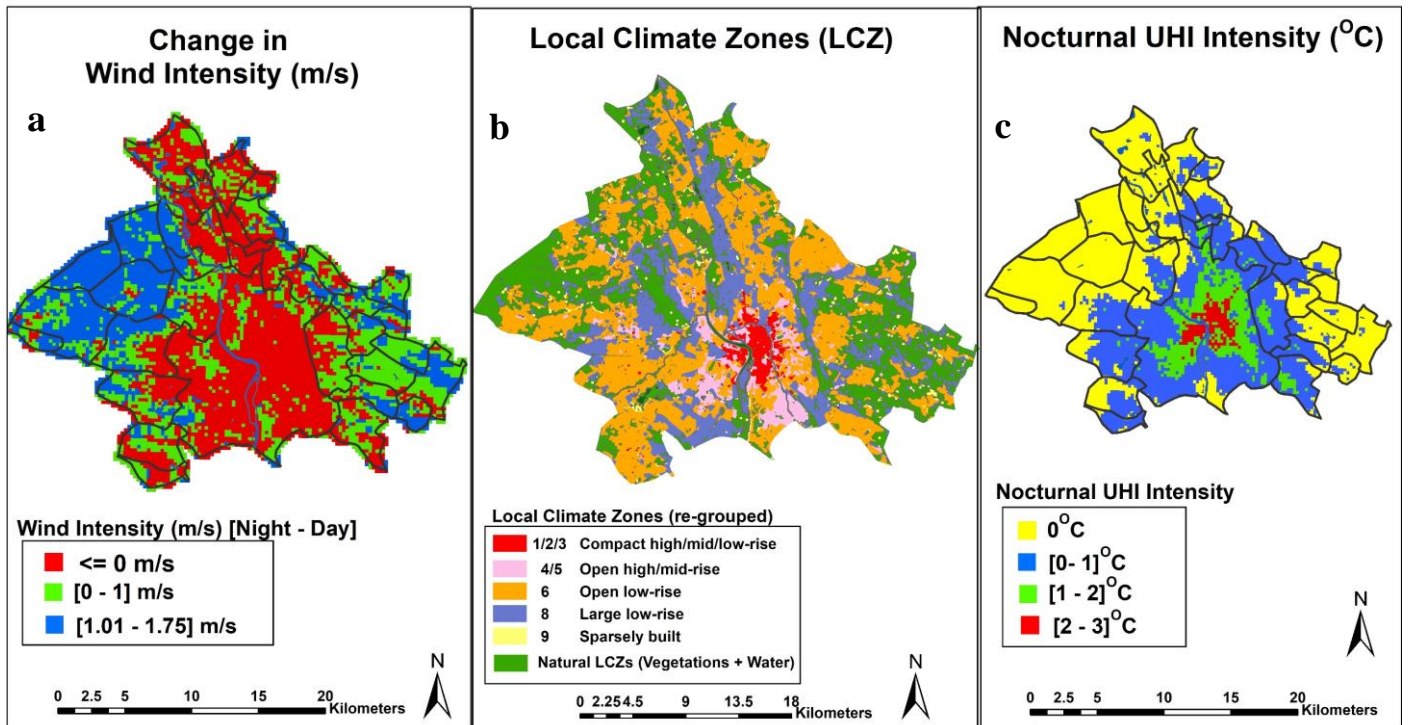


Figure 15: Comparison of (a) change in wind intensity map between the night-time and daytime, (b) Local Climate Zones re-grouped, and (c) the Nocturnal Urban Heat Island Intensity

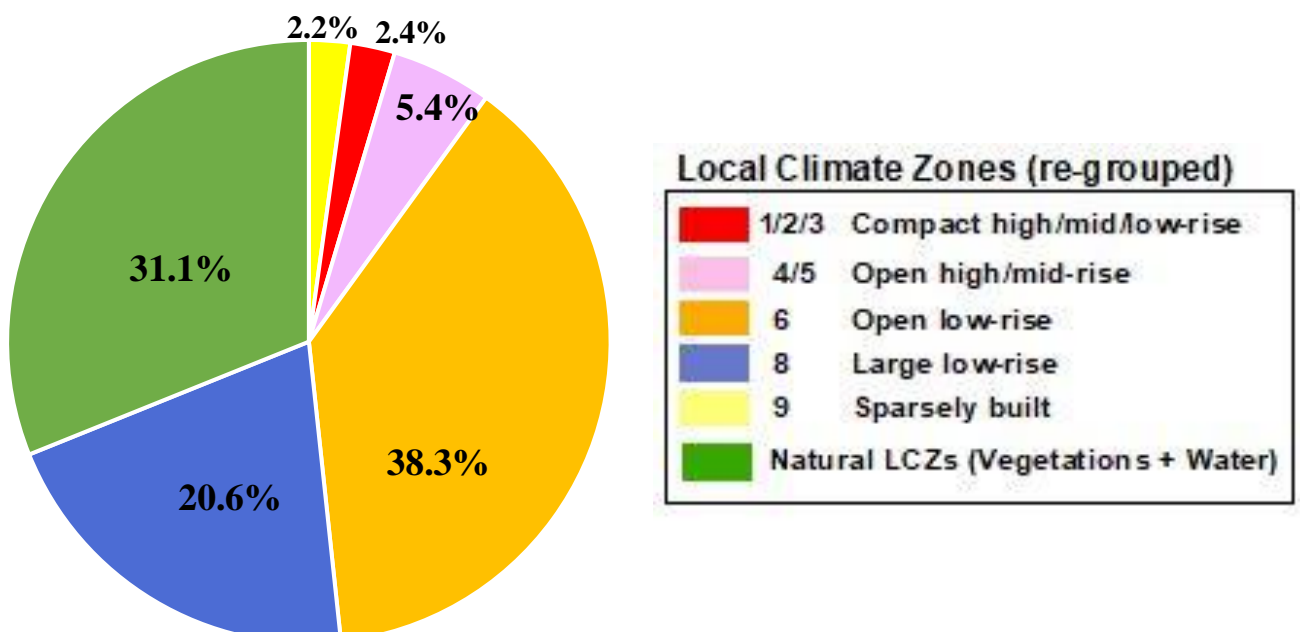


Figure 16: Distribution of area covered by each of the Built LCZs and the Natural LCZs

A visual inspection of the LCZ map and the pie-chart distribution (Figure 17) clearly reveals that the natural LCZ (i.e. all vegetation types and water) occupies 31.1% of the land area. Meanwhile, the most common built LCZ in Toulouse is the open low-rise (LCZ 6) category which covers 38.3% and thus reflects the city's low built density. Furthermore, the second-most common LCZ is the large low-rise (LCZ 8) class with 20.6% area covered which corresponds to the commercial and industrial districts dominant along major traffic routes away from the city-centre. Within the historical city centre, the most common LCZ is the compact mid-rise (LCZ 2) buildings with patches of open mid-rise (LCZ 5) and compact low-rise (LCZ 3) developments in its surrounding. Meanwhile, it should be noted that there are few informal settlements in Toulouse, hence the lightweight low-rise (LCZ 7) buildings are not present at the building block scale. Also due to the limitations of the MAPUCE database, heavy industry (LCZ 10) is also not represented.

Furthermore, from the change in wind intensity map in Figure 16a, regions covered in red represent those areas where there is either no change or a decrease in average wind velocity from daytime to night-time. While the green and blue coloured grids represent those regions with either between  $[0 - 1]$  m/s increase in wind velocity or between  $[1.01 - 1.75]$  m/s, respectively. Additionally, the Nocturnal UHI map shown in Figure 16c above clearly reveals the aggregated warming pattern (from all local weather types 7,8,9) of the city at night as compared to the previous daytime. It can be seen that the city centre (in red) has a UHI intensity of between  $[2-3]^{\circ}\text{C}$ , while the next urban regions surrounding the core of the city centre (in green and blue) has UHI intensity between  $[1-2]^{\circ}\text{C}$  and  $[0-1]^{\circ}\text{C}$  respectively. Meanwhile the surrounding rural suburban of the city (in yellow) experienced  $0^{\circ}\text{C}$  change in nocturnal UHI as compared to the previous daytime.

**Table 4: Summary of UHI Intensity and Wind Intensity across the LCZs.**

LOCAL CLIMATE ZONEs (re-grouped)		Urban/Rural Nocturnal Heat Island Intensity ( $\Delta^{\circ}\text{C}$ )			Change in Wind Intensity (Night-time - Daytime) (m/s)		
Zone #	Zone Title	Min	Average	Max	Min	Average	Max
1/2/3	Compact Zones (High/mid/low-rise)	0	2.57	3	-0.82	-0.20	0.52
4/5	Open High/mid-rise	0	1.52	3	-1.40	-0.13	1.72
6	Open low-rise	0	0.76	3	-1.48	0.20	1.75
8	Large low-rise	0	0.64	3	-1.39	0.14	1.70
9	Sparsely built	0	0.32	2	-0.82	0.47	1.75

The nocturnal thermal environment and the wind intensity for different LCZs in the Toulouse Metropolitan Area is described in Table 4 obtained from the Més0-NH simulations output. Significant nocturnal urban warming can be observed in all the LCZs. This nocturnal urban warming has a distinct decreasing pattern as one moves away from the densely built urban core towards the sparsely built suburban. This result is consistent with previous findings (Kwok et al. 2019), where the same decreasing pattern was observed for both air temperature and the mean radiant temperature in Toulouse. On the other hand, the change in wind intensity shows a gradual increase across the LCZ, from the inner urban core LCZ 1/2/3 to the outermost sparsely built LCZ 9. However, there was a slight variability in the increasing pattern from LCZ 6 to LCZ 8, which could be attributed to their “low-rise” urban morphology.

Nevertheless, areas with LCZ 1/2/3 - compact development (high/mid/low-rise) can be seen to have the strongest average nocturnal UHI intensity of 2.57°C. Consequently, the same compact LCZ zones recorded the highest decrease in the wind intensity (-0.20m/s) from daytime to night-time. This is expected since the urban-rural thermal gradient is at the highest at night-time because of the thermal properties of the building materials which tends to conserve the daytime heat which is later released at night-time. This coupled with the compact morphology of the urban core that tends to slow down the wind intensity and redistribution across the LCZ contributes to the warming of the LCZ 1/2/3.

Furthermore, among the built LCZs, the highest increase in wind intensity (0.47m/s) is observed in LCZ 9 (Sparsely built) which corresponds to the weakest nocturnal UHI intensity. It is deemed that since these areas are scattered all over the city with most located in the rural outskirts, their building fabric will tend to allow easy passage of the stronger prevailing rural wind into its street canyon during the day and even at night when the weather is close to calm situation. The end result is such that both the heating and the cooling of the LCZ fabric happens in a rapid manner thus leading to a near zero nocturnal heat island intensity.

Further analysis revealed that an increase in daytime to night-time wind intensity of 0.20m/s and 0.14m/s is observed for LCZ 6 and LCZ 8 respectively. This could be due to their spatial heterogeneity in urban form because of their locations at urban–rural boundaries, or perhaps as a result of the larger area covered by the LCZs. More so, Table 4 showed that LCZ 6 has the largest wind intensity range, which is consistent with previous findings on larger intra-LCZ variabilities in cities at night (Skarbit et al., 2017).

### 4.3 Visualizing Urban Breeze Circulation in Toulouse

The differential rate of heating between the built urban centres and the surrounding countryside is the main cause for the urban breeze circulation. The atmospheric conditions favouring the formation of this phenomenon is a strong insulation day coupled with low surface wind velocity and a deep boundary layer. Luckily, these atmospheric conditions were observed by (Hidalgo *et al.*, 2008) over the city of Toulouse and countryside during the Intensive Observation Period number 5 (IOP5, 3<sup>rd</sup> and 4<sup>th</sup> July 2004) of the CAPITOUL experiment (Feb. 2004 to Feb. 2005).

Therefore, to visualize the existence of this phenomenon, the wind characteristics on the 4<sup>th</sup> of July 2004 in the Meso-NH simulation output dataset used in this study was analysed such that the average wind pattern between 12:00 – 15:00UTC and 15:00 – 18:00UTC was evaluated. The resulting summertime urban breeze phenomenon is presented (Figure 18).

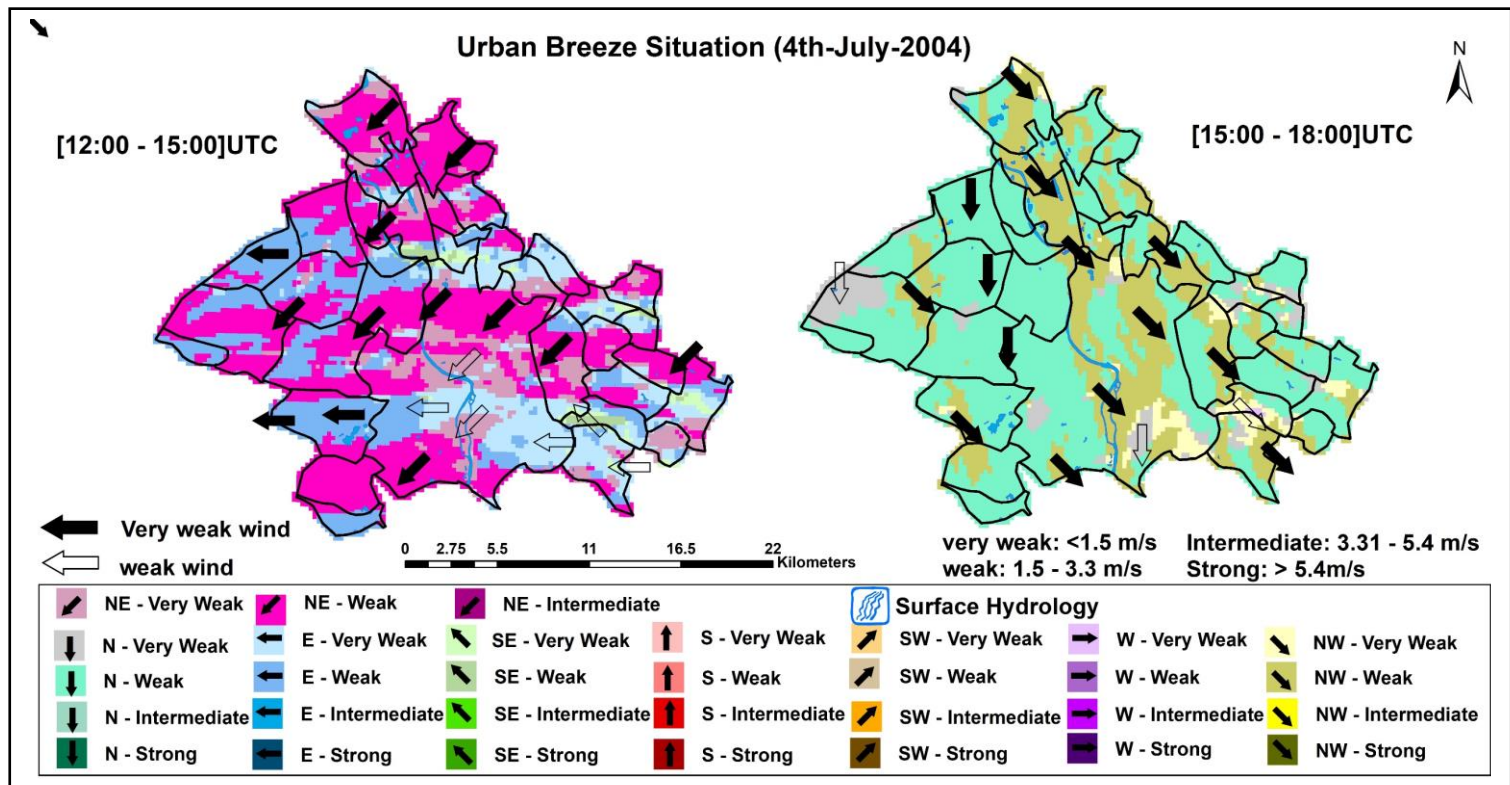


Figure 17: Urban Breeze Situation at 10m above ground in Toulouse Metropole on 4<sup>th</sup>/July/2004

From Figure 18, it is apparent that on the 4<sup>th</sup> of July, between 12:00- 15:00UTC, the dominant wind system at 10m above ground, was a weak East-Northeast (E-NE) pattern. This is expected since according to the weather clustering by Hidalgo & Jougla (2018), the most persistent weather type on July 4<sup>th</sup> is LWT 7- which is a typical sunny summer day weather with persistent but weak south-easterly wind and extreme temperature reaching 40°C. Thus, this extreme urban-rural horizontal temperature gradient which must have begun to develop from the previous day and the early morning, together with the weak wind intensity allows a

more turbulent boundary layer to build up. That is why for the few hours between 15:00 – 18:00 UTC, the wind system had switched to a NW-SE pattern, such that now, there is a near-surface wind advection from the less built-up northern part of the city, towards the core of the urban area as shown in Figure 18 above.

This surface convergence towards the urban centre is complimented by an upper boundary layer divergence of wind away from the centre towards the rural outskirts. This result further corroborates the previous aircraft measurement by Hidalgo et al. (2008a) where it was noted that the urban-breeze grew in intensity from 2 m/s at 12:00UTC to 5-6m/s at 18:00UTC. Similar results were also recorded by Lemonsu and Masson (2002), in the case of the city of Paris and its surrounding in July 1994.

Whilst the synoptic scenario on 4<sup>th</sup> of July was favourable to the development of an urban-breeze which could be considered as a positive situation since the fresh breeze from the rural outskirt could bring in some much needed cooler air into the already warm city centre, it is important to note that, urban breeze can also accentuate the diffusion of pollution from the industrial campuses in the suburban into the city centre especially as the horizontal extent of the breeze covers a large portion of the NW-SE mesoscale cross-section of the city. Meanwhile, with favourable atmospheric system, the anticyclonic urban-breeze could aid the formation of convective thunderstorm over the urban area as the wind advects towards the city centre leading to much heavier turbulent rainfall. A concise record of recent (1990–present) research related to how the thermodynamics of the urban climate affects precipitation is documented by Shepherd (2005).

Therefore, it is imperative that more work is still needed to understand the severity, frequency and horizontal extent of urban breeze across other major French agglomeration which will be very useful to predict the urban-rural pollution transport and the evaluation of air policy legislations.



#### 4.4 Wind Velocity Ratio Analysis

The wind velocity ratio is a unitless quantity defined as the ratio of wind speed measured at pedestrian level ( $V_p$ ) to that at the reference point -  $V_{ref}$  (Ng et al., 2011).

$$V_{Ratio} = \frac{V_p}{V_{ref}} \quad [2]$$

In this study, the  $V_p$  refers to the hourly mean of wind speed [m/s] at 2m pedestrian-height above the ground in the TOWN tiles (i.e. the urban areas), while  $V_{ref}$  is the reference hourly mean of wind speed [m/s] at 10m above average building height in urban areas. Hence, the results of the velocity ratio analysis in the urban areas are shown in figure 19.

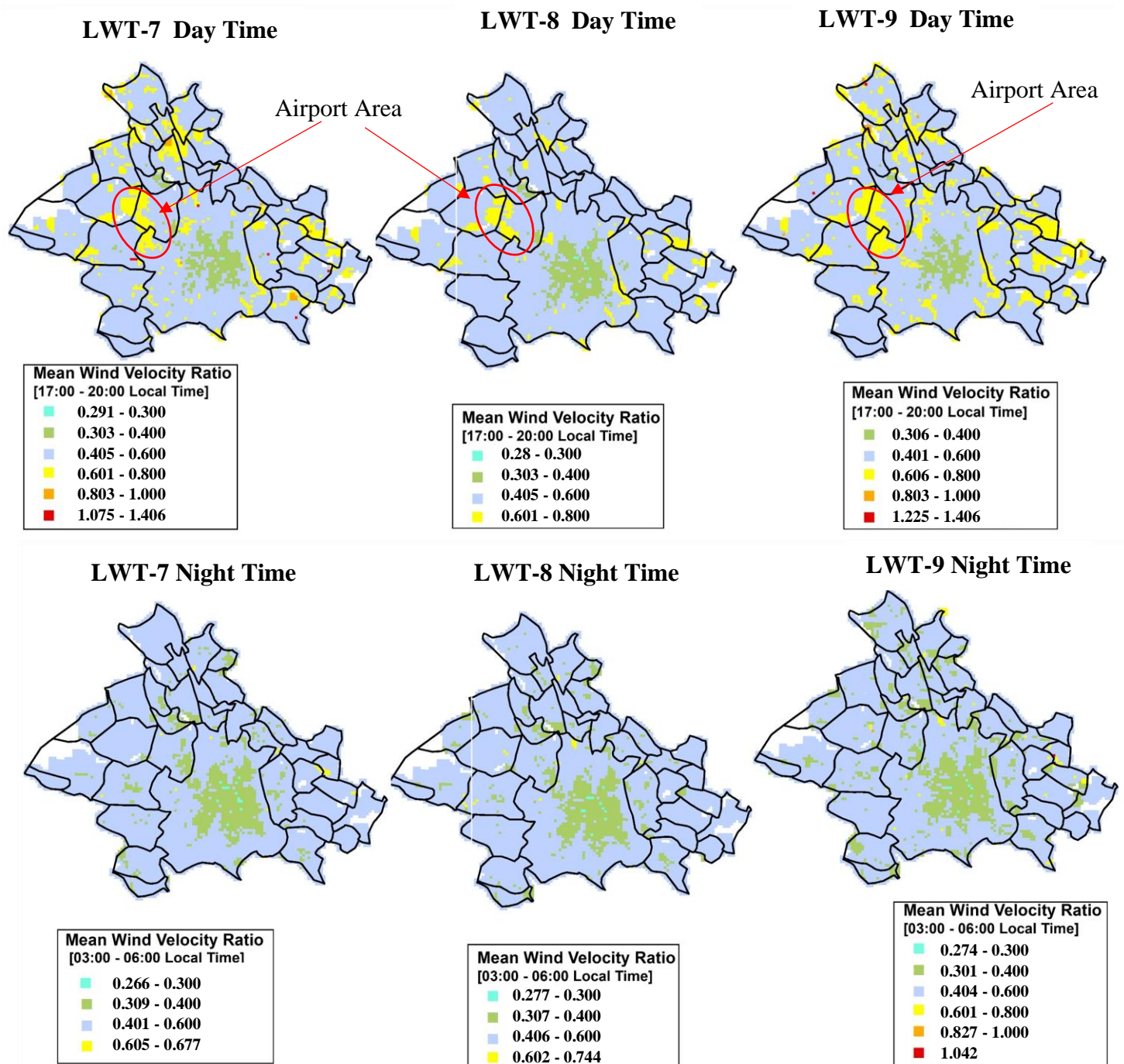


Figure 18: The mean wind velocity ratio at pedestrian level-2m during the daytime (17h - 20h local time) and night-time (03h - 06h local time) across the different local weather type 7, 8 and 9.



The daytime and night-time velocity ratio maps (Figure 19) clearly reveal both the general pattern and shape of the urban areas within the city, as high values of velocity ratio (yellow: 0.6 - 0.8) are found in open areas away from the centre, such as in the airport area towards the North West, while the lower values (green: 0.3 – 0.4) are mostly concentrated within the densely built up areas of the city centre. Meanwhile, the high velocity ratio is due to the prevalence of large open spaces and low buildings leading to low values of aerodynamical roughness length and building drag. More so, the maps shows the differential change in velocity ratio from daytime to night-time as lower values are predominant at night time, since there is less turbulent transport of momentum towards the surface, leading to the lower wind speed at the pedestrian-level at night.

Furthermore, figure 19 above also revealed that in the middle of the map, there exist pockets of very weak wind velocity ratio ranging between 0.2 - 0.3. These very weak values are due to the high building density in the city centre and could be as a result of the homogeneity of those built form in the centre. However, these very weak values will have a negative impact on the urban ventilation and consequently affect the thermal comfort of pedestrian, especially during night-time when there is a stable atmospheric condition with less transport of momentum.

Table 5: Summary of the velocity ratio for the different local weather types during the daytime and night-time

<b>Velocity Ratio</b>	<b>Daytime</b>			<b>Night-time</b>		
	<b>Min</b>	<b>Mean</b>	<b>Max</b>	<b>Min</b>	<b>Mean</b>	<b>Max</b>
LWT 7	0.291	0.447	1.406	0.266	0.390	0.677
LWT 8	0.284	0.427	0.754	0.277	0.390	0.744
LWT 9	0.306	0.460	1.477	0.274	0.387	1.042

Consequently, from table 5 showing the summarized values, it is evident that LWT-9 has the strongest velocity ratio across both timescales, while LWT-7 mean recorded the weakest velocity ratio within both timescales.

However, to better understand how the urban morphology affects the velocity ratio across the cityscape, the difference in daytime velocity ratio and night-time velocity ratio was compared with the building volume density map as illustrated in the next section.

### ➤ Relationship between wind Velocity ratio & Building Volume Density

A further analysis of the wind velocity ratio map was carried out by aggregating together the three velocity ratio maps of all the local weather types for daytime to get the estimate of the daytime mean velocity ratio, and likewise for the night time to evaluate the night-time mean velocity ratio (Figure 20).

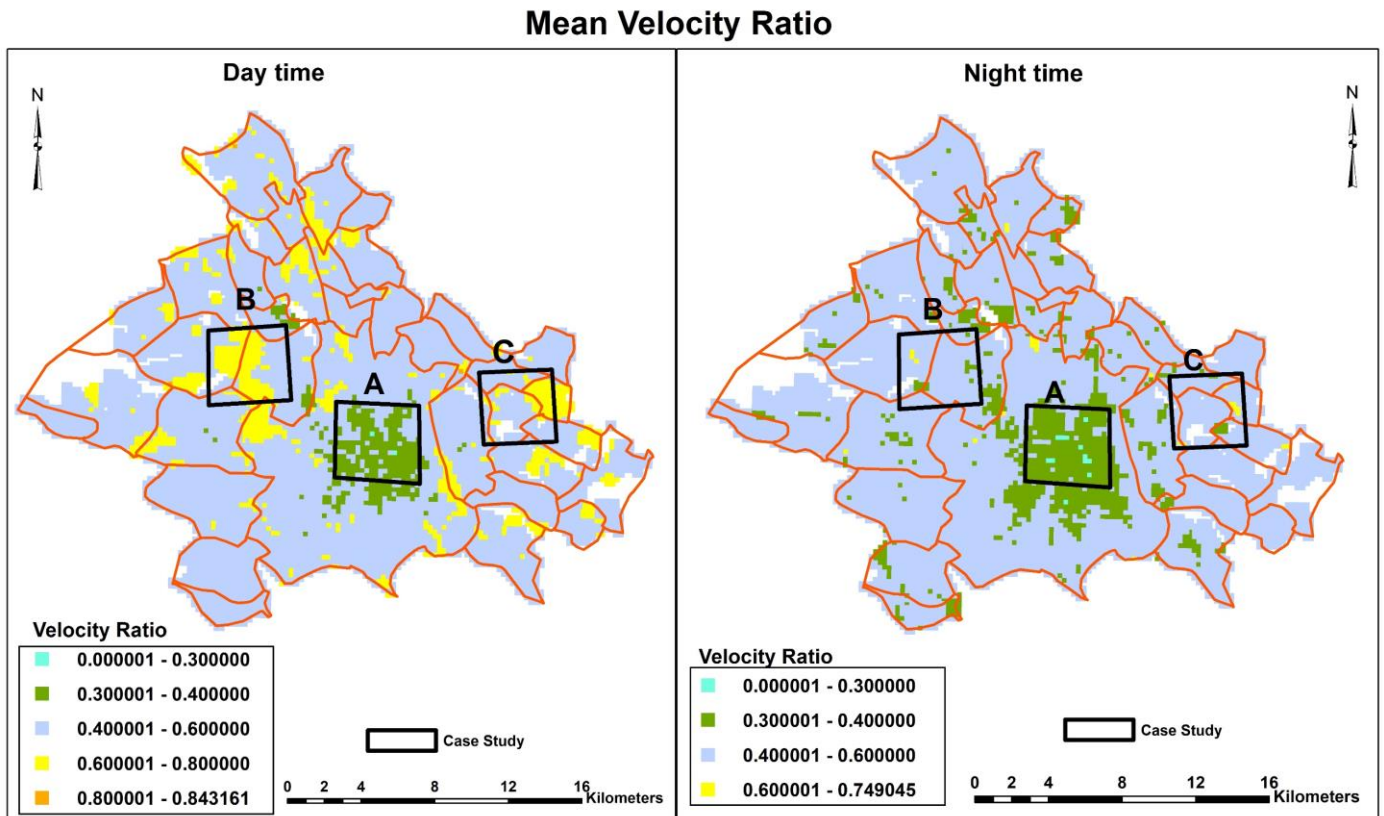


Figure 19: Aggregated mean velocity ratio across all local weather types during the daytime and night with the marked case study areas.

The aggregated spatiotemporal maps reveal the pattern of the wind velocity ratio in relation to the time of the day. During the daytime, strong velocity ratio values can be seen around the airport area and towards the eastern part of the city where there are more open spaces. At night, this ratio had decreased such that very weak velocity ratio could be observed in the city centre due to the less turbulence in the atmosphere which in turn lowers the speed.

Furthermore, these results were then compared with the building volume density (BVD) to examine how the wind velocity ratio is influenced by the underlying building volume density. However, in order to further understand how this is characterized across different urban built-up scenarios in the city, 3 sample case study areas were selected as follows (Figure 21);

**Case A [Urban Core]:** This is representative of the densely built up city centre,

**Case B [Airport Area]:** This represents the suburban scenario with more open spaces,

**Case C [Rural Area]:** This is representative of the rural areas with less buildings, but greatly influenced by high elevation.

### Building Volume Density Map

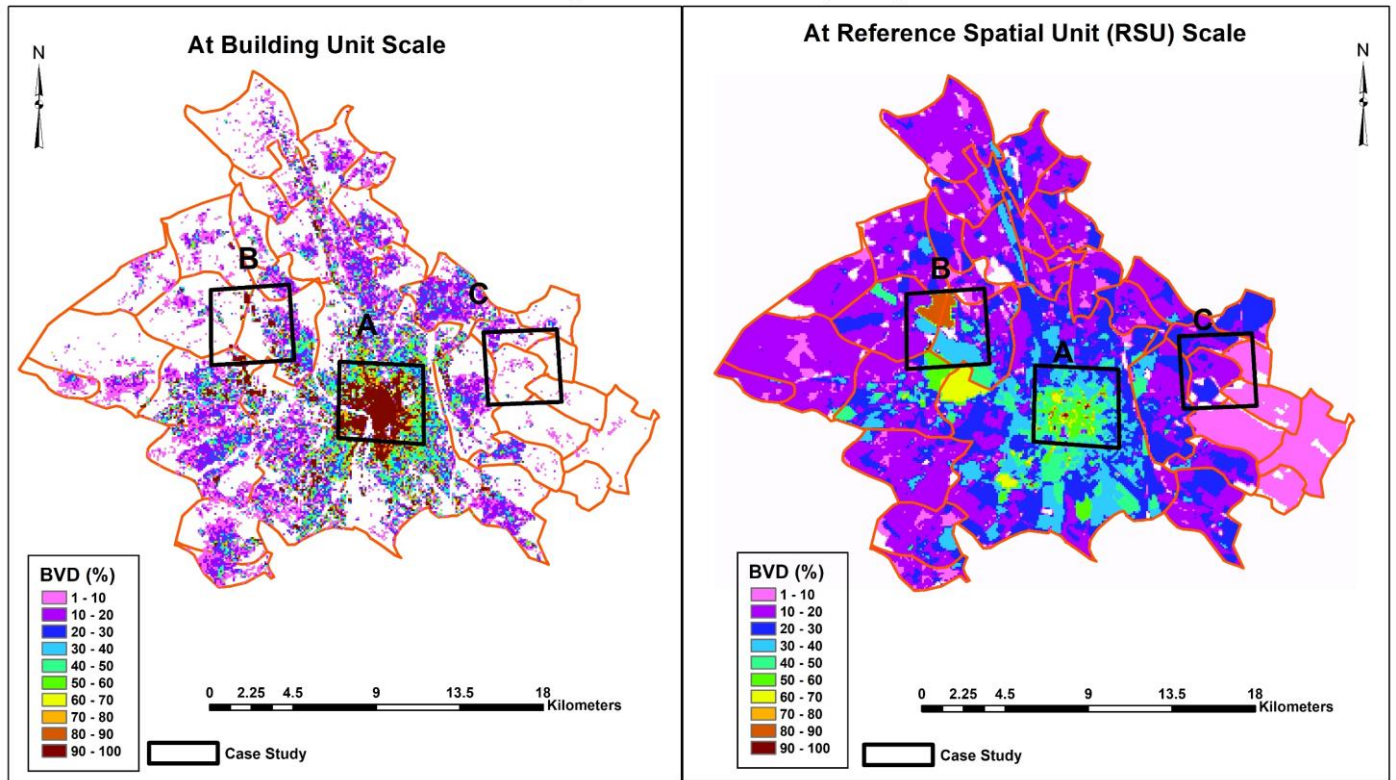


Figure 20: The Building Volume Density map for Toulouse based on the building unit scale(left) and the RSU scale (right) at 100m resolution.

Figure 21 above shows the characteristics differences in the building volume density maps derived from the building unit scale and the RSU scale respectively. The more detailed building unit scale data helps to identify areas with no buildings which could serve as the ventilation corridor to allow wind flowing into the city. However, with land use data available, concrete areas with no building can also be identified as it has implications on the thermal load of the city. From the figure above, it can be observed that high building volume density is mostly found in the city centre around the Capitole, Esquirol and Carmes metro stations. More so, scattered pixels of high building density are observed in the airport areas and other large commercial complexes around the city. This demonstrate the applicability of built-up volume as triggers of local heat island phenomena or their influence on local wind systems (Harlan et al. 2006).

Table 6: Summary of the relationship between building volume density and mean of the unitless velocity ratio during the day and night

	Building Volume Density (%)		Velocity Ratio			
			Day-time		Night-time	
	Mean	Max	Mean	Max	Mean	Max
Case A	13	86	0.384	0.562	0.355	0.495
Case B	9	100	0.529	0.732	0.454	0.699
Case C	2	15	0.429	0.790	0.374	0.749

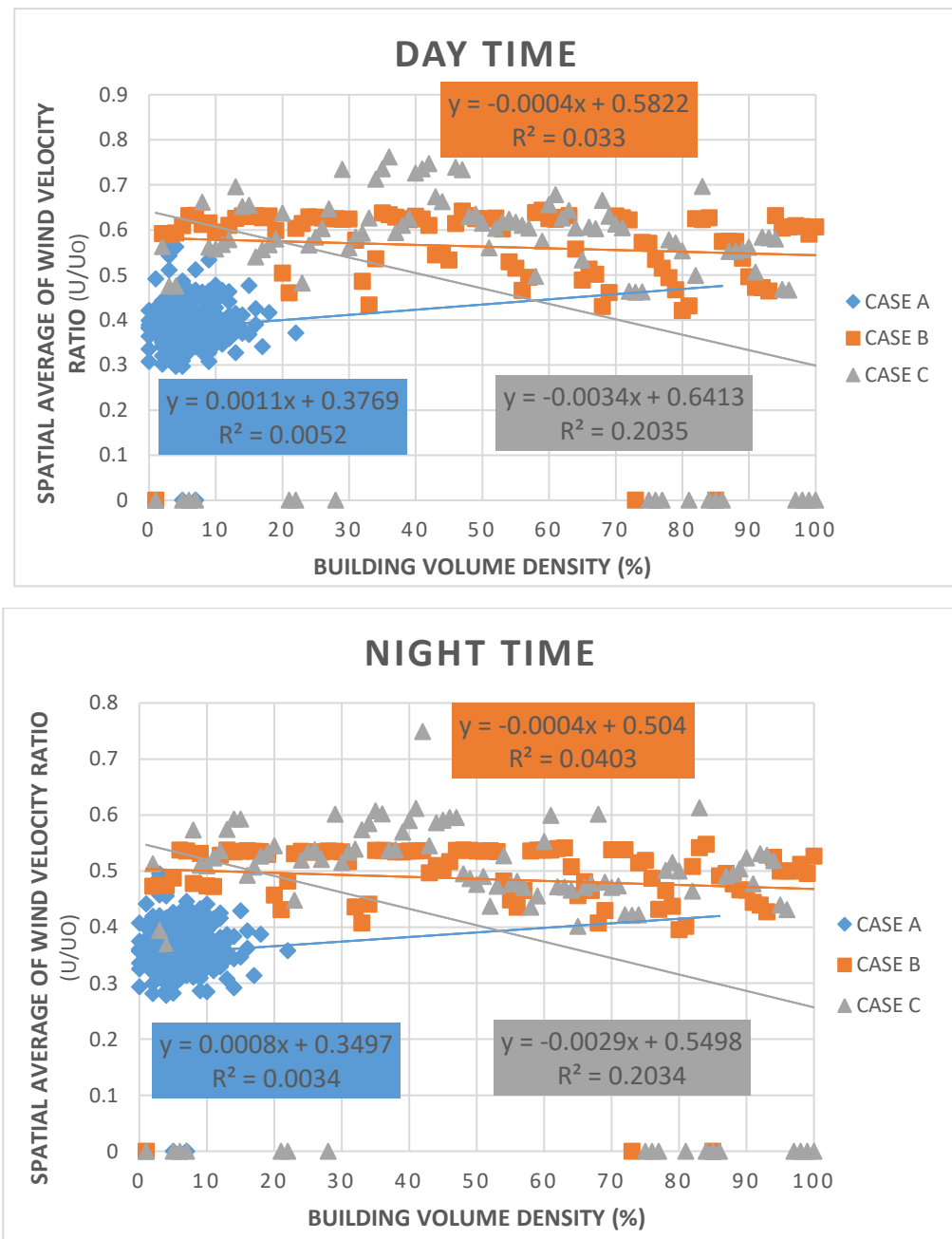


Figure 21: Spatial average of wind velocity ratio as compared with the building volume density for the different case studies during the daytime and night.

Table 6 presents the summary of the relationship between building volume density (BVD) and the mean velocity ratio for each case study areas during the daytime and night-time. It is revealed that CaseB (Airport) recorded the maximum building volume density (100%) per unit area of all the sampled cases. This is due to the presence of large bodied buildings at the airport terminals. Despite CaseB reporting the maximum BVD, CaseA (Urban Core) had the highest mean BVD of 13% because of the tall and close packed dense nature of the buildings in the centre. Of the three cases, CaseC (Rural Area) recorded the lowest BVD since it is in rural outskirts of the city with fewer built-up densities.

Furthermore, table 6 indicates that CaseC (Rural) recorded the maximum value of wind velocity ratio both during the daytime and night-time. This is expected as in this case, the surface wind velocity is accelerated because of the less obstructions from the fewer buildings in the rural vicinity. Consequently, the maximum velocity ratio recorded show a reducing pattern similar to the mean building volume density as one moves closer to the centre of the city (CaseC  $\leftarrow$  CaseB  $\leftarrow$  CaseA). Regardless of this, the highest mean value of the velocity ratio was recorded at the airport area (CaseB). This is because in this study, only the built-up grid points were considered and since CaseC is mostly rural with large vegetation cover, there are fewer data points considered in this case. Unlike in CaseB, with plenty open spaces around the airport complex with mostly urban built-up, more grid points were considered.

Nonetheless, figure 22 shows the graph of the spatial average of wind velocity ratio when plotted against the building volume density for all cases during the day and night-time. From the graph, it is apparent that only CaseA shows a positive characteristic between the mean velocity ratio and the BVD irrespective of the time of day. This could be due to the high density and compact nature of the buildings in the centre, as compared with the open spaces in Cases B and C which revealed a negative relationship between BVD and the velocity ratio. Consequently, for both time of the day, the urban core recorded the lowest  $R^2$  value (0.0052 for day, and 0.0034 for night-time), however CaseC in the rural recorded the highest  $R^2$  value (0.2035 in the day and 0.2034 in the night). This very high  $R^2$  value could be because of the high topography of the selected location (CaseC) in the rural eastern part of the city.

These findings is similar to previous work by Kubot and Miura et al (2000, 2002) in Japan and Malaysia, where they used a wind tunnel test to analysis the variation of gross building ratio in relation to the wind velocity ratio. Hence, this study has illustrated that irrespective of time of day, the relationship between BVD and VRatio tends to behave in a similar pattern with higher velocity ratio in daytime, thus, demonstrating how the urban surface morphology and small-scale orography could influence the wind field.

## 5. CONCLUSIONS

This chapter draws conclusion based on all the results. It also acknowledges the limitation of the research approach and recommends ways for further research.

### 5.1 Summary of Results

This thesis has attempted to examine the spatial characteristics of wind dynamics in relation to urban morphology and heat island in the metropolitan city of Toulouse using the local weather type classification through statistical analysis and GIS operations. Specifically, the urban surface database was used, while the 2004 summertime Meso-NH model data with 250m x 250m horizontal resolution at 10m above ground was extracted and analysed using R script and was then exported to shapefile (.shp) format for subsequent GIS spatial analysis.

To understand the wind propagation across the cityscape, a comparative analysis of the frequency and mean statistical methods was carried out. The results of the wind map revealed that the frequency approach showed more details and the distinct shape of the urban morphology. Further analysis revealed that the mean method tends to over-estimate the wind velocity by 1-2 m/s across the East-West profile during the daytime for all LWT. While at night, both methods show almost similar wind intensity pattern with occasional spikes in the frequency method. Consequently, observed temporal similarities between the mean and frequency East-West profile is that they both show the distinct presence of the urban centre with a drop in the wind speed across all local weather types irrespective of the time of day. This observed differences in the mean and frequency wind maps could be attributed to the fact that mean analysis is not a representation of the actual absolute values of the wind velocity but rather an aggregation of the daily average wind velocity. On the other hand, the frequency analysis simply extracts the most frequent actual wind velocity per day, hence this accounts for why frequency method represents the wind intensity as close to what is expected in the urban climatic conditions.

Furthermore, to understand how the nocturnal UHI varies across different urban characteristics in relations to changes in wind intensity, the local climate zones (LCZs) classification which characterizes built urban morphology was used. The results showed that LCZ-6 (open low-rise) is the most common building type in Toulouse covering 38.3% of the built area. Further results revealed that compact buildings LCZ-1/2/3 (compact high/mid/low-rise) which are common in the city-centre recorded the strongest average nocturnal UHI intensity of 2.57°C. Interestingly, this same compact LCZs recorded the highest decrease in wind intensity of -0.20 m/s from daytime to night-time. Meanwhile, the highest increase in average wind intensity of 0.47 m/s was observed in the sparsely built LCZ-9 which also corresponds to the



weakest nocturnal UHI intensity of  $0.32^{\circ}\text{C}$ . This is not surprising since the urban-rural thermal gradient is at the peak at night-time because of the thermal properties of the building materials that stores heat during day and releases it at night. Additional analysis reveals that the intra-LCZ variabilities of UHI and wind intensity can be explained by the distance to the city centre.

Consequently, the characteristics of the unitless wind velocity ratio in Toulouse was analysed. It was observed that the highest values of velocity ratio were found around the airport area. This is due to the prevalence of large open spaces and low buildings leading to low values of aerodynamical roughness length and building drag. Conversely, the very low values observed in the city centre are due to the high building density. Even so, lower values of the velocity ratio were observed at night, since there is less turbulent transport of momentum towards the surface, thus confirming previous studies. Furthermore, the characteristics of the spatial average wind velocity ratio in relation to different case studies with varied building volume density was examined. The results revealed that the higher the building volume density in a unit area, the lower the velocity ratio at the pedestrian level.

Additionally, to assist urban planners, attempts were made to visualize on a cartographic map the anticyclonic urban breeze circulation pattern which occurred on the 4th July 2004. The map confirm that for the few hours between 15:00 – 18:00UTC there was a breeze pattern which stretch across the NW-SE axis of the city with surface wind flowing from the peripheral northern areas towards the core of the city. Whilst the weather situation on that day was favourable to the development of an urban-breeze which could be considered as a positive event with the fresh breeze from the rural outskirt bringing in some much needed cooler air into the already warm city centre, it is important to note that this breeze can also aid the diffusion of pollution from the industrial factories in the suburban into the centre especially as the extent of the breeze covers a large portion of the NW-SE mesoscale cross-section.

In conclusion, this thesis has demonstrated that the morphology of the urban fabric and the wind flow characteristics has a great impact on the extent and intensity of the summertime urban heat island. Through this study, it has been revealed that a decrease of  $0.20\text{m/s}$  in diurnal average wind intensity in the city-centre resulted in a night-time UHI intensity of  $2.57^{\circ}\text{C}$ , while an increase of  $0.47\text{ m/s}$  in the sparsely built LCZ-9 was observed to have resulted in a nocturnal UHI intensity of  $0.32^{\circ}\text{C}$ . Knowing this new information, the urban planning agency of Toulouse can leverage on this knowledge to design more climate-sensitive urban neighbourhoods that would allow flow of natural wind ventilation which can contribute to the overall environmental sustainability and well-being of the entire city.



## 5.2 Implication of this study

A city-wide urban climate study such as this one in this research can help estimate the natural ventilation potential of a city and thus greatly assist city planning professionals incorporate climate knowledge to design and make data-driven decisions. By comparing in this study, the wind velocity ratio across various urban case scenarios, in addition to the mesoscale wind speed and nocturnal UHI across the different LCZs in the city, this thesis has contributed to the understanding of how to optimize the Toulouse urban climatic conditions to mitigate UHI effects and create liveable and sustainable urban environment in France. In addition, the urban breeze circulation visualized in this study can assist the environmental agency in the prediction of peak pollution perturbation pattern and the evaluation of air quality policy in the city and thus contribute to a more sus

Finally, it is important to mention here that the wind maps produced in this thesis is already been incorporated in a much bigger ongoing project by the Toulouse Metropole Planning Agency to understand the urban climate of the city.

## 5.3 Limitations of the Study

Upon completing this research, the following are some of the issues encountered:

- Whilst the 250 m x 250 m horizontal resolution of the Meso-NH data used in this thesis could be said to be appropriate for a city-wide urban climate study, it however has its limiting factor. Specifically, the resolution was too coarse and urban features such as roads and canals with less than 250m width are not fully resolved in the model. Thus, the results in this study is only limited to the mesoscale wind pattern and any small-scale wind effects cannot be inferred from this.
- Consequently, the U and V wind components used in this study are simulated at 10m above ground it is difficult to evaluate the wind flow pattern within the urban canopy.

## 5.4 Recommendations for Future Research

The following recommendations are suggested for future research:

- Firstly, since the analysis carried out in this research was based only on summer months heat island and wind intensity situations, thus, it is recommended that future study should examine more closely similar kind of analysis for the winter conditions. This will greatly help city planners investigate the seasonal changing effects of the wind flow on the thermal characteristics and pollution dispersion in the city,
- Further, given the low resolution of the model data used in this study, it is recommended that for future work, a much higher model resolution (possibly less than 100 m) should be simulated. While this would take up large computing resources and time to simulate over the entire city, it is therefore recommended that this higher resolution modelling could be simulated for much smaller portions of the city, such as areas with weaker wind intensity and high potential for extreme UHI intensity. This will provide a more detailed examination of the wind blocking areas in the centre and to better the wind dynamics at the district and neighbourhood scales,
- Lastly, it is recommended that for future study, the daytime UHI intensity should be considered as well. Also, other time periods, such as: late morning (09:00 - 12:00UTC) and late evening (19:00 - 22:00UTC) should be evaluated as well. This will further contribute to understanding the temporal evolution of the wind and thus give a holistic picture across the city,

## 6. REFERENCES

- ABREU-HARBICH, L., LABAKI, L.C. & MATZARAKIS, A., 2014. Thermal bioclimate in idealized urban street canyons in Campinas, Brazil. *Theoretical and Applied Climatology*. **115**(1), pp.333-340. Available from: 10.1007/s00704-013-0886-0.
- ADOLPHE, L., 2001. A Simplified Model of Urban Morphology: Application to an Analysis of the Environmental Performance of Cities. *Environment and Planning B: Planning and Design*. [viewed Apr 3, 2020]. Available from: 10.1068/b2631.
- AHMED, K.S., 2003. Comfort in urban spaces: defining the boundaries of outdoor thermal comfort for the tropical urban environments. *Energy and Buildings*. **35**(1), pp.103-110. [viewed Apr 6, 2020]. Available from: 10.1016/S0378-7788(02)00085-3.
- AKBARI, H., POMERANTZ, M. & TAHA, H., 2001. Cool surfaces and shade trees to reduce energy use and improve air quality in urban areas. *Solar Energy*. **70**(3), pp.295-310. [viewed Apr 3, 2020]. Available from: 10.1016/S0038-092X(00)00089-X.
- ALCOFORADO, M.J., ANDRADE, H. & VIERA, P., 2004. Weather and recreation at the Atlantic shore near Lisbon, Portugal: A study on applied local Climatology. In: A. MATZARAKIS, C. DE FREITAS and D. SCOTT eds., *Advances in Tourism Climatology* Freiburg: , pp. 38-48.
- BAKER, L.A., BRAZEL, A.J., SELOVER, N., MARTIN, C., MCINTYRE, N., STEINER, F.R., NELSON, A. & MUSACCHIO, L., 2002. Urbanization and warming of Phoenix (Arizona, USA): Impacts, feedbacks and mitigation. *Urban Ecosystems*. **6**(3), pp.183-203. Available from: 10.1023/A:1026101528700.
- BECHTEL, B., ALEXANDER, P.J., BÖHNER, J., CHING, J., CONRAD, O., FEDDEMA, J., MILLS, G., SEE, L. AND STEWART, I. (2015) Mapping local climate zones for a worldwide database of the form and function of cities. *ISPRS International Journal of Geo-Information*, **4**(1), 199–219.
- CANTAT, O., 2004. The Parisian urban heat island according to the types of weather. *Norois. Environnement, Aménagement, Société*. (191), pp.75-102. [viewed Apr 6, 2020]. Available from: 10.4000/norois.1373.
- CANTAT, O. & SAVOURET, E., 2013. L'évolution des « types de temps » depuis 1951 à Caen-Carpique (Basse-Normandie, France).
- CARREGA, P., 2004. Avant-propos sur les « types de temps ». *Norois. Environnement, Aménagement, Société*. (191), pp.7-9. [viewed Apr 8, 2020]. Available from: 10.4000/norois.982.
- EDUSSURIYA, P., CHAN, A. & YE, A., 2011. Urban morphology and air quality in dense residential environments in Hong Kong. Part I: District-level analysis. *Atmospheric Environment*. **45**(27), pp.4789-4803. [viewed Apr 3, 2020]. Available from: 10.1016/j.atmosenv.2009.07.061.

- ELIASSON, I., 2000. The use of climate knowledge in urban planning. *Landscape and Urban Planning*. **48**(1), pp.31-44. [viewed Apr 3, 2020]. Available from: 10.1016/S0169-2046(00)00034-7.
- ERELL, E., PEARLMUTTER, D. & WILLIAMSON, T., 2011. *Urban Microclimate : Designing the Spaces Between Buildings*. 1st ed. London: Routledge.
- FREW, T., BAKER, D. & DONEHUE, P., 2016. Performance based planning in Queensland: A case of unintended plan-making outcomes. *Land use Policy*. **50**, pp.239-251. [viewed Apr 3, 2020]. Available from: 10.1016/j.landusepol.2015.10.007.
- GELETI C, J. AND LEHNERT, M. (2016) GIS-based delineation of local climate zones: the case of medium-sized central European cities. *Moravian Geographical Reports*, 24(3), 2–12.
- GIANNOPOULOU, K., SANTAMOURIS, M., LIVADA, I., GEORGAKIS, C. & CAOURIS, Y., 2010. The Impact of Canyon Geometry on Intra Urban and Urban: Suburban Night Temperature Differences Under Warm Weather Conditions. *Pure and Applied Geophysics*. **167**(11), pp.1433-1449. Available from: 10.1007/s00024-010-0099-8.
- GOLANY, G.S., 1996. Urban design morphology and thermal performance. *Atmospheric Environment*. **30**(3), pp.455-465. [viewed Apr 6, 2020]. Available from: 10.1016/1352-2310(95)00266-9.
- HANG, J. & LI, Y., 2011. Age of air and air exchange efficiency in high-rise urban areas and its link to pollutant dilution. *Atmospheric Environment*. **45**(31), pp.5572-5585. [viewed Apr 3, 2020]. Available from: 10.1016/j.atmosenv.2011.04.051.
- HARLAN, S.L.; BRAZEL, A.J.; PRASHAD, L.; STEFANOV, W.L.; LARSEN, L. (2006). Neighbourhood microclimates and vulnerability to heat stress. *Soc. Sci. Med.* 2006, 63, 2847–2863.
- HE, B., 2018. Potentials of meteorological characteristics and synoptic conditions to mitigate urban heat island effects. *Urban Climate*. **24**, pp.26-33. Available from: <https://doi.org/10.1016/j.uclim.2018.01.004>.
- HIDALGO, J., MASSON, V. & PIGEON, G., 2008. Urban-breeze circulation during the CAPITOUL experiment: numerical simulations. *Meteorology and Atmospheric Physics*. **102**(3), pp.243. Available from: 10.1007/s00703-008-0345-0.
- HIDALGO, J., PIGEON, G. & MASSON, V., 2008. Urban-breeze circulation during the CAPITOUL experiment: observational data analysis approach. *Meteorology and Atmospheric Physics*. **102**(3), pp.223-241. Available from: 10.1007/s00703-008-0329-0.
- HIDALGO, J. & JOUGLA, R., 2018. On the use of local weather types classification to improve climate understanding: An application on the urban climate of Toulouse. *Plos One*. **13**(12), pp.e0208138. [viewed Apr 1, 2020]. Available from: 10.1371/journal.pone.0208138.

HIDALGO, J., MASSON, V. & BAEHR, C., 2014. From daily climatic scenarios to hourly atmospheric forcing fields to force Soil-Vegetation-Atmosphere transfer models. *Frontiers in Environmental Science*. **2** [viewed Apr 1, 2020]. Available from: 10.3389/fenvs.2014.00040.

HWANG, R., LIN, T. & MATZARAKIS, A., 2011. Seasonal effects of urban street shading on long-term outdoor thermal comfort. *Building and Environment*. **46**(4), pp.863-870. [viewed Apr 6, 2020]. Available from: 10.1016/j.buildenv.2010.10.017.

KATO, S. & HUANG, H., 2009. Ventilation efficiency of void space surrounded by buildings with wind blowing over built-up urban area. *Journal of Wind Engineering & Industrial Aerodynamics*. **7-8**(97), pp.358-367. [viewed Apr 6, 2020]. Available from: 10.1016/j.jweia.2009.05.003.

KIM, Y. & BAIK, J., 2002. Maximum Urban Heat Island Intensity in Seoul. *Journal of Applied Meteorology - J APPL METEOROL*. **41**, pp.651-659. Available from: 10.1175/1520-0450(2002)0412.0.CO;2.

KRESS, R., (1979). Regionale luftaustauschprozesse und ihre Bedeutung Fur die Raumliche planung. Dortmund, Germany.

KUBOTA, T., MIURA, M., TOMINAGA, Y. AND MOCHIDA, A.(2000) Wind tunnel tests on the nature of regional wind flow in the 270m square residential area, using the real model: Effects of arrangement and structural patterns of buildings on the nature of regional wind flow part 1. J. Archit. Plann. Environ. Eng. AI, No. 529, 109-116 (in Japanese).

KUBOTA, T., MIURA, M., TOMINAGA, Y. AND MOCHIDA, A. (2000) Standards of Gross Building Coverage ratio in major cities for the planning of residential areas in consideration of wind flow, effects of arrangement and structural Patterns of buildings on the nature of regional wind flow part 2. J. Archit. Plann. Environ. Eng. AI, No. 556, 107-114 (in Japanese)

KWOK YT, SCHOETTER R, LAU KK-L, ET AL. (2019). How well does the local climate zone scheme discern the thermal environment of Toulouse (France)? An analysis using numerical simulation data. *Int J Climatology*. 2019; 39:5292–5315. <https://doi.org/10.1002/joc.6140>

LESBEGUERIES, J., LACHICHE, N., BRAUD, A., SKUPINSKI, G., PUISSANT, A., PERRET, J. (2012). A platform for spatial data labeling in an urban context, Geospatial free and open source software in the 21st century (2012) 49–61

LEMONSU A. AND MASSON V. (2002). Simulation of a Summer Urban Breeze Over Paris. *Boundary Layer Meteorology* 104: 463-490.

MAPUCE., 2016. *Urban Climate Maps Strategy for MAPUCE*.

MAPUCE, 2019. MAPUCE final Project Report. Accessed on 10-08-2020. Available at [http://www.umn-cnm.fr/ville.climat/IMG/pdf/rapport\\_scientifique\\_mapuce\\_v1.2.pdf](http://www.umn-cnm.fr/ville.climat/IMG/pdf/rapport_scientifique_mapuce_v1.2.pdf)

MASSON V., 2000: A Physically-based scheme for the Urban Energy Budget in atmospheric models. *Boundary-Layer Meteorol.*, 94, 357-397

MASSON, V., GOMES, L., PIGEON, G., LIOUSSE, C., PONT, V., LAGOUARDE, J.-., VOOGT, J., SALMOND, J., OKE, T.R., HIDALGO, J., LEGAIN, D., GARROUSTE, O., LAC, C., CONNAN, O., BRIOTTET, X., LACHÉRADE, S. & TULET, P., 2008. The Canopy and Aerosol Particles Interactions in TOulouse Urban Layer (CAPITOUL) experiment. *Meteorology and Atmospheric Physics*. **102**(3), pp.135. Available from: 10.1007/s00703-008-0289-4.

MEMON, R.A. & LEUNG, D.Y.C., 2010. Impacts of environmental factors on urban heating. *Journal of Environmental Sciences*. **22**(12), pp.1903-1909. [viewed Apr 3, 2020]. Available from: 10.1016/S1001-0742(09)60337-5.

MORRIS, C.J.G., SIMMONDS, I. & PLUMMER, N., 2001. Quantification of the Influences of Wind and Cloud on the Nocturnal Urban Heat Island of a Large City. *Journal of Applied Meteorology*. **40**(2), pp.169-182. Available from: 10.1175/1520-0450(2001)0402.0.CO;2.

NG, E., YUAN, C., CHEN, L., REN, C., FUNG, J.C.H. (2011). Improving the wind environment in high-density cities by understanding urban morphology and surface roughness: a study in Hong Kong. *Landscape Urban Plan*, 101, 59-74. [accessed Jul 23 2020].

NIU, J., LIU, J., LEE, T., LIN, Z., MAK, C., TSE, K., TANG, B. & KWOK, K.C.S., 2015. A new method to assess spatial variations of outdoor thermal comfort: Onsite monitoring results and implications for precinct planning. *Building and Environment*. **91**, pp.263-270. [viewed Apr 3, 2020]. Available from: 10.1016/j.buildenv.2015.02.017.

OKE, T.R., 1987. *Boundary Layer Climates*. Second ed. Routledge.

OKE T (2005) Towards better scientific communication in urban climate. *Theor Appl Climatol*, 84: 179–90

R CORE TEAM 2019. R: A language and environment for statistical computing. R Foundation for Statistical Computing, Vienna, Austria. URL <https://www.R-project.org/>.

RAJAGOPALAN, P., HIEN, W.N. & WAI DAVID, C.K., 2008. Microclimatic modeling of the urban thermal environment of Singapore to mitigate urban heat island. *Solar Energy*. **82**(8), pp.727-745. [viewed Apr 6, 2020]. Available from: 10.1016/j.solener.2008.02.008.

RAJAGOPALAN, P., LIM, K.C. & JAMEI, E., 2014a. Urban heat island and wind flow characteristics of a tropical city. *Solar Energy*. **107**, pp.159-170. Available from: <https://doi.org/10.1016/j.solener.2014.05.042>.

RAJAGOPALAN, P., LIM, K.C. & JAMEI, E., 2014b. Urban heat island and wind flow characteristics of a tropical city. *Solar Energy*. **107**, pp.159-170. Available from: 10.1016/j.solener.2014.05.042.

SANTAMOURIS, M., DING, L., FIORITO, F., OLDFIELD, P., OSMOND, P., PAOLINI, R., PRASAD, D. & SYNNEFA, A., 2017. Passive and active cooling for the outdoor built environment – Analysis and assessment of the cooling potential of mitigation technologies



using performance data from 220 large scale projects. *Solar Energy*. **154**, pp.14-33. [viewed Apr 3, 2020]. Available from: 10.1016/j.solener.2016.12.006.

SANTAMOURIS, M. & GEORGAKIS, C., 2003. Energy and indoor climate in urban environments: recent trends. *Building Services Engineering Research and Technology*. **24**(2), pp.69-81. Available from: 10.1191/0143624403bt065oa.

SANTAMOURIS, M., GEORGAKIS, C. & NIACHOU, A., 2008. On the estimation of wind speed in urban canyons for ventilation purposes—Part 2: Using of data driven techniques to calculate the more probable wind speed in urban canyons for low ambient wind speeds. *Building and Environment*. **43**(8), pp.1411-1418. Available from: <https://doi.org/10.1016/j.buildenv.2007.01.042>.

SANTAMOURIS, M., 2011. Heat Island Research in Europe: The State of the Art. *Advances in Building Energy Research*. **1**(1), pp.123-150. [viewed Apr 3, 2020]. Available from: 10.1080/17512549.2007.9687272.

SANTAMOURIS, M. & KOLOKOTSA, D., 2016. *Urban Climate Mitigation Techniques*. 1st ed. Location: Routledge.

SHASHUA-BAR, L., TZAMIR, Y. & HOFFMAN, M.E., 2004. Thermal effects of building geometry and spacing on the urban canopy layer microclimate in a hot-humid climate in summer. *International Journal of Climatology*. **24**(13), pp.1729-1742. [viewed Apr 6, 2020]. Available from: 10.1002/joc.1092.

SHEPHERD, J.M., 2005. A Review of Current Investigations of Urban-Induced Rainfall and Recommendations for the Future. *Earth Interactions*. **9**(12), pp.1-27. Available from: 10.1175/EI156.1.

SHIRZADI, M., NAGHASHZADEGAN, M. & A. MIRZAEI, P., 2018. Improving the CFD modelling of cross-ventilation in highly-packed urban areas. *Sustainable Cities and Society*. **37**, pp.451-465. [viewed Apr 3, 2020]. Available from: 10.1016/j.scs.2017.11.020.

STATHOPOULOS, T., WU, H. & ZACHARIAS, J., 2004. Outdoor human comfort in an urban climate. *Building and Environment*. **39**(3), pp.297-305. [viewed Apr 3, 2020]. Available from: 10.1016/j.buildenv.2003.09.001.

STEWART, I.D. & OKE, T.R., 2012. Local Climate Zones for Urban Temperature Studies. *Bulletin of the American Meteorological Society*. **93**(12), pp.1879-1900. Available from: 10.1175/BAMS-D-11-00019.1.

STEWART, I.D. AND T.R. OKE, (2009). Classifying urban climate field sites by ‘local climate zone’. The case of Nagana Japan. The seventh international conference on Urban climate, 29 June - 3 July 2009, Yokohama, Japan.

STEWART, I. D. (2011). Redefining the Urban Heat Island, PhD Thesis, University of British Columbia (<https://circle.ubc.ca/handle/2429/38069>, accessed June 8, 2020)

STEWART, I.D., OKE, T.R. AND KRAYENHOFF, E.S. (2014) Evaluation of the “local climate zone” scheme using temperature observations and model simulations. *International Journal of Climatology*, 34(4), 1062–1080.

SKARBIT, N., STEWART, I.D., UNGER, J. AND GÁL, T. (2017) Employing an urban meteorological network to monitor air temperature conditions in the “local climate zones” of Szeged, Hungary. *International Journal of Climatology*, 37(S1), 582–596.

TALEB, D. & ABU-HIJLEH, B., 2013. Urban heat islands: Potential effect of organic and structured urban configurations on temperature variations in Dubai, UAE. *Renewable Energy*. **50**, pp.747-762. [viewed Apr 6, 2020]. Available from: 10.1016/j.renene.2012.07.030.

VOOGT, J.A. & OKE, T.R., 2003. Thermal remote sensing of urban climates. *Remote Sensing of Environment*. **86**(3), pp.370-384. [viewed Apr 5, 2020]. Available from: 10.1016/S0034-4257(03)00079-8.

WANG, X., LI, Y. & HANG, J., 2017. A combined fully-resolved and porous approach for building cluster wind flows. *Building Simulation*. **10**(1), pp.97-109. Available from: 10.1007/s12273-016-0305-4.

WATTS, N., AMANN, M., AYEB-KARLSSON, S., BELESOVA, K., BOULEY, T., BOYKOFF, M., BYASS, P., CAI, W., CAMPBELL-LENDRUM, D., CHAMBERS, J., COX, P.M., DALY, M., DASANDI, N., DAVIES, M., DEPLEDGE, M., DEPOUX, A., DOMINGUEZ-SALAS, P., DRUMMOND, P., EKINS, P., FLAHAULT, A., FRUMKIN, H., GEORGESON, L., GHANEI, M., GRACE, D., GRAHAM, H., GROJSMAN, R., HAINES, A., HAMILTON, I., HARTINGER, S., JOHNSON, A., KELMAN, I., KIESEWETTER, G., KNIVETON, D., LIANG, L., LOTT, M., LOWE, R., MACE, G., SEWE, M.O., MASLIN, M., MIKHAYLOV, S., MILNER, J., LATIFI, A.M., MORADI-LAKEH, M., MORRISSEY, K., MURRAY, K., NEVILLE, T., NILSSON, M., ORESZCZYN, T., OWFI, F., PENCHEON, D., PYE, S., RABBANIHA, M., ROBINSON, E., ROCKLÖV, J., SCHÜTTE, S., SHUMAKE-GUILLEMOT, J., STEINBACH, R., TABATABAEI, M., WHEELER, N., WILKINSON, P., GONG, P., MONTGOMERY, H. & COSTELLO, A., 2018. The Lancet Countdown on health and climate change: from 25 years of inaction to a global transformation for public health. *The Lancet*. **391**(10120), pp.581-630. [viewed Apr 3, 2020]. Available from: 10.1016/S0140-6736(17)32464-9.

WIJEYESEKERA, DEVAPRIYA & NAZARI, BAHAREH & LIM, SIN & ZAINORABIDIN, ADNAN & A, JOHN. (2012). Investigation into the Urban Heat Island effects from Asphalt Pavements. SSRN Electronic Journal. ISSN 1923-6662.

WMO (2018). Chapter 5: Measurement of Surface Wind. Available at: [https://www.wmo.int/pages/prog/www/IMOP/publications/CIMO-Guide/Prelim 2018 ed/8 I 5 en MR clean.pdf](https://www.wmo.int/pages/prog/www/IMOP/publications/CIMO-Guide/Prelim%202018%20ed/8%20I%205%20en%20MR%20clean.pdf)

WMO., 2019 *European heatwave sets new temperature records*. [viewed Apr 1, 2020]. Available from: <https://public.wmo.int/en/media/news/european-heatwave-sets-new-temperature-records>.

WONG, N.H. & YU, C., 2005. Study of green areas and urban heat island in a tropical city. *Habitat International*. **29**(3), pp.547-558. [viewed Apr 3, 2020]. Available from: 10.1016/j.habitatint.2004.04.008.

YANG, L. & LI, Y., 2011. Thermal conditions and ventilation in an ideal city model of Hong Kong. *Energy and Buildings*. **43**(5), pp.1139-1148. [viewed Apr 6, 2020]. Available from: 10.1016/j.enbuild.2010.06.005.

YIM, S.H.L., FUNG, J.C.H., LAU, A.K.H. & KOT, S.C., 2009. Air ventilation impacts of the “wall effect” resulting from the alignment of high-rise buildings. *Atmospheric Environment*. **43**(32), pp.4982-4994. [viewed Apr 3, 2020]. Available from: 10.1016/j.atmosenv.2009.07.002.

ZHANG, Y., GU, Z., CHENG, Y. & LEE, S., 2011. Effect of real-time boundary wind conditions on the air flow and pollutant dispersion in an urban street canyon—Large eddy simulations. *Atmospheric Environment*. **45**(20), pp.3352-3359. [viewed Apr 6, 2020]. Available from: 10.1016/j.atmosenv.2011.03.055.

# APPENDIX

# APPENDIX I

## Local Weather Types Classification

2192 2004-01-01 0	2219 2004-01-28 3	2246 2004-02-24 0	2273 2004-03-22 3	2300 2004-04-18 5
2193 2004-01-02 3	2220 2004-01-29 3	2247 2004-02-25 5	2274 2004-03-23 3	2301 2004-04-19 2
2194 2004-01-03 3	2221 2004-01-30 5	2248 2004-02-26 3	2275 2004-03-24 3	2302 2004-04-20 9
2195 2004-01-04 0	2222 2004-01-31 5	2249 2004-02-27 0	2276 2004-03-25 3	2303 2004-04-21 2
2196 2004-01-05 9	2223 2004-02-01 5	2250 2004-02-28 3	2277 2004-03-26 3	2304 2004-04-22 6
2197 2004-01-06 0	2224 2004-02-02 5	2251 2004-02-29 3	2278 2004-03-27 0	2305 2004-04-23 3
2198 2004-01-07 5	2225 2004-02-03 5	2252 2004-03-01 3	2279 2004-03-28 5	2306 2004-04-24 9
2199 2004-01-08 5	2226 2004-02-04 5	2253 2004-03-02 3	2280 2004-03-29 2	2307 2004-04-25 9
2200 2004-01-09 10	2227 2004-02-05 5	2254 2004-03-03 9	2281 2004-03-30 2	2308 2004-04-26 9
2201 2004-01-10 4	2228 2004-02-06 5	2255 2004-03-04 9	2282 2004-03-31 1	2309 2004-04-27 1
2202 2004-01-11 8	2229 2004-02-07 0	2256 2004-03-05 0	2283 2004-04-01 2	2310 2004-04-28 4
2203 2004-01-12 1	2230 2004-02-08 9	2257 2004-03-06 6	2284 2004-04-02 0	2311 2004-04-29 6
2204 2004-01-13 0	2231 2004-02-09 9	2258 2004-03-07 3	2285 2004-04-03 9	2312 2004-04-30 0
2205 2004-01-14 6	2232 2004-02-10 9	2259 2004-03-08 3	2286 2004-04-04 9	2313 2004-05-01 5
2206 2004-01-15 0	2233 2004-02-11 9	2260 2004-03-09 9	2287 2004-04-05 3	2314 2004-05-02 1
2207 2004-01-16 5	2234 2004-02-12 9	2261 2004-03-10 9	2288 2004-04-06 3	2315 2004-05-03 8
2208 2004-01-17 6	2235 2004-02-13 5	2262 2004-03-11 5	2289 2004-04-07 3	2316 2004-05-04 3
2209 2004-01-18 3	2236 2004-02-14 9	2263 2004-03-12 5	2290 2004-04-08 0	2317 2004-05-05 3
2210 2004-01-19 3	2237 2004-02-15 3	2264 2004-03-13 6	2291 2004-04-09 3	2318 2004-05-06 3
2211 2004-01-20 3	2238 2004-02-16 3	2265 2004-03-14 5	2292 2004-04-10 3	2319 2004-05-07 3
2212 2004-01-21 3	2239 2004-02-17 0	2266 2004-03-15 5	2293 2004-04-11 3	2320 2004-05-08 3
2213 2004-01-22 3	2240 2004-02-18 3	2267 2004-03-16 5	2294 2004-04-12 3	2321 2004-05-09 9
2214 2004-01-23 6	2241 2004-02-19 3	2268 2004-03-17 2	2295 2004-04-13 3	2322 2004-05-10 0
2215 2004-01-24 6	2242 2004-02-20 2	2269 2004-03-18 9	2296 2004-04-14 0	2323 2004-05-11 9
2216 2004-01-25 5	2243 2004-02-21 5	2270 2004-03-19 3	2297 2004-04-15 5	2324 2004-05-12 6
2217 2004-01-26 6	2244 2004-02-22 3	2271 2004-03-20 3	2298 2004-04-16 6	2325 2004-05-13 2
2218 2004-01-27 3	2245 2004-02-23 0	2272 2004-03-21 3	2299 2004-04-17 0	2326 2004-05-14 3

2327 2004-05-15 9	2356 2004-06-13 9	2385 2004-07-12 2	2414 2004-08-10 7	2443 2004-09-08 7
2328 2004-05-16 9	2357 2004-06-14 9	2386 2004-07-13 9	2415 2004-08-11 7	2444 2004-09-09 7
2329 2004-05-17 7	2358 2004-06-15 9	2387 2004-07-14 9	2416 2004-08-12 8	2445 2004-09-10 1
2330 2004-05-18 7	2359 2004-06-16 8	2388 2004-07-15 9	2417 2004-08-13 8	2446 2004-09-11 8
2331 2004-05-19 9	2360 2004-06-17 8	2389 2004-07-16 7	2418 2004-08-14 7	2447 2004-09-12 8
2332 2004-05-20 7	2361 2004-06-18 9	2390 2004-07-17 2	2419 2004-08-15 7	2448 2004-09-13 7
2333 2004-05-21 7	2362 2004-06-19 6	2391 2004-07-18 7	2420 2004-08-16 8	2449 2004-09-14 8
2334 2004-05-22 4	2363 2004-06-20 3	2392 2004-07-19 7	2421 2004-08-17 1	2450 2004-09-15 8
2335 2004-05-23 9	2364 2004-06-21 5	2393 2004-07-20 8	2422 2004-08-18 7	2451 2004-09-16 9
2336 2004-05-24 5	2365 2004-06-22 7	2394 2004-07-21 7	2423 2004-08-19 8	2452 2004-09-17 9
2337 2004-05-25 2	2366 2004-06-23 8	2395 2004-07-22 7	2424 2004-08-20 8	2453 2004-09-18 5
2338 2004-05-26 9	2367 2004-06-24 8	2396 2004-07-23 8	2425 2004-08-21 8	2454 2004-09-19 8
2339 2004-05-27 8	2368 2004-06-25 8	2397 2004-07-24 8	2426 2004-08-22 7	2455 2004-09-20 8
2340 2004-05-28 9	2369 2004-06-26 7	2398 2004-07-25 9	2427 2004-08-23 7	2456 2004-09-21 8
2341 2004-05-29 9	2370 2004-06-27 8	2399 2004-07-26 9	2428 2004-08-24 8	2457 2004-09-22 9
2342 2004-05-30 8	2371 2004-06-28 8	2400 2004-07-27 9	2429 2004-08-25 8	2458 2004-09-23 9
2343 2004-05-31 8	2372 2004-06-29 9	2401 2004-07-28 7	2430 2004-08-26 8	2459 2004-09-24 8
2344 2004-06-01 8	2373 2004-06-30 9	2402 2004-07-29 8	2431 2004-08-27 9	2460 2004-09-25 3
2345 2004-06-02 8	2374 2004-07-01 8	2403 2004-07-30 8	2432 2004-08-28 8	2461 2004-09-26 3
2346 2004-06-03 3	2375 2004-07-02 9	2404 2004-07-31 9	2433 2004-08-29 8	2462 2004-09-27 9
2347 2004-06-04 9	2376 2004-07-03 9	2405 2004-08-01 7	2434 2004-08-30 8	2463 2004-09-28 9
2348 2004-06-05 8	2377 2004-07-04 7	2406 2004-08-02 4	2435 2004-08-31 8	2464 2004-09-29 5
2349 2004-06-06 7	2378 2004-07-05 8	2407 2004-08-03 8	2436 2004-09-01 7	2465 2004-09-30 9
2350 2004-06-07 2	2379 2004-07-06 1	2408 2004-08-04 8	2437 2004-09-02 7	2466 2004-10-01 7
2351 2004-06-08 7	2380 2004-07-07 8	2409 2004-08-05 8	2438 2004-09-03 7	2467 2004-10-02 7
2352 2004-06-09 5	2381 2004-07-08 2	2410 2004-08-06 7	2439 2004-09-04 7	2468 2004-10-03 7
2353 2004-06-10 7	2382 2004-07-09 9	2411 2004-08-07 7	2440 2004-09-05 7	2469 2004-10-04 2
2354 2004-06-11 8	2383 2004-07-10 8	2412 2004-08-08 7	2441 2004-09-06 2	2470 2004-10-05 2
2355 2004-06-12 8	2384 2004-07-11 3	2413 2004-08-09 7	2442 2004-09-07 1	2471 2004-10-06 8



2472 2004-10-07 7	2501 2004-11-05 0	2530 2004-12-04 0	2559 2005-01-02 3	2559 2005-01-02 3
2473 2004-10-08 2	2502 2004-11-06 3	2531 2004-12-05 3	2560 2005-01-03 0	2560 2005-01-03 0
2474 2004-10-09 4	2503 2004-11-07 3	2532 2004-12-06 0	2561 2005-01-04 5	2561 2005-01-04 5
2475 2004-10-10 7	2504 2004-11-08 0	2533 2004-12-07 0	2562 2005-01-05 9	2562 2005-01-05 9
2476 2004-10-11 1	2505 2004-11-09 6	2534 2004-12-08 0	2563 2005-01-06 5	2563 2005-01-06 5
2477 2004-10-12 1	2506 2004-11-10 3	2535 2004-12-09 0	2564 2005-01-07 5	2564 2005-01-07 5
2478 2004-10-13 5	2507 2004-11-11 6	2536 2004-12-10 0	2565 2005-01-08 5	2565 2005-01-08 5
2479 2004-10-14 3	2508 2004-11-12 0	2537 2004-12-11 5	2566 2005-01-09 5	2566 2005-01-09 5
2480 2004-10-15 6	2509 2004-11-13 3	2538 2004-12-12 5	2567 2005-01-10 2	2567 2005-01-10 2
2481 2004-10-16 4	2510 2004-11-14 3	2539 2004-12-13 5	2568 2005-01-11 5	2568 2005-01-11 5
2482 2004-10-17 5	2511 2004-11-15 3	2540 2004-12-14 5	2569 2005-01-12 5	2569 2005-01-12 5
2483 2004-10-18 7	2512 2004-11-16 3	2541 2004-12-15 9	2570 2005-01-13 0	2570 2005-01-13 0
2484 2004-10-19 7	2513 2004-11-17 3	2542 2004-12-16 5	2571 2005-01-14 5	2571 2005-01-14 5
2485 2004-10-20 2	2514 2004-11-18 0	2543 2004-12-17 3	2572 2005-01-15 5	2572 2005-01-15 5
2486 2004-10-21 8	2515 2004-11-19 3	2544 2004-12-18 3	2573 2005-01-16 5	2573 2005-01-16 5
2487 2004-10-22 7	2516 2004-11-20 0	2545 2004-12-19 6	2574 2005-01-17 5	2574 2005-01-17 5
2488 2004-10-23 2	2517 2004-11-21 5	2546 2004-12-20 3	2575 2005-01-18 6	2575 2005-01-18 6
2489 2004-10-24 2	2518 2004-11-22 5	2547 2004-12-21 5	2576 2005-01-19 3	2576 2005-01-19 3
2490 2004-10-25 4	2519 2004-11-23 0	2548 2004-12-22 0	2577 2005-01-20 3	2577 2005-01-20 3
2491 2004-10-26 6	2520 2004-11-24 0	2549 2004-12-23 3	2578 2005-01-21 3	2578 2005-01-21 3
2492 2004-10-27 5	2521 2004-11-25 5	2550 2004-12-24 0	2579 2005-01-22 3	2579 2005-01-22 3
2493 2004-10-28 5	2522 2004-11-26 0	2551 2004-12-25 3	2580 2005-01-23 3	2580 2005-01-23 3
2494 2004-10-29 4	2523 2004-11-27 5	2552 2004-12-26 3	2581 2005-01-24 3	2581 2005-01-24 3
2495 2004-10-30 5	2524 2004-11-28 5	2553 2004-12-27 3	2582 2005-01-25 3	2582 2005-01-25 3
2496 2004-10-31 6	2525 2004-11-29 3	2554 2004-12-28 3	2583 2005-01-26 3	2583 2005-01-26 3
2497 2004-11-01 0	2526 2004-11-30 0	2555 2004-12-29 3	2584 2005-01-27 3	2584 2005-01-27 3
2498 2004-11-02 5	2527 2004-12-01 2	2556 2004-12-30 3	2585 2005-01-28 3	2585 2005-01-28 3
2499 2004-11-03 5	2528 2004-12-02 5	2557 2004-12-31 3	2586 2005-01-29 3	2586 2005-01-29 3
2500 2004-11-04 9	2529 2004-12-03 0	2558 2005-01-01 3	2587 2005-01-30 3	2587 2005-01-30 3

2588 2005-01-31 3	2603 2005-02-15 3
2589 2005-02-01 3	2604 2005-02-16 3
2590 2005-02-02 3	2605 2005-02-17 3
2591 2005-02-03 3	2606 2005-02-18 3
2592 2005-02-04 0	2607 2005-02-19 3
2593 2005-02-05 5	2608 2005-02-20 3
2594 2005-02-06 5	2609 2005-02-21 3
2595 2005-02-07 2	2610 2005-02-22 5
2596 2005-02-08 2	2611 2005-02-23 0
2597 2005-02-09 5	2612 2005-02-24 0
2598 2005-02-10 0	2613 2005-02-25 5
2599 2005-02-11 9	2614 2005-02-26 9
2600 2005-02-12 2	2615 2005-02-27 3
2601 2005-02-13 6	2616 2005-02-28 3
2602 2005-02-14 3	

# APPENDIX II

## R Script used in the study

### Preparatory Script for Wind Analysis

Full Script available for download at:

[https://drive.google.com/drive/folders/1hGu9F0SJSshTn16IqLcbRNZN\\_RuCMNnx?usp=sharing](https://drive.google.com/drive/folders/1hGu9F0SJSshTn16IqLcbRNZN_RuCMNnx?usp=sharing)

```
1 ##### PREPARATORY SCRIPT FOR WIND #####
2 ##### H. Ibitolu 20200526 #####
3 #####
4 #####
5
6 ## This script is the pre-treatment for the wind data Analysis.
7 ## This script loads the wind data and aggregates for 36 hours for each day of the LWT occurrence
8
9 #HI
10 setwd("D:/Toulouse_CNRS/Internship_January/Data/for_Henry/03_Toulouse_CAPITOUL_250m_untar/")
11 source("D:/Toulouse_CNRS/Internship_January/Data/for_Henry/03_Toulouse_CAPITOUL_250m_untar/FFDuv.R")
12
13 # #JH
14 # setwd('/media/julia/My Passport/work/PROYECTOS_en_curso/MAPUCE/13_Simulations_Robert/Robert_simulations2018/06_carto_3H/02_online20180717/')
15 # source('01_Scripts/FFDuv.R')
16
17 #This is the start and end date
18 date_start = "2004-03-01"
19 date_end = "2005-02-28"
20
21 #HI
22 rep_base = "D:/Toulouse_CNRS/Internship_January/Data/for_Henry/03_Toulouse_CAPITOUL_250m_untar/"
23 #JH
24 #rep_base = '03_Toulouse_CAPITOUL_250m_untar/'
25
26 # Reading LWT prduced in the Article of Hidalgo et al. (2014)
27 #HI
28 weather_types_file = read.table(paste(rep_base,"weathertypes_Toulouse_Hidalgo_etal_2014.txt",sep=""))
29 #JH
30 #weather_types_file = read.table(paste(rep_base,"Weather_Types_Toulouse_Hidalgo_etal_2014.txt",sep=""))
31 ind_start = which(as.character(weather_types_file[,2])==date_start) ### This describes the starting point for the LWT base on the date_start
32 weather_types_file = weather_types_file[-(1:(ind_start-1)),]
33
34 #This creates the folder to store the results
35 dir.create('results/')
36 dir.create('results/data_main/')
37
38
39 ##### Here, we assigned the variable needed. Where tt_trait = The weather_type variable needed (i.e- from 1:10),
40 ##### and sais_trait = Seasons Variable (i.e- 4 seasons 1:4 )
41 ##### This sample script assumes we want to select LWT= 7 for the Summer (Jun,Jul,Aug) season
42
43
44 tt_temp = c(7,8,9) ###For LWT number X
45 sais_trait = 3 ###For Summer season
46 #varlab = c('UMME') # test for one variable
47 varlab = c('UMME', 'VMME')
48
49
50 for (lwt in 1:length(tt_temp)) { #This iterates for each LWT
51   tt_trait = tt_temp[lwt]
52   print(paste("LWT", tt_trait))
53
54   for (v in 1:length(variab)) { # for each variable
55     var = variab[v]
56     print(var)
57
58     for (t in 1:length(tt_trait)) {#for each LWT
59       ti=Sys.time()
60       tt = tt_trait[t]
61       print('TT')
62       print(tt)
63     }
64   }
65
66   uu_TT = NULL
67   vv_TT = NULL
68   var_TT = NULL
69   dates_tt = NULL
70   ind_tt = which(weather_types_file[,3]==tt)# LWT index
71   print("ind_tt")
72   print(ind_tt) # There are 50 days of LWT 9 in the simulation, those are the index 3 4 9 10 18 34 35 51 55 56 57 70 72 76 77 80 84 87 89 90 96 105 106 107 110 121
73   # 122 124 125 131 135 136 137 147 148 149 153 180 200 201 206 207 211 212 214 249 290 311 348 363
74
75   if (length(ind_tt)!=0) {
76     dates = weather_types_file[ind_tt,2]#dates du TT dans toute la serie de simulations
77     dates = paste(substring(as.character(dates),1,4),substring(as.character(dates),6,7),substring(as.character(dates),9,10),sep='')#dates en caracter
78     mois = substring(dates,5,6) #extraction des mois
79
80     print("dates")
81     print(dates) # those are the dates for LWT 9 "20040303" "20040304" "20040309" "20040310" "20040318" "20040403" "20040404" "20040420" "20040424" "20040425" "20040426" "20040509"
82     # "20040511" "20040515" "20040516" "20040519" "20040523" "20040526" "20040528" "20040529" "20040604" "20040613" "20040614" "20040615" "20040618" "20040629" "20040630" "20040702"
83     # "20040703" "20040709" "20040713" "20040714" "20040715" "20040725" "20040726" "20040727" "20040731" "20040827" "20040916" "20040917" "20040922" "20040923" "20040927" "20040928"
84     # "20040930" "20041104" "20041215" "20050105" "20050211" "20050226"
85
86     # reading the data: 41 directories each containing directories with dates and then data
87     print("Now start reading in the files from 1:41")
88     # for (i in 1:1) {#test for first directory where there are 3 LWT days "20040303" "20040304" "20040309"
89     for (i in 1:41) {
90       print(paste('i =',i))
91       rep = paste(rep_base,"TIME_DEP_PART_",i,sep='')
92       for (j in 1:length(list.files(rep))) { # j is the day, there are 9 days in each directory i
93         print(paste('j =',j))
94         rep_date = list.files(rep)[j]
95         if (rep_date!="20050228") {
96           ind_date = which(dates==rep_date) #how many LWT dates are in this directory ?
97           print('ind_date =')
98           print (ind_date)
99           if (length(ind_date)!=0) {# if there are one or more load the data
100             dates_tt = c(dates_tt,dates[ind_date])
101             print('dates_tt =')
102             print(dates_tt)
103             load(paste(rep,'/',rep_date,'/REFER/',var,sep=""))
104             var_temp = LSTsvals_day
105             print(var_temp[1,])
106
107             if (j!=length(list.files(rep))) { # if i'm not in the last file of the directory I also load the day j+1
108               rep_date_temp = list.files(rep)[j+1]
109               load(paste(rep,'/',rep_date_temp,'/REFER/',var,sep=""))
110               var_temp = cbind(var_temp,LSTsvals_day)
111               print('im not in the last file of the directory so I load also the day j+1')
112               print('rep_date_temp')
113               print (rep_date_temp)
114             }
115             print(var_temp[1,])
116
117             else { # if im already in the last day (j=9) of the repertory i, I take the first day of the repertory i+1
118               if (i!=41) {
119                 print('Im here i=41')
120                 rep_temp = paste(rep_base,"TIME_DEP_PART_",i+1,sep='')
121                 rep_date_temp = list.files(rep_temp)[1]
122                 load(paste(rep_temp,'/',rep_date_temp,'/REFER/',var,sep=""))
123                 var_temp = cbind(var_temp,LSTsvals_day)
124                 print('rep_temp')
125                 print(rep_temp)
126                 print('rep_date_temp')
127                 print(rep_date_temp)
128                 print('dim(var_temp)')
129                 print(dim(var_temp))
130               }
131             }
132           }
133         }
134       }
135     }
136   }
137 }
138
139
140
141
142
143
144
145
146
147
148
149
150
151
152
153
154
155
156
157
158
159
160
161
162
163
164
165
166
167
168
169
170
171
172
173
174
175
176
177
178
179
180
181
182
183
184
185
186
187
188
189
190
191
192
193
194
195
196
197
198
199
200
201
202
203
204
205
206
207
208
209
210
211
212
213
214
215
216
217
218
219
220
221
222
223
224
225
226
227
228
229
230
231
232
233
234
235
236
237
238
239
240
241
242
243
244
245
246
247
248
249
250
251
252
253
254
255
256
257
258
259
260
261
262
263
264
265
266
267
268
269
270
271
272
273
274
275
276
277
278
279
280
281
282
283
284
285
286
287
288
289
290
291
292
293
294
295
296
297
298
299
300
301
302
303
304
305
306
307
308
309
310
311
312
313
314
315
316
317
318
319
320
321
322
323
324
325
326
327
328
329
330
331
332
333
334
335
336
337
338
339
340
341
342
343
344
345
346
347
348
349
350
351
352
353
354
355
356
357
358
359
360
361
362
363
364
365
366
367
368
369
370
371
372
373
374
375
376
377
378
379
380
381
382
383
384
385
386
387
388
389
390
391
392
393
394
395
396
397
398
399
400
401
402
403
404
405
406
407
408
409
410
411
412
413
414
415
416
417
418
419
420
421
422
423
424
425
426
427
428
429
430
431
432
433
434
435
436
437
438
439
440
441
442
443
444
445
446
447
448
449
450
451
452
453
454
455
456
457
458
459
460
461
462
463
464
465
466
467
468
469
470
471
472
473
474
475
476
477
478
479
480
481
482
483
484
485
486
487
488
489
490
491
492
493
494
495
496
497
498
499
500
501
502
503
504
505
506
507
508
509
510
511
512
513
514
515
516
517
518
519
520
521
522
523
524
525
526
527
528
529
530
531
532
533
534
535
536
537
538
539
540
541
542
543
544
545
546
547
548
549
550
551
552
553
554
555
556
557
558
559
560
561
562
563
564
565
566
567
568
569
570
571
572
573
574
575
576
577
578
579
580
581
582
583
584
585
586
587
588
589
590
591
592
593
594
595
596
597
598
599
600
601
602
603
604
605
606
607
608
609
610
611
612
613
614
615
616
617
618
619
620
621
622
623
624
625
626
627
628
629
630
631
632
633
634
635
636
637
638
639
640
641
642
643
644
645
646
647
648
649
650
651
652
653
654
655
656
657
658
659
660
661
662
663
664
665
666
667
668
669
670
671
672
673
674
675
676
677
678
679
680
681
682
683
684
685
686
687
688
689
690
691
692
693
694
695
696
697
698
699
700
701
702
703
704
705
706
707
708
709
710
711
712
713
714
715
716
717
718
719
720
721
722
723
724
725
726
727
728
729
730
731
732
733
734
735
736
737
738
739
740
741
742
743
744
745
746
747
748
749
750
751
752
753
754
755
756
757
758
759
760
761
762
763
764
765
766
767
768
769
770
771
772
773
774
775
776
777
778
779
780
781
782
783
784
785
786
787
788
789
790
791
792
793
794
795
796
797
798
799
800
801
802
803
804
805
806
807
808
809
810
811
812
813
814
815
816
817
818
819
820
821
822
823
824
825
826
827
828
829
830
831
832
833
834
835
836
837
838
839
840
841
842
843
844
845
846
847
848
849
850
851
852
853
854
855
856
857
858
859
860
861
862
863
864
865
866
867
868
869
870
871
872
873
874
875
876
877
878
879
880
881
882
883
884
885
886
887
888
889
890
891
892
893
894
895
896
897
898
899
900
901
902
903
904
905
906
907
908
909
910
911
912
913
914
915
916
917
918
919
920
921
922
923
924
925
926
927
928
929
930
931
932
933
934
935
936
937
938
939
940
941
942
943
944
945
946
947
948
949
950
951
952
953
954
955
956
957
958
959
960
961
962
963
964
965
966
967
968
969
970
971
972
973
974
975
976
977
978
979
980
981
982
983
984
985
986
987
988
989
990
991
992
993
994
995
996
997
998
999
1000
```

```

128 print(dim(var_temp))
129 print(var_temp[1,])
130 }
131 } # if im in the last day (j=9) of i=41 I finish
132 if (dim(var_temp)[1]>24) {var_TT = cbind(var_TT,var_temp[,1:36])} # 36h wanted (from 01h UTC for day j to 12h UTC for the day j+1)
133 print('I select 36h per LWT')
134 print(var_TT[1,])
135 }
136 print(paste('dim(var_TT)', dim(var_TT)))# 57600 grid points, 1800 (=50 days x 36 hours)
137 } # # end condition if (length(ind_dat)!=0)
138 } # end condition if (rep_date!="20050228")
139 } # end boolean statement for j
140 } # end boolean statement for i
141 }
142 # from here the important matrix are dates_tt and var_TT 57600 grid points, 1800 (=50 days x 36 hours)
143 # "dates_tt = "20040303" "20040304" "20040309" "20040310" "20040318" "20040403" "20040404" "20040420" "20040424" "20040425" "20040426" "20040509" "20040511" "20040515" "20040516" "20040519"
144 # "20040523" "20040526" "20040528" "20040529" "20040604" "20040613" "20040614" "20040615" "20040618" "20040629" "20040630" "20040702" "20040703" "20040709" "20040713" "20040714" "20040715"
145 # "20040725" "20040726" "20040727" "20040731" "20040827" "20040916" "20040917" "20040922" "20040923" "20040927" "20040928" "20040930" "20041104" "20041215" "20050105" "20050211" "20050226"
146 }
147 ### This is to extract the dates that the particular weather type occurred for a particular season
148 mois = substring(dates_tt,5,6)
149 ind_djf = which(mois=="12" | mois=="01" | mois=="02")
150 ind_mam = which(mois=="03" | mois=="04" | mois=="05")
151 ind_jja = which(mois=="06" | mois=="07" | mois=="08")
152 ind_son = which(mois=="09" | mois=="10" | mois=="11")
153 }
154 for (s in 1:length(sais_trait)) {
155   sais = sais_trait[s]
156   print(paste('sais',sais)) # 18 days for LWT 9 -> 21 22 23 24 25 26 27 28 29 30 31 32 33 34 35 36 37 38
157 }
158 if (sais==1) {ind_sais = ind_djf}
159 if (sais==2) {ind_sais = ind_mam}
160 if (sais==3) {ind_sais = ind_jja}
161 if (sais==4) {ind_sais = ind_son}
162 print('ind_sais for the selected LWT')
163 print(ind_sais)
164 if (length(ind_sais)!=0) {
165   dir.create(paste('results/data_main/TT_',tt,'/sais_',sais,sep=''))
166   var_TT_sais = matrix(nrow=dim(var_TT)[1],ncol=length(ind_sais)*36)
167   for (i in 1:length(ind_sais)) {
168     var_TT_sais[(1+36*(i-1)): (36*i)] = var_TT[(1+36*(ind_sais[i]-1)): (36*ind_sais[i])]
169   }
170   print('index')
171   print((1+36*(i-1)))#index for var_TT_sais
172   print(36*i)#index for var_TT_sais
173   print((1+36*(ind_sais[i]-1)))#index for var_TT
174   print((36*ind_sais[i]))#index for var_TT
175   }
176   var_TT_sais = as.data.frame(var_TT_sais)
177   write.table(var_TT_sais,file=paste('results/data_main/TT_',tt,'/sais_',sais,'/36hours_',var,'_TT',tt,'_sais',sais,'.txt',sep=''))# lines = grid points ; rows= time (number of days x
178   } # end condition if length(ind_sais)!=0
179 } # end for s
180 } # end condition if length(ind_tt)!=0
181 } # fin condition if length(ind_tt)!=0
182 }
183 }
184 t2=Sys.time()
185 print(t2-t1)
186 }
187 } # end for t in 1:length(tt_trait)
188 } # end for v in 1:length(variab)
189 } #end lwt in 1:length(tt_temp)

```



# Main Script for Wind Analysis

```
1 #####
2 ### MAIN SCRIPT WIND ANALYSIS ##
3 [##### H. Ibitolu 20200615 #####]
4 #####
5
6 ## This is the main script for the wind data Analysis.
7 ## This script loads the pre-processed wind data
8
9 ## HI
10 setwd("D:/Toulouse_CNRS/Internship_January/Data/for_Henry/03_Toulouse_CAPITOUL_250m_untar/")
11 ## JH
12 # setwd("D:/Toulouse_CNRS/Internship_January/Data/for_Henry/03_Toulouse_CAPITOUL_250m_untar/results_sample/data_main/TT_7/sais_3/wind/")
13
14 ## HI
15 source("D:/Toulouse_CNRS/Internship_January/Data/for_Henry/03_Toulouse_CAPITOUL_250m_untar/FFDDuv.R")
16 ##JH
17 # source('01_scripts/FFDDuv.R')
18
19 library(rgdal)
20 library(sf)
21
22 #This is the start and end date
23 date_start = "2004-03-01"
24 date_end = "2005-02-28"
25
26 ## HI
27 rep_base = "D:/Toulouse_CNRS/Internship_January/Data/for_Henry/03_Toulouse_CAPITOUL_250m_untar/"
28 ##JH
29 rep_base = '03_Toulouse_CAPITOUL_250m_untar/'
30
31 load(paste(rep_base,'CONSTANTS_AND_README/LONS',sep=''))
32 lon = LST$vals
33 load(paste(rep_base,'CONSTANTS_AND_README/LATS',sep=''))
34 lat = LST$vals
35
36 lonlat_points = SpatialPoints(cbind(lon,lat),CRS("+init=epsg:4326"))
37 lonlat = spttransform(lonlat_points,CRS("+init=epsg:2154"))
38
39 # Reading LWT prduced in the Article of Hidalgo et al. (2014)
40 ## HI
41 weather_types_file = read.table(paste(rep_base,"weathertypes_Toulouse_Hidalgo_etal_2014.txt",sep=''))
42 ##JH
43 #weather_types_file = read.table(paste(rep_base,"weather_Types/Weathertypes_Toulouse_Hidalgo_etal_2014.txt",sep=''))
44 ind_start = which(as.character(weather_types_file[,2])==date_start) ### This describes the starting point for the LWT base on the date_start
45 weather_types_file = weather_types_file[-(1:(ind_start-1)),]
46
47 #This creates the folder to store the results
48 dir.create('results_4class/')
49 dir.create('results_4class/data_main/')
50 dir.create('results_4class/data_main/Day/')
51
52 #### Here, we assigned the variable needed. Where tt_trait = The weather_type variable needed (i.e- from 0:10),
53 #### and sais_trait = Seasons Variable (i.e.- 4 seasons 1:4 )
54 #### This sample script assumes we want to select LWT= 7 during the Summer (Jun,Jul,Aug) season
55
56 echelle_FF= c(0, 1.5, 3.3, 5.4, 10.7, 13.8, 17.1, 24.4) # Beaufort scale m/s
57 echelle_DD = c(22.5,67.5,112.5,157.5,202.5,247.5,292.5,337.5) ## Wind direction
58
59 tt_temp = c(9,8,7) ###For LWT number X
60 sais_trait = 3 ###For Summer season
61
62 for (lwt in 1:length(tt_temp)) { #This iterates for each LWT
63   tt_trait = tt_temp[lwt]
64   print(paste("LWT", tt_trait))
65 }
66
67 for (t in 1:length(tt_trait)) {
68   ti=Sys.time()
69   tt = tt_trait[t]
70   print(paste('TT',tt))
71   #dir.create(paste('results/data_main/TT_',tt,sep=''))
72
73   uu_TT = NULL
74   vv_TT = NULL
75   dates_tt = NULL
76   ind_tt = which(weather_types_file[,3]==tt)
77
78   ### This is to extract and get the dates that the particular weather type appeared
79   if (length(ind_tt)!=0) {
80     dates = weather_types_file[ind_tt,2]
81     dates = paste(substring(as.character(dates),1,4),substring(as.character(dates),6,7),substring(as.character(dates),9,10),sep='')
82
83     month = substring(dates,5,6)
84     ind_djf = which(month=="12" | month=="01" | month=="02")
85     ind_mam = which(month=="03" | month=="04" | month=="05")
86     ind_jja = which(month=="06" | month=="07" | month=="08")
87     ind_son = which(month=="09" | month=="10" | month=="11")
88
89     ### This is for seasons characteristics
90     for (s in 1:length(sais_trait)) {
91       sais = sais_trait[s]
92       print(paste('sais',sais))
93       dir.create(paste('results_4class/data_main/Day/TT_',tt,sep=''))
94       dir.create(paste('results_4class/data_main/Day/TT_',tt,'/sais_',sais,sep=''))
95
96       if (sais==1) {ind_sais = ind_djf}
97       if (sais==2) {ind_sais = ind_mam}
98       if (sais==3) {ind_sais = ind_jja}
99       if (sais==4) {ind_sais = ind_son}
100
101       ### This is to assign the date we wanted to evaluate based on the seasons we choose
102       if (length(ind_sais)!=0) {
103         dates_wanted = dates[ind_sais]
104
105         #####
106
107         print(" Step 1 - Reading the data into a variable")
108
109         Data_variab = c('UMME', 'VMME')
110         |
111         for (d in 1:length(Data_variab)) { # for each variable
112           Data_var = Data_variab[d]
113           print(Data_var)
114
115           data_temp <- read.table(file=paste('results/data_main/TT_',tt,'/sais_',sais,'/36hours_',Data_var,'_TT',tt,'_sais',sais,'.txt',sep='')) #lines = grid points ; rows= time (number of days x 36h)
116
117           print(" Step 2 - Extracting the required time interval") #to extract the time period from 03h--06h local time, which is equivalent to 01h-04h GMT (model time).
118
119           #indices <- lapply(seq(25, ncol(data_temp), 36), function(X) X:(X+3)) ## For extracting Night time (01-04)GMT --- (03-06)LT
120           indices <- lapply(seq(15, ncol(data_temp), 36), function(X) X:(X+3)) ## For Day time (15-18)GMT --- (17-20)LT
121           columns <- lapply(indices, function(X) data_temp[, X ])
122
123           data_temp_extract <- do.call(cbind, columns)
124
125           print(paste("Step 3 - Calculating the required means values for", Data_var)) # calculate the required mean for each day that the LWT appears in summer
126
127           data_temp_mean <- sapply(split.default(data_temp_extract, ((1:ncol(data_temp_extract))-1)%/4 + 1), rowMeans)
128
129           print(" Now writing into table the uu_vv mean")
130           ##write.table(data_temp_mean,file=paste('results_4class/data_main/Night/TT_',tt,'/sais_',sais,'/mean_',Data_var,'_TT',tt,'_sais',sais,'.txt',sep='')) ##For Night time
131           write.table(data_temp_mean,file=paste('results_4class/data_main/Day/TT_',tt,'/sais_',sais,'/Day_mean_',Data_var,'_TT',tt,'_sais',sais,'.txt',sep='')) ## For Day time
132         } #End the for (d in 1:length(Data_variab))
133
134         print("Step 4a - Converting the daily mean uu_vv to ff_dd")
135         UMME_mean <- read.table(file=paste('results_4class/data_main/Day/TT_',tt,'/sais_',sais,'/Day_mean_UMME_TT',tt,'_sais',sais,'.txt',sep=''))
136         VMME_mean <- read.table(file=paste('results_4class/data_main/Day/TT_',tt,'/sais_',sais,'/Day_mean_VMME_TT',tt,'_sais',sais,'.txt',sep=''))
137
138         FF_TT = uv2ffdd(UMME_mean,VMME_mean)[[1]]
139         DD_TT = uv2ffdd(UMME_mean,VMME_mean)[[2]]
140
141         print("Step 4b - Now writing into table the FF and DD for all the days of the LWT")
142         write.table(FF_TT,file=paste('results_4class/data_main/Day/TT_',tt,'/sais_',sais,'/Day_FF_TT',tt,'_sais',sais,'.txt',sep=''))
143         write.table(DD_TT,file=paste('results_4class/data_main/Day/TT_',tt,'/sais_',sais,'/Day_DD_TT',tt,'_sais',sais,'.txt',sep=''))
144
145         #####
146       }
147     }
148   }
149 }
```

```

145 print("Step 4c - Creating the .shp for the FF and DO which is then exported to QGIS")
146 dir.create(paste('results_4class/data_main/Day/TT_',tt,'/sais_',sais,'/wind/',sep = '')) #set the working directory to store the .shp
147
148 for (dd in 1:length(dates_wanted)) { #This is to extract the data for each day of the LWT
149   each_day = dates_wanted[dd]
150
151   FF_TT_Day <- FF_TT[, dd]
152   DO_TT_Day <- DO_TT[, dd]
153
154   FF_TT_proj = as.data.frame(FF_TT_Day)
155   coordinates(FF_TT_proj) = coordinates(lonlat)
156   proj4string(FF_TT_proj) = CRS("+init=epsg:2154")
157   writeOGR(FF_TT_proj, paste('results_4class/data_main/Day/TT_',tt,'/sais_',sais,'/wind/FF_1720LT_D', dd,'_T',tt,'_sais',sais,'.shp',sep=''), layer= "proj_FF_TT" , driver='ESRI Shapefile')
158
159   DO_TT_proj = as.data.frame(DO_TT_Day)
160   coordinates(DO_TT_proj) = coordinates(lonlat)
161   proj4string(DO_TT_proj) = CRS("+init=epsg:2154")
162   writeOGR(DO_TT_proj, paste('results_4class/data_main/Day/TT_',tt,'/sais_',sais,'/wind/DO_1720LT_D', dd,'_T',tt,'_sais',sais,'.shp',sep=''), layer= "proj_DO_TT" , driver='ESRI Shapefile')
163
164 } #End dd in 1:length(dates_wanted)
165
166
167 print("Step 5a - Now find the mean and write into table and shapefile")
168 FF_TT_mean = as.data.frame(rowMeans(FF_TT))
169 DO_TT_mean = as.data.frame(rowMeans(DO_TT))
170 write.table(FF_TT_mean, file=paste('results_4class/data_main/Day/TT_',tt,'/sais_',sais,'/Day_FF_TT_mean',tt,'_sais',sais,'.txt',sep=''))
171 write.table(DO_TT_mean, file=paste('results_4class/data_main/Day/TT_',tt,'/sais_',sais,'/Day_DO_TT_mean',tt,'_sais',sais,'.txt',sep=''))
172
173 FF_TT_mean_proj = as.data.frame(FF_TT_mean)
174 coordinates(FF_TT_mean_proj) = coordinates(lonlat)
175 proj4string(FF_TT_mean_proj) = CRS("+init=epsg:2154")
176 writeOGR(FF_TT_mean_proj, paste('results_4class/data_main/Day/TT_',tt,'/sais_',sais,'/wind/Mean_FF_1720LT_TT',tt,'_sais',sais,'.shp',sep=''), layer= "proj_FF_TT" , driver='ESRI Shapefile')
177
178 DO_TT_mean_proj = as.data.frame(DO_TT_mean)
179 coordinates(DO_TT_mean_proj) = coordinates(lonlat)
180 proj4string(DO_TT_mean_proj) = CRS("+init=epsg:2154")
181 writeOGR(DO_TT_mean_proj, paste('results_4class/data_main/Day/TT_',tt,'/sais_',sais,'/wind/Mean_DO_1720LT_TT',tt,'_sais',sais,'.shp',sep=''), layer= "proj_DO_TT" , driver='ESRI Shapefile')
182
183 print("Step 5b - Now determine the wind threshold and write into a table")
184 # transition to thresholds
185 print("Transition to thresholds")
186 var_S = matrix(nrow=nrow(FF_TT_mean)[1], ncol=dim(FF_TT_mean)[2])
187
188 for (h in 1:dim(FF_TT_mean)[2]) {
189   # traitement pour chacune des classes ; c'est un peu barbare mais c'est le seul endroit qui n'est pas réellement optimisé
190   # et ou il faut donc faire attention si des modifs sont faites.
191   # Grosso modo, on retient les jours pour lesquels on a un certain DO et une certaine FF ;
192   # les différents seuils pour DO et FF sont écrits plus haut
193
194   #### Transitions for Beaufort Scale : 4 types of wind Speed classes: (0, 1.5, 3.3, 5.4)m/s
195   var_S[which(DO_TT_mean[,h]>echelle_DO[1] | DO_TT_mean[,h]>echelle_DO[8]) & FF_TT_mean[,h]>echelle_FF[1] & FF_TT_mean[,h]<echelle_FF[2],h] = 1
196   var_S[which(DO_TT_mean[,h]<echelle_DO[1] | DO_TT_mean[,h]>echelle_DO[8]) & FF_TT_mean[,h]>echelle_FF[2] & FF_TT_mean[,h]<echelle_FF[3],h] = 2
197   var_S[which(DO_TT_mean[,h]<echelle_DO[1] | DO_TT_mean[,h]>echelle_DO[8]) & FF_TT_mean[,h]>echelle_FF[3] & FF_TT_mean[,h]<echelle_FF[4],h] = 3
198   var_S[which(DO_TT_mean[,h]<echelle_DO[1] | DO_TT_mean[,h]>echelle_DO[8]) & FF_TT_mean[,h]>echelle_FF[4],h] = 4
199
200   var_S[which(DO_TT_mean[,h]>echelle_DO[1] & DO_TT_mean[,h]<echelle_DO[2] & FF_TT_mean[,h]>echelle_FF[1] & FF_TT_mean[,h]<echelle_FF[2],h] = 5
201   var_S[which(DO_TT_mean[,h]>echelle_DO[1] & DO_TT_mean[,h]<echelle_DO[2] & FF_TT_mean[,h]>echelle_FF[2] & FF_TT_mean[,h]<echelle_FF[3],h] = 6
202   var_S[which(DO_TT_mean[,h]>echelle_DO[1] & DO_TT_mean[,h]<echelle_DO[2] & FF_TT_mean[,h]>echelle_FF[3] & FF_TT_mean[,h]<echelle_FF[4],h] = 7
203   var_S[which(DO_TT_mean[,h]>echelle_DO[1] & DO_TT_mean[,h]<echelle_DO[2] & FF_TT_mean[,h]>echelle_FF[4],h] = 8
204
205   var_S[which(DO_TT_mean[,h]>echelle_DO[2] & DO_TT_mean[,h]<echelle_DO[3] & FF_TT_mean[,h]>echelle_FF[1] & FF_TT_mean[,h]<echelle_FF[2],h] = 9
206   var_S[which(DO_TT_mean[,h]>echelle_DO[2] & DO_TT_mean[,h]<echelle_DO[3] & FF_TT_mean[,h]>echelle_FF[2] & FF_TT_mean[,h]<echelle_FF[3],h] = 10
207   var_S[which(DO_TT_mean[,h]>echelle_DO[2] & DO_TT_mean[,h]<echelle_DO[3] & FF_TT_mean[,h]>echelle_FF[3] & FF_TT_mean[,h]<echelle_FF[4],h] = 11
208   var_S[which(DO_TT_mean[,h]>echelle_DO[2] & DO_TT_mean[,h]<echelle_DO[3] & FF_TT_mean[,h]>echelle_FF[4],h] = 12
209
210   var_S[which(DO_TT_mean[,h]>echelle_DO[3] & DO_TT_mean[,h]<echelle_DO[4] & FF_TT_mean[,h]>echelle_FF[1] & FF_TT_mean[,h]<echelle_FF[2],h] = 13
211   var_S[which(DO_TT_mean[,h]>echelle_DO[3] & DO_TT_mean[,h]<echelle_DO[4] & FF_TT_mean[,h]>echelle_FF[2] & FF_TT_mean[,h]<echelle_FF[3],h] = 14
212   var_S[which(DO_TT_mean[,h]>echelle_DO[3] & DO_TT_mean[,h]<echelle_DO[4] & FF_TT_mean[,h]>echelle_FF[3] & FF_TT_mean[,h]<echelle_FF[4],h] = 15
213   var_S[which(DO_TT_mean[,h]>echelle_DO[3] & DO_TT_mean[,h]<echelle_DO[4] & FF_TT_mean[,h]>echelle_FF[4],h] = 16
214
215   var_S[which(DO_TT_mean[,h]>echelle_DO[4] & DO_TT_mean[,h]<echelle_DO[5] & FF_TT_mean[,h]>echelle_FF[1] & FF_TT_mean[,h]<echelle_FF[2],h] = 17
216   var_S[which(DO_TT_mean[,h]>echelle_DO[4] & DO_TT_mean[,h]<echelle_DO[5] & FF_TT_mean[,h]>echelle_FF[2] & FF_TT_mean[,h]<echelle_FF[3],h] = 18
217   var_S[which(DO_TT_mean[,h]>echelle_DO[4] & DO_TT_mean[,h]<echelle_DO[5] & FF_TT_mean[,h]>echelle_FF[3] & FF_TT_mean[,h]<echelle_FF[4],h] = 19
218   var_S[which(DO_TT_mean[,h]>echelle_DO[4] & DO_TT_mean[,h]<echelle_DO[5] & FF_TT_mean[,h]>echelle_FF[4],h] = 20
219
220   var_S[which(DO_TT_mean[,h]>echelle_DO[5] & DO_TT_mean[,h]<echelle_DO[6] & FF_TT_mean[,h]>echelle_FF[1] & FF_TT_mean[,h]<echelle_FF[2],h] = 21
221   var_S[which(DO_TT_mean[,h]>echelle_DO[5] & DO_TT_mean[,h]<echelle_DO[6] & FF_TT_mean[,h]>echelle_FF[2] & FF_TT_mean[,h]<echelle_FF[3],h] = 22
222   var_S[which(DO_TT_mean[,h]>echelle_DO[5] & DO_TT_mean[,h]<echelle_DO[6] & FF_TT_mean[,h]>echelle_FF[3] & FF_TT_mean[,h]<echelle_FF[4],h] = 23
223   var_S[which(DO_TT_mean[,h]>echelle_DO[5] & DO_TT_mean[,h]<echelle_DO[6] & FF_TT_mean[,h]>echelle_FF[4],h] = 24
224
225   var_S[which(DO_TT_mean[,h]>echelle_DO[6] & DO_TT_mean[,h]<echelle_DO[7] & FF_TT_mean[,h]>echelle_FF[1] & FF_TT_mean[,h]<echelle_FF[2],h] = 25
226   var_S[which(DO_TT_mean[,h]>echelle_DO[6] & DO_TT_mean[,h]<echelle_DO[7] & FF_TT_mean[,h]>echelle_FF[2] & FF_TT_mean[,h]<echelle_FF[3],h] = 26
227   var_S[which(DO_TT_mean[,h]>echelle_DO[6] & DO_TT_mean[,h]<echelle_DO[7] & FF_TT_mean[,h]>echelle_FF[3] & FF_TT_mean[,h]<echelle_FF[4],h] = 27
228   var_S[which(DO_TT_mean[,h]>echelle_DO[6] & DO_TT_mean[,h]<echelle_DO[7] & FF_TT_mean[,h]>echelle_FF[4],h] = 28
229
230   var_S[which(DO_TT_mean[,h]>echelle_DO[7] & DO_TT_mean[,h]<echelle_DO[8] & FF_TT_mean[,h]>echelle_FF[1] & FF_TT_mean[,h]<echelle_FF[2],h] = 29
231   var_S[which(DO_TT_mean[,h]>echelle_DO[7] & DO_TT_mean[,h]<echelle_DO[8] & FF_TT_mean[,h]>echelle_FF[2] & FF_TT_mean[,h]<echelle_FF[3],h] = 30
232   var_S[which(DO_TT_mean[,h]>echelle_DO[7] & DO_TT_mean[,h]<echelle_DO[8] & FF_TT_mean[,h]>echelle_FF[3] & FF_TT_mean[,h]<echelle_FF[4],h] = 31
233   var_S[which(DO_TT_mean[,h]>echelle_DO[7] & DO_TT_mean[,h]<echelle_DO[8] & FF_TT_mean[,h]>echelle_FF[4],h] = 32
234 } # fin boucle for h
235
236 var_S = as.data.frame(var_S)
237 write.table(var_S, file=paste('results_4class/data_main/TT_',tt,'/sais_',sais,'/wind_4class_thresholds_T',tt,'_sais',sais,'.txt',sep=''))
238 write.table(var_S, file=paste('results_4class/data_main/Day/TT_',tt,'/sais_',sais,'/Day_wind_4class_thres_T',tt,'_sais',sais,'.txt',sep=''))
239
240
241 var_S_proj = as.data.frame(var_S)
242 coordinates(var_S_proj) = coordinates(lonlat)
243 proj4string(var_S_proj) = CRS("+init=epsg:2154")
244 writeOGR(var_S_proj, paste('results_4class/data_main/TT_',tt,'/sais_',sais,'/wind/proj_wind_4class_thresholds_T',tt,'_sais',sais,'.shp',sep=''), driver='ESRI Shapefile', layer='seuil_final') ## For Night time
245 writeOGR(var_S_proj, paste('results_4class/data_main/Day/TT_',tt,'/sais_',sais,'/wind/proj_Day_wind_4class_thres_T',tt,'_sais',sais,'.shp',sep=''), driver='ESRI Shapefile', layer='seuil_final') ## For Day time
246
247
248 rm(var_S_proj)
249
250 } # end condition - if (length(ind_sais)!=0)
251
252 } # end boolean statement for - s
253
254 } # end condition - if (length(ind_tt)!=0)
255 t2=Sys.time()
256 print(t2-t1)
257 } # end boolean for t
258 } # lwt in 1:length(tt_temp))
259

```



## Preparatory Script for Wind Velocity Ratio Analysis

```
1 #####
2 ## SCRIPT VELOCITY RATIO ANALYSIS ##
3 ## H. Ibitolu 20200305 #####
4 #####
5
6 ## This script is the preparation for the wind vel Ratio Analysis.
7 ## This script loads the wind vel Ratio data and aggregates it to have only one single data.
8 #####JH*** to allow portability between platforms please name the files and folders without spaces and using _ as in this exemple 03_Toulouse_CAPITOU_250m_untar
9
10 #HI
11 setwd("D:/Toulouse_CNRS/Internship_January/Data/for_Henry/03_Toulouse_CAPITOU_250m_untar/")
12
13 # JH
14 # setwd('/media/julia/My Passport/work/PROYECTOS_en_curso/MAPUCE/13_Simulations_Robert/Robert_simulations2018/06_carto_JH/02_online20180717/')
15
16 #This is the start and end date
17 date_start = "2004-03-01"
18 date_end = "2005-02-28"
19
20 rep_base = "D:/Toulouse_CNRS/Internship_January/Data/for_Henry/03_Toulouse_CAPITOU_250m_untar/"
21
22 #JH
23 #rep_base = '03_Toulouse_CAPITOU_250m_untar/'
24
25 #####JH*** you don't need to do this. You are not using WFF10MM_ISBA... variables but the integrated ones: WFF10MM
26 # reading the constant variables over time (urban morphology variables)
27 load(paste(rep_base,'/CONSTANTS_AND_README/FRAC_NATURE',sep=''))
28 FRAC_NATURE <- LST$vals
29 load(paste(rep_base,'/CONSTANTS_AND_README/FRAC_TOWN',sep=''))
30 FRAC_TOWN <- LST$vals
31 load(paste(rep_base,'/CONSTANTS_AND_README/FRAC_WATER',sep=''))
32 FRAC_WATER <- LST$vals
33
34 # Reading LWT prduced in the Article of Hidalgo et al. (2014)
35 #HI
36 weather_types_file = read.table(paste(rep_base,"weathertypes_Toulouse_Hidalgo_etal_2014.txt",sep=''))
37 #JH
38 weather_types_file = read.table(paste(rep_base,"Weather_Types/Weathertypes_Toulouse_Hidalgo_etal_2014.txt",sep=''))
39 ind_start = which(as.character(weather_types_file[,2])==date_start) ## This describes the starting point for the LWT base on the date_start
40 weather_types_file = weather_types_file[-(1:(ind_start-1)),]
41
42
43 #This creates the folder to store the results
44 dir.create('results/')
45 dir.create('results/vel_ratio/')
46 dir.create('results/vel_ratio/data_prep/')
47
48
49 ##### Here, we assigned the variable needed. Where tt_trait = The weather_type variable needed (i.e- from 1:9),
50 ##### and sais_trait = Seasons Variable (i.e.- 4 seasons 1:4 )
51 ##### This sample script assumes we want to select LWT= 7 during the Summer (Jun,Jul,Aug) season
52
53 #
54 # tt_trait = 7 ##For LWT=7
55 #
56 # sais_trait = 3 ##For Summer season
57
58 tt_temp = c(7,8) ##For LWT number X
59 sais_trait = 3 ##For Summer season
60 #variab = c('UMME') # test for one variable
61 variab = c('VRAT_ISBA_2m', 'VRAT_TEB_2m')
62
63 # for (t in 1:length(tt_trait)) {
64 # ti=Sys.time()
65 # tt = tt_trait[t]
66 # print(paste('TT',tt))
67 # dir.create(paste('results2/data_main/TT_',tt,sep=''))
68 #
69 # uu_TT = NULL
70 # vv_TT = NULL
71 # dates_tt = NULL
72 # ind_tt = which(weather_types_file[,3]==tt)
73 #
74
75 for (lwt in 1:length(tt_temp)) { #This iterates for each LWT
76 tt_trait = tt_temp[lwt]
77 print(paste("LWT", tt_trait))
78
79 for (v in 1:length(variab)) { # for each variable
80 var = variab[v]
81 print(var)
82
83 for (t in 1:length(tt_trait)) {#for each LWT
84 ti=Sys.time()
85 tt = tt_trait[t]
86 print('TT')
87 print(tt)
88 dir.create(paste('results/vel_ratio/data_prep/TT_',tt,sep=''))
89
90 VRAT_ISBA = NULL
91 VRAT_TEB = NULL
92 var_TT = NULL
93 dates_tt = NULL
94 ind_tt = which(weather_types_file[,3]==tt)# LWT index
95 print("ind_tt")
96 print(ind_tt)
97
98 ## This is to extract and get the dates that the particular weather type appeared
99 if (length(ind_tt)!=0) {
100 dates = weather_types_file[ind_tt,2]
101 dates = paste(substring(as.character(dates),1,4),substring(as.character(dates),6,7),substring(as.character(dates),9,10),sep='')
102 month = substring(dates,5,6)
103
104 print("dates")
105 print(dates)
106
107 # reading the data: 41 directories each containing directories with dates and then data
108 print("Now start reading in the files from 1:41")
109 # for (i in 1:1) {#test for first directory where there are 3 LWT days "20040303" "20040304" "20040309"
110 for (i in 1:41) {
111 print(paste('i=',i))
112 rep = paste(rep_base,'TIME_DEP_PART_',i,sep='')
113 for (j in 1:length(list.files(rep))) { # j is the day, there are 9 days in each directory i
114 print(paste('j=',j))
115 rep_date = list.files(rep)[j]
116 if (rep_date!="20050228") {
117 ind_date = which(dates==rep_date) #how many LWT dates are in this directory ?
118 print('ind_date =')
119 print(ind_date)
120 if (length(ind_date)!=0) {# if there are one or more load the data
121 dates_tt = c(dates_tt,dates[ind_date])
122 print('dates_tt =')
123 print(dates_tt)
124 load(paste(rep,'/',rep_date,'/REFER/',var,sep=''))
125 var_temp = LST$vals_day
126 print(var_temp[1,])
127
128 if (j!=length(list.files(rep))) { # if i'm not in the last file of the directory I also load the day J+1
129 rep_date_temp = list.files(rep)[j+1]
130 load(paste(rep,'/',rep_date_temp,'/REFER/',var,sep=''))
131 var_temp = cbind(var_temp,LST$vals_day)
132 print("im not in the last file of the directory so I load also the day J+1")
133 print('rep_date_temp')
134 print(rep_date_temp)
135 print(var_temp[1,])
136 }
137
138 } else { # if im already in the last day (j=9) of the repertory i, I take the first day of the repertory i+1
139 if (i!=41) {
140 print("Im here i!=41")
141 rep_temp = paste(rep_base,'TIME_DEP_PART_',i+1,sep='')
142 rep_date_temp = list.files(rep)[1]
143 load(paste(rep_temp,'/',rep_date_temp,'/REFER/',var,sep=''))
144 var_temp = cbind(var_temp,LST$vals_day)
145 print('rep_temp')
```

```

146     print(rep_temp)
147     print(rep_date_temp)
148     print(rep_date_temp)
149     print(dim(var_temp))
150     print(dim(var_temp))
151     print(var_temp[1,])
152 }
153 } # if im in the last day (j=9) of i=41 I finish
154 if (dim(var_temp)[1]>24) {var_TT = cbind(var_TT,var_temp[,1:36])} # 36h wanted (from 01h UTC for day j to 12h UTC for the day j+1)
155 print('I select 36h per LWT')
156 print(var_TT[1,])
157 }
158 print(paste('dim(var_TT)', dim(var_TT)))# 57600 grid points, 1800 (=50 days x 36 hours)
159 } # end condition if (length(ind_dat)!=0)
160 } # end condition if (rep_date!='20050228')
161 } # end boolean statement for j
162 } # end boolean statement for i
163 }
164 ### This is to extract the dates that the particular weather type occurred for a particular season
165 mois = substring(dates_tt,s,6)
166 ind_djf = which(mois=='12' | mois=='01' | mois=='02')
167 ind_mam = which(mois=='03' | mois=='04' | mois=='05')
168 ind_jja = which(mois=='06' | mois=='07' | mois=='08')
169 ind_son = which(mois=='09' | mois=='10' | mois=='11')
170
171 for (s in 1:length(sais_trait)) {
172     sais = sais_trait[s]
173     print(paste('sais',sais)) # 18 days for LWT 9 -> 21 22 23 24 25 26 27 28 29 30 31 32 33 34 35 36 37 38
174
175     if (sais==1) {ind_sais = ind_djf}
176     if (sais==2) {ind_sais = ind_mam}
177     if (sais==3) {ind_sais = ind_jja}
178     if (sais==4) {ind_sais = ind_son}
179     print('ind_sais for the selected LWT')
180     print(ind_sais)
181     if (length(ind_sais)!=0) {
182         dir.create(paste('results/vel_ratio/data_prep/TT_',tt,'/sais_',sais,sep=''))
183         var_TT_sais = matrix(nrow=dim(var_TT)[1],ncol=length(ind_sais)*36)
184         for (i in 1:length(ind_sais)) {
185             var_TT_sais[, (1+36*(i-1)): (36*i)] = var_TT[, (1+36*(ind_sais[i]-1)): (36*ind_sais[i])]
186             print('index')
187             print((1+36*(i-1)))#index for var_TT_sais
188             print(36*i)#index for var_TT_sais
189             print((1+36*(ind_sais[i]-1)))#index for var_TT
190             print((36*ind_sais[i]))#index for var_TT
191         }
192         var_TT_sais = as.data.frame(var_TT_sais)
193         write.table(var_TT_sais,file=paste('results/vel_ratio/data_prep/TT_',tt,'/sais_',sais,'/36hours_',var,'_TT',tt,'_sais',sais,'.txt',sep=''))# lines = grid points ; rows= time (number of days x 36h)
194     } # end condition if length(ind_sais)!=0
195 } # end for s
196
197 } # end for s
198
199 } # fin condition if length(ind_tt)!=0
200
201 t2=Sys.time()
202 print(t2-t1)
203
204 #rm(var_TT_sais)
205 #rm(var_TT)
206
207 } # end for t in 1:length(tt_trait)
208
209 } # end for v in 1:length(variab)
210
211 } #end lwt in 1:length(tt_temp)
212

```

## Main Script for Wind Velocity Ratio Analysis

```

1 #####
2 ### SCRIPT VELOCITY RATIO ANALYSIS ###
3 ### H. Ibitolu 20200305 ###
4 #####
5
6 ## This script is the main script for the wind velocity Ratio Analysis.
7 ## This script loads the wind vel Ratio data and aggregates it to have only one single data.
8 #####H#### to allow portability between platforms please name the files and folders without spaces and using _ as in this exemple 03_Toulouse_CAPITOU_250m_untar
9
10 ## HI
11 setwd("D:/Toulouse_CNRS/Internship_January/Data/for_Henry/03_Toulouse_CAPITOU_250m_untar/")
12 ## JH
13 # setwd("D:/Toulouse_CNRS/Internship_January/Data/for_Henry/03_Toulouse_CAPITOU_250m_untar/results_sample/data_main/TT_7/sais_3/wind/")
14
15 ## HI
16 source("D:/Toulouse_CNRS/Internship_January/Data/for_Henry/03_Toulouse_CAPITOU_250m_untar/FFDDuv.R")
17 ##JH
18 # source('01_scripts/FFDDuv.R')
19
20
21 library(rgdal)
22 library(sf)
23
24 #This is the start and end date
25 date_start = "2004-03-01"
26 date_end = "2005-02-28"
27
28 ## HI
29 rep_base = "D:/Toulouse_CNRS/Internship_January/Data/for_Henry/03_Toulouse_CAPITOU_250m_untar/"
30 ##JH
31 #rep_base = '03_Toulouse_CAPITOU_250m_untar/'
32
33 load(paste(rep_base, 'CONSTANTS_AND_README/LONS', sep=''))
34 lon = LST$vals
35 load(paste(rep_base, 'CONSTANTS_AND_README/LATS', sep=''))
36 lat = LST$vals
37
38 lonlat_points = SpatialPoints(cbind(lon, lat), CRS("+init=epsg:4326"))
39 lonlat = spttransform(lonlat_points, CRS("+init=epsg:2154"))
40
41 # Reading LWT prduced in the Article of Hidalgo et al. (2014)
42 ## HI
43 weather_types_file = read.table(paste(rep_base, "weathertypes_Toulouse_Hidalgo_etal_2014.txt", sep=''))
44 ##JH
45 #weather_types_file = read.table(paste(rep_base, "weather_Types/Weathertypes_Toulouse_Hidalgo_etal_2014.txt", sep=''))
46 ind_start = which(as.character(weather_types_file[,2])==date_start) ## This describes the starting point for the LWT base on the date_start
47 weather_types_file = weather_types_file[-(1:(ind_start-1)),]
48
49 #This creates the folder to store the results
50 #dir.create('results/vel_ratio/data_main/')
51 #dir.create('results/vel_ratio/data_main/day/') ## For Day time
52 dir.create('results/vel_ratio/data_main/night/') ## For Night time
53
54 #### Here, we assigned the variable needed. Where tt_trait = The weather_type variable needed (i.e- from 0:10),
55 #### and sais_trait = Seasons Variable (i.e- 4 seasons 1:4 )
56 #### This sample script assumes we want to select LWT= 7 during the Summer (Jun, Jul, Aug) season
57
58 tt_temp = c(9,8,7) ###For LWT number X
59 sais_trait = 3 ###For Summer season
60
61 for (lwt in 1:length(tt_temp)) { #This iterates for each LWT
62   tt_trait = tt_temp[lwt]
63   print(paste("LWT", tt_trait))
64
65   for (t in 1:length(tt_trait)) {
66     ti=Sys.time()
67     tt = tt_trait[t]
68     print(paste('TT', tt))
69
70
71     VRAT_ISBA = NULL
72     VRAT_TEB = NULL
73     dates_tt = NULL
74     ind_tt = which(weather_types_file[,3]==tt)
75
76     ## This is to extract and get the dates that the particular weather type appeared
77     if (length(ind_tt)!=0) {
78       dates = weather_types_file[ind_tt,2]
79       dates = paste(substring(as.character(dates),1,4), substring(as.character(dates),6,7), substring(as.character(dates),9,10), sep='')
80
81       month = substring(dates,5,6)
82       ind_djf = which(month=="12" | month=="01" | month=="02")
83       ind_mam = which(month=="03" | month=="04" | month=="05")
84       ind_jja = which(month=="06" | month=="07" | month=="08")
85       ind_son = which(month=="09" | month=="10" | month=="11")
86
87       ## This is for seasons characteristics
88       for (s in 1:length(sais_trait)) {
89         sais = sais_trait[s]
90         print(paste('sais', sais))
91         # dir.create(paste('results/vel_ratio/data_main/Day/TT_', tt, sep='')) ## For Day time
92         # dir.create(paste('results/vel_ratio/data_main/Day/TT_', tt, '/', sais, sep=''))
93         dir.create(paste('results/vel_ratio/data_main/Night/TT_', tt, sep='')) ## For Night time
94         dir.create(paste('results/vel_ratio/data_main/Night/TT_', tt, '/', sais, sep=''))
95
96         if (sais==1) {ind_sais = ind_djf}
97         if (sais==2) {ind_sais = ind_mam}
98         if (sais==3) {ind_sais = ind_jja}
99         if (sais==4) {ind_sais = ind_son}
100
101         #### This is to assign the date we wanted to evaluate based on the seasons we choose
102         if (length(ind_sais)!=0) {
103           dates_wanted = dates[ind_sais]
104
105           #####
106           print(" Step 1 - Reading the data into a variable")
107           Data_variab = c('VRAT_ISBA_2m', 'VRAT_TEB_2m')
108
109           for (d in 1:length(Data_variab)) { # for each variable
110             Data_var = Data_variab[d]
111             print(Data_var)
112
113             data_temp <- read.table(file=paste('results/vel_ratio/data_prep/TT_', tt, '/', sais, '/', 36hours, Data_var, '_TT', tt, '_sais', sais, '.txt', sep='')) # rows = grid points ; columns= time (number of days x 36h)
114
115             print(" Step 2 - Extracting the required time interval") #to extract the time period from 03h-06h local time, which is equivalent to 01h-04h GMT (model time).
116
117             indices <- lapply(seq(25, ncol(data_temp), 36), function(X) X:(X+3)) ## For Night time : (01-04)GMT --- (03-06)LT
118             # indices <- lapply(seq(15, ncol(data_temp), 36), function(X) X:(X+3)) ## For Day time : (15-18)GMT --- (17-20)LT
119             columns <- lapply(indices, function(X) data_temp[, X])
120
121             data_temp_extract <- do.call(cbind, columns)
122
123
124             print(paste("Step 3 - Calculating the required means values for", Data_var)) # calculate the required mean for each day that the LWT appears in season 3
125             data_temp_mean <- sapply(split.default(data_temp_extract, ((1:ncol(data_temp_extract))-1)%4 + 1), rowMeans)
126
127             print(" Now writing into table the VRAT_ISBA and VRAT_TEB for the entire period")
128             ## This gives the daily mean velocity Ratio of each day of occurrence of the LWT
129             # write.table(data_temp_mean, file=paste('results/vel_ratio/data_main/Day/TT_', tt, '/', sais, '/', 'Day_mean', Data_var, '_TT', tt, '_sais', sais, '.txt', sep='')) ## For Day time
130             write.table(data_temp_mean, file=paste('results/vel_ratio/data_main/Night/TT_', tt, '/', sais, '/', 'Night_mean', Data_var, '_TT', tt, '_sais', sais, '.txt', sep='')) ## For Night time
131
132
133
134
135
136
137
138
139
140
141
142
143
144
145
146
147
148
149
150
151
152
153
154
155
156
157
158
159
160
161
162
163
164
165
166
167
168
169
170
171
172
173
174
175
176
177
178
179
180
181
182
183
184
185
186
187
188
189
190
191
192
193
194
195
196
197
198
199
200
201
202
203
204
205
206
207
208
209
210
211
212
213
214
215
216
217
218
219
220
221
222
223
224
225
226
227
228
229
230
231
232
233
234
235
236
237
238
239
240
241
242
243
244
245
246
247
248
249
250
251
252
253
254
255
256
257
258
259
260
261
262
263
264
265
266
267
268
269
270
271
272
273
274
275
276
277
278
279
280
281
282
283
284
285
286
287
288
289
290
291
292
293
294
295
296
297
298
299
300
301
302
303
304
305
306
307
308
309
310
311
312
313
314
315
316
317
318
319
320
321
322
323
324
325
326
327
328
329
330
331
332
333
334
335
336
337
338
339
340
341
342
343
344
345
346
347
348
349
350
351
352
353
354
355
356
357
358
359
360
361
362
363
364
365
366
367
368
369
370
371
372
373
374
375
376
377
378
379
380
381
382
383
384
385
386
387
388
389
390
391
392
393
394
395
396
397
398
399
400
401
402
403
404
405
406
407
408
409
410
411
412
413
414
415
416
417
418
419
420
421
422
423
424
425
426
427
428
429
430
431
432
433
434
435
436
437
438
439
440
441
442
443
444
445
446
447
448
449
450
451
452
453
454
455
456
457
458
459
460
461
462
463
464
465
466
467
468
469
470
471
472
473
474
475
476
477
478
479
480
481
482
483
484
485
486
487
488
489
490
491
492
493
494
495
496
497
498
499
500
501
502
503
504
505
506
507
508
509
510
511
512
513
514
515
516
517
518
519
520
521
522
523
524
525
526
527
528
529
530
531
532
533
534
535
536
537
538
539
540
541
542
543
544
545
546
547
548
549
550
551
552
553
554
555
556
557
558
559
560
561
562
563
564
565
566
567
568
569
570
571
572
573
574
575
576
577
578
579
580
581
582
583
584
585
586
587
588
589
590
591
592
593
594
595
596
597
598
599
600
601
602
603
604
605
606
607
608
609
610
611
612
613
614
615
616
617
618
619
620
621
622
623
624
625
626
627
628
629
630
631
632
633
634
635
636
637
638
639
640
641
642
643
644
645
646
647
648
649
650
651
652
653
654
655
656
657
658
659
660
661
662
663
664
665
666
667
668
669
670
671
672
673
674
675
676
677
678
679
680
681
682
683
684
685
686
687
688
689
690
691
692
693
694
695
696
697
698
699
700
701
702
703
704
705
706
707
708
709
710
711
712
713
714
715
716
717
718
719
720
721
722
723
724
725
726
727
728
729
730
731
732
733
734
735
736
737
738
739
740
741
742
743
744
745
746
747
748
749
750
751
752
753
754
755
756
757
758
759
760
761
762
763
764
765
766
767
768
769
770
771
772
773
774
775
776
777
778
779
780
781
782
783
784
785
786
787
788
789
790
791
792
793
794
795
796
797
798
799
800
801
802
803
804
805
806
807
808
809
810
811
812
813
814
815
816
817
818
819
820
821
822
823
824
825
826
827
828
829
830
831
832
833
834
835
836
837
838
839
840
841
842
843
844
845
846
847
848
849
850
851
852
853
854
855
856
857
858
859
860
861
862
863
864
865
866
867
868
869
870
871
872
873
874
875
876
877
878
879
880
881
882
883
884
885
886
887
888
889
890
891
892
893
894
895
896
897
898
899
900
901
902
903
904
905
906
907
908
909
910
911
912
913
914
915
916
917
918
919
920
921
922
923
924
925
926
927
928
929
930
931
932
933
934
935
936
937
938
939
940
941
942
943
944
945
946
947
948
949
950
951
952
953
954
955
956
957
958
959
960
961
962
963
964
965
966
967
968
969
970
971
972
973
974
975
976
977
978
979
980
981
982
983
984
985
986
987
988
989
990
991
992
993
994
995
996
997
998
999
1000

```



```

135 } #End the for (d in 1:length(data_variab))
136
137 print("Step 4 - Now find the mean and write into table and shapefile")
138
139 # dir.create(paste('results/vel_ratio/data_main/Day/TT_',tt,'/sais_',sais,'/VRAT_output/',sep = '')) ## For Day time
140 dir.create(paste('results/vel_ratio/data_main/Night/TT_',tt,'/sais_',sais,'/VRAT_output/',sep = '')) ## For Night time
141
142 ## Reading back in, the table of the daily mean velocity Ratio
143 # VRAT_ISBA_daily <- read.table(file=paste('results/vel_ratio/data_main/Day/TT_',tt,'/sais_',sais,'/Day_mean_VRAT_ISBA_2m_TT',tt,'_sais',sais,'.txt',sep='')) ### For Day time
144 # VRAT_TEB_daily <- read.table(file=paste('results/vel_ratio/data_main/Day/TT_',tt,'/sais_',sais,'/Day_mean_VRAT_TEB_2m_TT',tt,'_sais',sais,'.txt',sep=''))
145 VRAT_ISBA_daily <- read.table(file=paste('results/vel_ratio/data_main/Night/TT_',tt,'/sais_',sais,'/Night_mean_VRAT_ISBA_2m_TT',tt,'_sais',sais,'.txt',sep='')) ## For Night time
146 VRAT_TEB_daily <- read.table(file=paste('results/vel_ratio/data_main/Night/TT_',tt,'/sais_',sais,'/Night_mean_VRAT_TEB_2m_TT',tt,'_sais',sais,'.txt',sep=''))
147
148 ## Find the mean for the entire days using the RowMeans function
149 VRAT_ISBA_mean = as.data.frame(rowMeans(VRAT_ISBA_daily))
150 VRAT_TEB_mean = as.data.frame(rowMeans(VRAT_TEB_daily))
151
152 ### This gives the total mean velocity Ratio for the entire days of the LWT occurrence
153 # write.table(VRAT_ISBA_mean,file=paste('results/vel_ratio/data_main/Day/TT_',tt,'/sais_',sais,'/Total_mean_VRAT_ISBA_1720LT_TT',tt,'_sais',sais,'.txt',sep='')) ## For Day time
154 # write.table(VRAT_TEB_mean,file=paste('results/vel_ratio/data_main/Day/TT_',tt,'/sais_',sais,'/Total_mean_VRAT_TEB_1720LT_TT',tt,'_sais',sais,'.txt',sep=''))
155 write.table(VRAT_ISBA_mean,file=paste('results/vel_ratio/data_main/Night/TT_',tt,'/sais_',sais,'/Total_mean_VRAT_ISBA_0306LT_TT',tt,'_sais',sais,'.txt',sep='')) ## For Night time
156 write.table(VRAT_TEB_mean,file=paste('results/vel_ratio/data_main/Night/TT_',tt,'/sais_',sais,'/Total_mean_VRAT_TEB_0306LT_TT',tt,'_sais',sais,'.txt',sep=''))
157
158 VRAT_ISBA_mean_proj = as.data.frame(VRAT_ISBA_mean)
159 coordinates(VRAT_ISBA_mean_proj) = coordinates(lonlat)
160 proj4string(VRAT_ISBA_mean_proj) = CRS("+init=epsg:2154")
161 # writeOGR(VRAT_ISBA_mean_proj, paste('results/vel_ratio/data_main/Day/TT_',tt,'/sais_',sais,'/VRAT_output/Mean_VRAT_ISBA_1720LT_TT',tt,'_sais',sais,'.shp',sep=''), layer= "proj_FF_TT" , driver='ESRI Shapefile')## For Day time
162 writeOGR(VRAT_ISBA_mean_proj, paste('results/vel_ratio/data_main/Night/TT_',tt,'/sais_',sais,'/VRAT_output/Mean_VRAT_ISBA_0306LT_TT',tt,'_sais',sais,'.shp',sep=''), layer= "proj_FF_TT" , driver='ESRI Shapefile')## For Night ti
163
164 VRAT_TEB_mean_proj = as.data.frame(VRAT_TEB_mean)
165 coordinates(VRAT_TEB_mean_proj) = coordinates(lonlat)
166 proj4string(VRAT_TEB_mean_proj) = CRS("+init=epsg:2154")
167 # writeOGR(VRAT_TEB_mean_proj, paste('results/vel_ratio/data_main/Day/TT_',tt,'/sais_',sais,'/VRAT_output/Mean_VRAT_TEB_1720LT_TT',tt,'_sais',sais,'.shp',sep=''), layer= "proj_DD_TT" , driver='ESRI Shapefile')## For Day time
168 writeOGR(VRAT_TEB_mean_proj, paste('results/vel_ratio/data_main/Night/TT_',tt,'/sais_',sais,'/VRAT_output/Mean_VRAT_TEB_0306LT_TT',tt,'_sais',sais,'.shp',sep=''), layer= "proj_DD_TT" , driver='ESRI Shapefile')## For Night ti
169
170 } # end condition - if (length(ind_sais)!=0)
171
172 } # end boolean statement for - s
173
174 } # end condition - if (length(ind_tt)!=0)
175 t2=Sys.time()
176 print(t2-t1)
177 } # end boolean for t
178 } # lwt in 1:length(tt_temp))
179

```